# Technical and financial feasibility study of solar water heating system

Thesis submitted in partial fulfillment

for the award of Degree

## Doctor of Philosophy

By


## SHAILENDRA SINGH

**RAJIV GANDHI INSTITUTE OF PETROLEUM TECHNOLOGY**
**JAIS-229304**


PRE18001 2024

## CERTIFICATE

It is certified that the work contained in the thesis titled *"**Technical and financial feasibility study of solar water heating system**" by "**Shailendra Singh**"* has been carried out under our supervision and that this work has not been submitted elsewhere for a degree.

It is further certified that the student has fulfilled all the requirements of the Comprehensive, Candidacy, and SOTA/Open seminar.

**Dr. Atul Sharma**
(Supervisor)

**Dr. Amritanshu Shukla**
(Co-Supervisor)

## DECLARATION BY THE CANDIDATE

I, "***Shailendra Singh***", certify that the work embodied in this thesis is my own bonafide work and carried out by me under the supervision of "***Dr. Atul Sharma***" and "***Dr. Amritanshu Shukla***" from August 2018 to January 2023 at the ***Department of Sciences and Humanities***, Rajiv Gandhi Institute of Petroleum Technology, Jais. The matter embodied in this thesis has not been submitted for the award of any other degree. I declare that I have faithfully acknowledged and given credits to the research workers wherever their works have been cited in my work in this thesis. I further declare that I have not willfully copied any other's work, paragraphs, text, data, results, etc., reported in journals, books, magazines, reports dissertations, theses, etc., or available on websites and have not included them in this thesis and have not cited as my own work.

Date:

Place:

**Shailendra Singh**

## CERTIFICATE BY THE SUPERVISOR(S)

It is certified that the above statement made by the student is correct to the best of our knowledge.

| | | |
|---|---|---|
| **Dr. Atul Sharma** | **Dr. Amritanshu Shukla** | **Dr. A.K. Choubey** |
| (Supervisor) | (Co-Supervisor) | (Head of the Department, Sciences and Humanities) |

## CERTIFICATE

CERTIFIED that the work contained in the thesis titled **Technical and financial feasibility study of solar water heating system** by **Mr. Shailendra Singh** has been carried out under our supervision. It is also certified that he fulfilled the mandatory requirement of TWO quality publications that arose out of his thesis work.

It is further certified that the two publications (copies enclosed) of the aforesaid **Mr. Shailendra Singh** have been published in the Journals indexed by –

(a) SCI

(b) SCI Extended

(c) SCOPUS

(d) *Non-indexed Journals –
(only in special cases)
(*Please enclosed DPGC resolution in this regard)

| | | |
|---|---|---|
| **Dr. Atul Sharma** | **Dr. Amritanshu Shukla** | **Dr. Praveen Kumar Srivastava** |
| (Supervisor) | (Co-supervisor) | (DPGC Convenor) |

## COPYRIGHT TRANSFER CERTIFICATE

**Title of the Thesis:** Technical and financial feasibility study of solar water heating system

**Name of the Student:** Shailendra Singh

### Copyright Transfer

The undersigned hereby assigns to the Rajiv Gandhi Institute of Petroleum Technology Jais all rights under copyright that may exist in and for the above thesis submitted for the award of the DOCTOR OF PHILOSOPHY.

Date: ___________________

Place:

*SHAILENDRA SINGH*

*Roll No.-PRE18-001*

**Note:** However, the author may reproduce or authorize others to reproduce material extracted verbatim from the thesis or derivative of the thesis for the author's personal use provided that the source and the Institute's copyright notice are indicated.

**Dedicated To**

# My Parents

# ACKNOWLEDGMENT

*First and foremost, I would like to express my sincere gratitude to my thesis advisor* ***Dr. Atul Sharma*** *and my co-advisor* ***Dr. Amritanshu Shukla*** *for providing me an opportunity and believing in me to pursue research in this very interesting field. I am extremely thankful for their continuous support, and guidance throughout my Ph.D. journey. Their scholarly advice and scientific approach have helped me a lot to accomplish this work.*

*I would like to convey my sincere thanks to the Director RGIPT, Prof. A.S.K. Sinha for his kind support and for providing me a platform to undertake my doctoral research work. He has always been a true inspiration for me.*

*I would like to acknowledge and give my warmest thanks to Dr. A.K. Choubey, Head of, the Department of Sciences and Humanities for his kind support. I would also like to thank my RPEC committee members for their encouragement and for providing insightful comments and suggestions.*

*My sincere thanks also go to Prof. C.R. Chen, Kun Shan University, Taiwan, Prof. D. Buddhi, Vice-Chancellor, Uttarakhand University, Dehradun, Dr. Anil Kumar, Coordinator, Centre for Energy and Environment, Delhi Technological University, Delhi, Dr. Hitesh Panchal, Assistant Professor, Government Engineering College, Patan for their kind help and suggestion throughout my study.*

*I am extremely grateful to my parents, for their love, care, prayers, and continuing support to complete this research work.*

*I am also thankful to my senior Dr. Abhishek Anand, for their constant support that made my Ph.D. journey enjoyable and unforgettable.*

*Shailendra Singh*

# TABLE OF CONTENTS

# LIST OF FIGURES

# LIST OF TABLES

# LIST OF ABBREVIATIONS

Nomenclature

English letters

| | |
|---|---|
| $Q$ | *energy flux (W)* |
| $Q_l$ | *heat loss from the solar collector (W)* |
| $A$ | *area ($m^2$)* |
| $I$ | *total solar radiation on the surface of the collector ($W/m^2$)* |
| $T$ | *temperature (℃)* |
| $U_l$ | *heat loss coefficient ($W/m^2K$)* |
| $F_R$ | *collector heat removal factor* |
| $\dot{m}$ | *mass flow rate (kg/s)* |
| $C_{pc}$ | *specific heat of collector fluid (J/kg K)* |
| $C_{ps}$ | *specific heat of the storage tank's fluid (J/kg K)* |
| $T_{si}$ | *inlet fluid temperature of heat exchanger (℃)* |
| $F'_R$ | *exchanger heat removal factor* |
| $T_r$ | *required hot water temperature (℃)* |
| $Q_L$ | *heat load (W)* |
| $U$ | *heat loss coefficient for the storage tank ($W/m^2K$)* |
| $T'_{tk}$ | *final temperature of water in the storage tank (℃)* |
| $C$ | *total initial cost of the project* |
| $IG$ | *incentives and grants* |
| $C_{ener}$ | *annual energy savings or income* |
| $C_{capa}$ | *annual capacity savings or income* |
| $C_{RE}$ | *annual renewable energy production credit income* |
| $C_{GHG}$ | *GHG reduction income* |
| $C_{O\&M}$ | *yearly operation and maintenance costs incurred by the clean energy project* |
| $C_{fuel}$ | *annual cost of fuel or electricity* |
| $N_{PCF}$ | *year to positive cash flow* |
| $\widetilde{C_n}$ | *after-tax cash flow* |
| $N$ | *project life in years* |
| $C_n$ | *cash flow for year n* |
| $T_{sky}$ | *sky temperature (℃)* |
| $L_{sky}$ | *sky radiation* |
| $L_{clear}$ | *clear sky radiation* |
| $L_{cloudy}$ | *cloudy sky radiation* |
| $c$ | *fraction of the sky covered by clouds* |
| $K_d$ | *diffuse fraction* |
| $\bar{K}_T$ | *monthly average clearness index* |
| $\bar{H}_T$ | *monthly average radiation in the plane of the collector* |
| $\bar{H}_b$ | *monthly average beam radiation* |
| $\bar{R}_b$ | *geometrical factor* |
| $\bar{H}_d$ | *monthly average diffuse radiation* |
| $t$ | *time (min.)* |

| | |
|---|---|
| $z$ | *vertical distance (m)* |
| $T_0$ | *amplitude of the temperature fluctuation at the surface (℃)* |
| $e_{base}$ | *GHG emission factor for the base case* |
| $e_{prop}$ | *GHG emission factor for the proposed case* |
| $E_{prop}$ | *proposed case of annual electricity required* |
| $e_{cr}$ | *credit fee for GHG emission reduction* |
| $\dot{Q_w}$ | *stored heat per unit time without PCMs in the ordinary heat storage tank (W)* |
| $\dot{m}_w$ | *mass flow rate of hot water required (kg/s)* |
| $c_{p,w}$ | *specific heat of water (J/kg K)* |
| $T_h$ | *hot water temperature required for domestic application (℃)* |
| $T_c$ | *temperature of cold water (℃)* |
| $T_{max}$ | *maximum temperature of water in the storage tank without PCM (℃)* |
| $T_{mean}$ | *mean temperature of water in the storage tank without PCM (℃)* |
| $t_w$ | *time for storage of warm water in the ordinary heat storage tank without PCM* |
| $m$ | *mass (kg)* |
| $m_{PCM}$ | *mass of PCM* |
| $C_{P,PCM-L}$ | *liquid-state specific heat of PCM* |
| $C_{P,PCM-S}$ | *solid-state specific heat of PCM* |
| $H$ | *total volumetric enthalpy (J/m$^3$)* |
| $f$ | *melt fraction* |
| $h$ | *sensible volumetric enthalpy (J/m$^3$)* |
| $k$ | *thermal conductivity (W/m K)* |
| $x$ | *space coordinate (m)* |
| $y$ | *space coordinate (m)* |
| $\Delta x, dx$ | *length in x direction (m)* |
| $\Delta y, dy$ | *length in y direction (m)* |

Greek letters

| | |
|---|---|
| $\tau$ | *transmittance of the collector* |
| $\varepsilon$ | *effectiveness of the heat exchanger* |
| $\sigma$ | *stefan-boltzman constant* |
| $\eta_o$ | *optical efficiency of the collector* |
| $\beta$ | *slope of the collector* |
| $\rho_g$ | *on-ground reflectivity* |
| $\omega$ | *frequency for the $i^{th}$ month* |
| $\lambda_{prop}$ | *fraction of electricity lost for the proposed case* |
| $\lambda$ | *latent heat of fusion (kJ/kg)* |
| $\alpha$ | *thermal diffusivity (m$^3$/s)* |
| $\alpha_f$ | *thermal diffusivity of the fin (m$^2$/s)* |

Subscripts

| | |
|---|---|
| *u* | *useful* |
| *i* | *incident* |
| *c* | *solar collector* |
| *a* | *ambient* |
| *top* | *top side of solar collector* |
| *back* | *back side of solar collector* |
| *edge* | *edge side of solar collector* |
| *fi* | *inlet fluid of solar collector* |
| *s* | *storage tank's fluid* |
| *fo* | *outlet fluid of solar collector* |
| *tk* | *storage tank* |

Superscripts

| | |
|---|---|
| *o* | *old value* |
| *k* | *interaction level* |

Abbreviations

| | |
|---|---|
| *NSM* | *National solar mission* |
| *SWH* | *Solar water heater* |
| *PCM* | *Phase change material* |
| *SPP* | *Simple payback period* |
| *EPP* | *Equity payback period* |
| *IRR* | *Internal rate of return* |
| *MIRR* | *Modified internal rate of return* |
| *NPV* | *Net Present Value* |
| *GHG* | *Greenhouse gas* |
| *PVsyst* | *Photovoltaic systems* |
| *HOMER* | *Hybrid optimization model for electric renewables* |
| *SAM* | *System advisor model* |
| *RETScreen* | *Renewable energy technologies screen* |
| *EM* | *Energy model* |
| *SRHLC* | *Solar resource and heating load calculation* |
| *CA* | *Cost analysis* |
| *GHG* | *Greenhouse gas* |
| *FA* | *financial analysis* |
| *SRA* | *Sensitivity and risk analysis* |
| *CDM* | *Clean development mechanism* |
| *CERs* | *Certified emissions reductions* |
| *NASA* | *National aeronautics and space administration* |
| *TES* | *Thermal energy storage* |
| *SHPD* | *Sodium hydrogen phosphate dodecahydrate* |
| *NE* | *N-Eicosane* |
| *LA* | *Lauric acid* |
| *PW* | *Paraffin wax* |

| | |
|---|---|
| *SAT* | *Sodium acetate trihydrate* |
| *PA* | *Palmitic acid* |
| *MA* | *Myristic acid* |
| *SA* | *Stearic acid* |

# PREFACE

The solar water heating (SWH) system is one of the most commonly available and used techniques utilizing solar energy for water heating. It helps achieve the goal of sustainability and is prevalent in curbing carbon emissions for the mitigation of global warming. Though the technique is easy to use and easily available, the usage of SWH systems needs to be increased in residential, commercial, and industrial sectors quantitatively. Also, on a qualitative basis, SWH systems need to be improved due to their low thermal efficiency, bulky design, and high cost of equipment. Also, the financial and environmental benefits need to be explored to prepare future pathways for energy security and sustainability.

The first chapter of the thesis begins with a brief description of clean sources of energy and their importance for the fulfillment of energy needs of today's scenario. The chapter also includes the basics of solar energy along with its world scenario. In this chapter, the progress of solar energy programs in India has been presented. The introduction of solar active and passive systems has also been presented. After these sections, a detailed introduction to SWH systems and their classifications have been presented. In the next section of the chapter, the limitations of the SWH systems and recent advancements in it have been discussed. In the last section of the chapter, methods of improvement of the SWH system have been suggested.

In the second chapter, detailed mathematical formalism and simulation details have been presented. This chapter begins with a detailed energy balance analysis of the solar collector, heat exchanger, and water storage tank. After this, financial feasibility analysis has been discussed through various terms like simple payback period (SPP), equity payback period (EPP), and internal rate of return (IRR). The next section provides the environmental analysis of sky radiation, tilted irradiance, cold water temperature, and greenhouse gas emission reduction. The last section of this chapter explains the simulation details for the selection of the software tool and the simulation methodology of the selected software.

In the third chapter, a detailed feasibility analysis of the SWH system for domestic applications has been provided through the RETScreen clean energy management software. It is one of the most powerful tools for the simulation of SWH projects and also has been adopted by many studies around the world. In this chapter, the SWH project model has been simulated to evaluate energy production, savings, the solar fraction (SF), costs of the project, greenhouse gas (GHG) emission reductions, financial viability, and risk analysis for the proposed SWH project at different geographical locations across seven cities in India. The study shows that all sites have more than 60 % of SF and the gross GHG emission reduction for 25 years of project life is 739 $tCO_2$. The payback period obtained for seven occupants for the typical household is between 7 - 10 years except for Delhi and Indore. It can also be observed from the simulation analysis that at least 50 % of incentives must be provided by the government to make such installation feasible.

In the fourth chapter, the techno-comparative study of the SWH system for residential, commercial, and industrial applications has been performed. The three different geographical locations have been selected namely Leh, Amethi (Jais), and Ludhiana districts. The performance of SWH project models is evaluated by an SF. The average values of SF obtained are 74, 64.48, and 13 correspond to residential, commercial, and industrial models. It is also found that the cumulative value of GHG emission reduction potential for residential, commercial, and industrial sectors are 155.9 $tCO_2$, 2419.3 $tCO_2$, and 492.3 $tCO_2$ per year for 25 years of project life.

In the fifth chapter, a design mechanism of the storage tank of the SWH system for thermal improvement has been suggested by the application of encapsulated phase change materials (PCMs). The effect of encapsulated PCM is measured by the effectiveness factor of PCM through the mathematical formulation for the storage tank of the SWH system. According to the desired range of thermophysical properties and melting temperature of encapsulated PCM, here eleven PCMs have been simulated like Sodium hydrogen phosphate dodecahydrate (SHPD), OM 37, N-Eicosane (NE), Lauric acid (LA), Paraffin wax (PW), OM 48, Paraffin wax C20-33 (PW-C20-33), Sodium acetate trihydrate (SAT), Myristic acid (MA), Palmitic acid (PA), and Stearic acid (SA). Among all the considered PCMs the SHPD has been found with the highest value of effectiveness factor of 3.27. So, it is the most recommended PCM for the storage tank of the SWH system. In this chapter, the prediction of the melt fraction of PCM inside container materials has also been performed by making a coding program in the FORTRAN programming language. Here majorly used container materials are glass, stainless steel, tin, aluminum, aluminum mixed, and copper. Through the analysis, copper container material was found to have of high melting rate for all PCMs so it is the most recommended container material.

In the sixth chapter, the summary, conclusion of the present work, and recommendations for future research work have been presented.

# Chapter 1: Introduction

## 1.1 Introduction to clean sources of energy

The most abundant clean sources of energy available around the globe at no price are solar energy, wind energy, biomass energy, biofuel energy, hydro energy, and ocean energy, as shown in Figure 1.1.

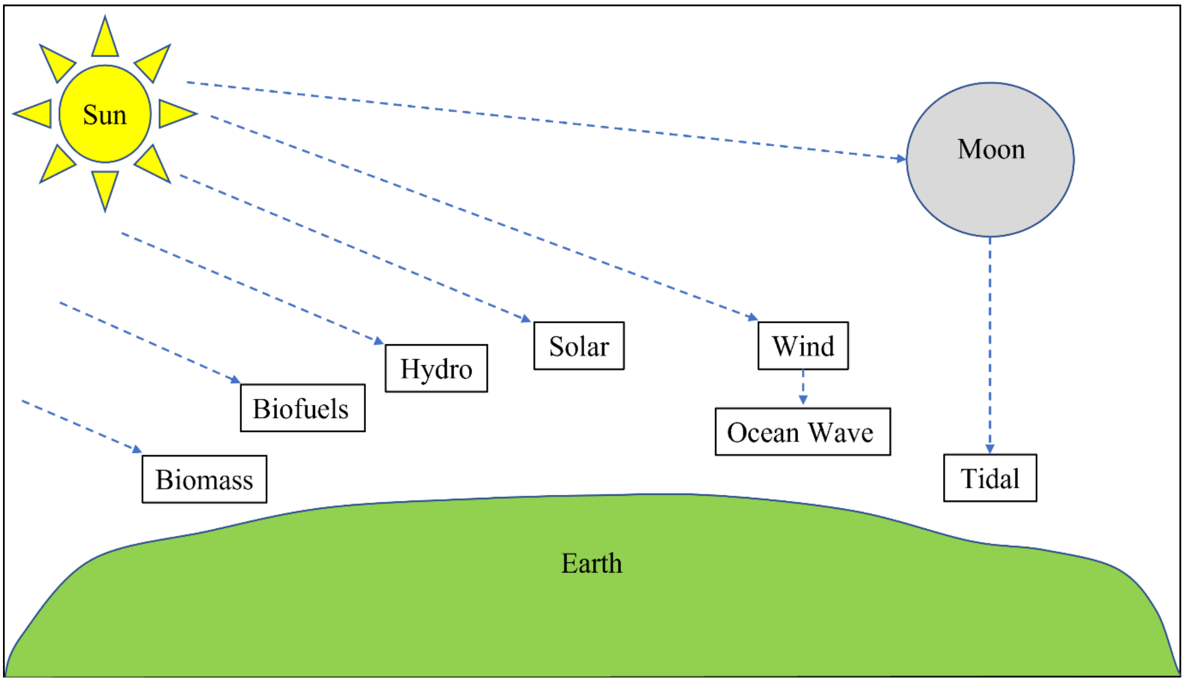


**Figure 1.1. Sources of clean energy**

These sources of clean energy are available from the evaluation of our planet. But could not be explored enough in the previous era of time due to a lack of knowledge about their importance. The journey of human civilization has grown along with the rise of energy needs. To fulfill our energy needs we have explored the fossil fuels like coal, crude oil, natural gas, etc. However, due to excessive population growth and the industrial revolution, these conventional sources of energy are depleting day by day and energy demand with crises increases extremely. So, it seems that very soon these sources of energy will be completely eradicated. It is evident that clean sources of energy are accessible for an infinite time everywhere and these are non-polluting [1]. The exploration of these sources of energy is essential for a sustainable solution and being environmentally friendly. These sources have the excessive potential for curbing environmental pollution. In recent years we have seen the consequent effects of environmental pollution [2].

The biggest adverse effect of environmental pollution comes in the form of global warming. It is expected that it is likely to cause a 1.5 °C rise in the average surface temperature of the earth between 2030 and 2052 if the current rate of emission continues [3]. The exploration of conventional sources of energy is the major reason for producing greenhouse gases (GHG) and these gases are responsible for global warming.

We should look forward to curbing GHG emissions by changing our conventional energy technology into non-conventional energy technology. Worldwide we have sufficient potential for clean sources as shown in Figure 1.2. These sources have enriched potential to fulfill energy needs around the globe.

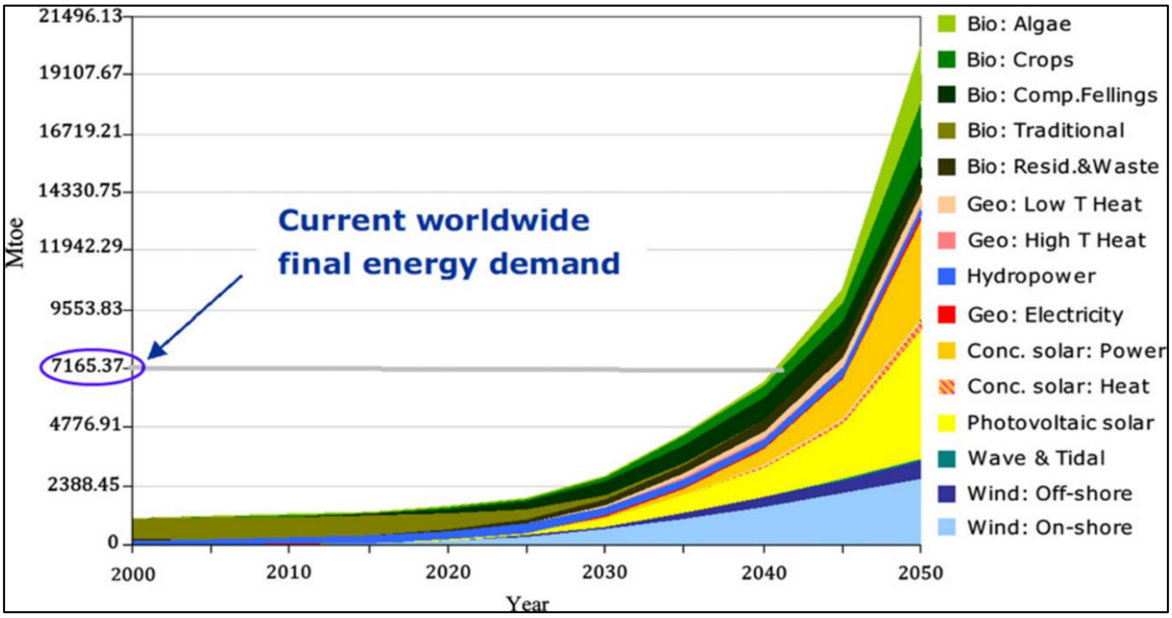


**Figure 1.2. Global potential of clean energy sources [4]**

## 1.2 Solar energy and World scenario

Solar energy is one of the most attractive forms of energy that is available in the form of light and heat in the daytime everywhere around the world. It is the cleanest form of energy that is free from all environmental pollution. It is available everywhere for useful conversion for end-users around the globe [5,6]. Unlike fossil fuels, it does not require transport from one place to another place and it does not emit any harmful by-products.

Solar energy reaches our planet in the form of solar radiation. These radiations are electromagnetic and emitted by the Sun due to nuclear fusion reactions. The range of the electromagnetic spectrum varies from gamma rays to radio waves. The effective surface temperature at which this radiation energy is emitted and coming from the Sun is 5800 K, and the core temperature can reach as high as maintained at $10^6$ K [7]. These radiations when hit by the earth's atmosphere then scattering and absorption process takes place, due to this process some part of the radiation is absorbed, some part is reflected towards the sky, and some part is radiated by the earth's crust as shown in Figure 1.3.

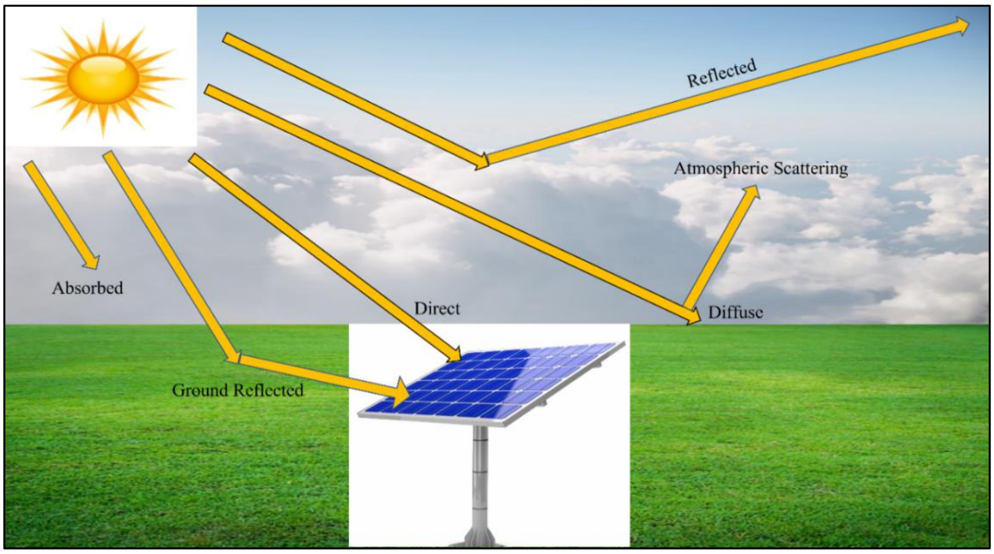


**Figure 1.3. Direct and diffuse solar radiation**

The energy of solar radiation hitting the collector is converted into a useful form to fulfill the demand by using appropriate solar technology systems. But one thing that should be acknowledged here is that the intensity of solar radiation differs from place to place on the earth's surface, it depends on the position of the sun in the sky concerning the earth's surface, the latitude of the place, the season of the place, time of the day, and length of the day. The peak of radiant energy from the Sun is at around 474 nm and about 98 % of the radiant energy lies in the wavelength range from 300 nm to 4000 nm [7]. About 31 % of incoming solar radiation is reflected by the earth's atmosphere and surface. It has been revealed by many studies that the Sun emits energy in one second is far greater than the energy consumption of the whole world's population [4,6]. It is also noted that it emits radiation at the rate of $3.8\times10^{23}$ kW and about $1.8\times10^{14}$ kW is reaching our planet [8,9].

Many countries around the world are receiving solar radiation in enriched quantities as shown in Figure 1.4.

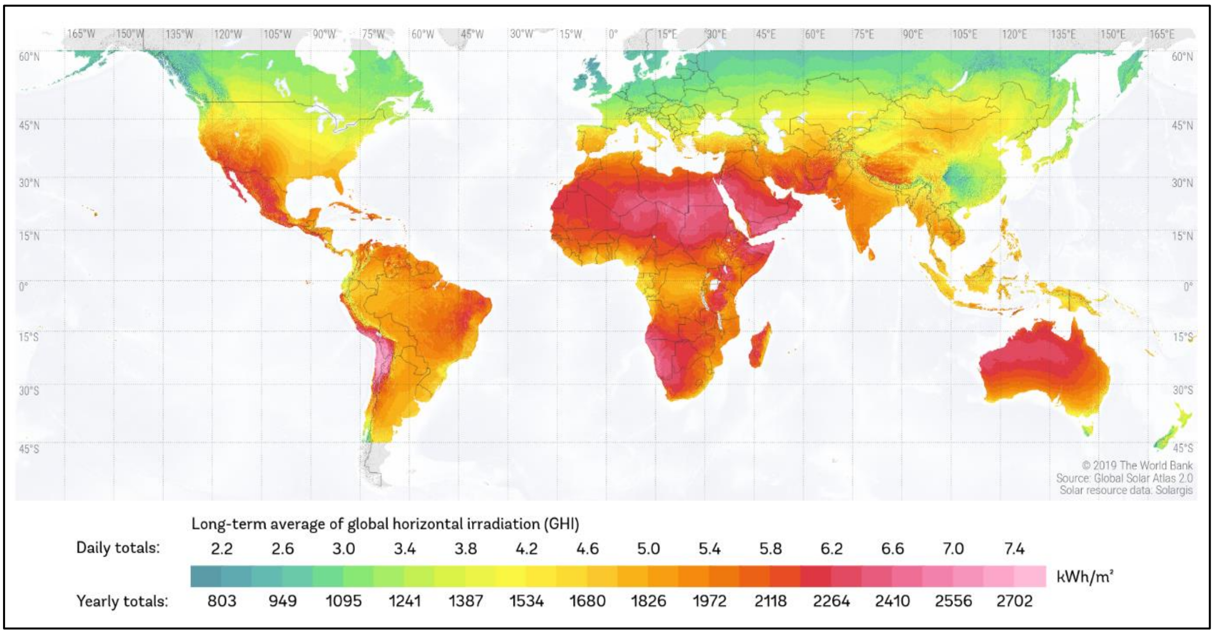


**Figure 1.4. Global solar radiation [10]**

Currently, it is a big challenge to convert the available solar energy in large for different applications, especially for developing countries this energy could not be converted into beneficial applications. Particularly it is happening in countries like India, Pakistan, Sri Lanka, Nepal, Bhutan, Maldives, Myanmar, Indonesia, Malaysia, Philippines, Thailand, etc. Many developed countries have been successful to a large extent in converting solar energy into useful thermal applications around the world. Around the globe, the solar energy potential in terms of the global solar thermal market has increased by 3 % in the year 2021. Once again China emerges as the largest global market with a growth of 1 % from a 3 % global increase. For the year 2021, China installed a solar thermal system of 18 $GW_{th}$ capacity out of 21 $GW_{th}$ global thermal capacity. The percentage share of installation in China is approximately 86 % overall. Even other countries like Italy (83 %), Brazil (28 %), the United States (19 %), Greece (18 %), Poland (17 %), India (16 %), and Mexico (7 %) have also positively raised their solar thermal markets [11]. Fortunately, India is receiving about 5000 trillion kWh of solar energy in a year, and in another way, it is receiving solar radiation of 4 -7 $kWh/m^2/d$ for 250 - 300 sunny days in a year [12]. So, India has an excellent opportunity for harnessing this solar energy into useful solar-based energy technology applications.

### 1.3 Progress of solar energy programs in India

Solar energy technologies are based on solar radiation for example solar water heaters, solar dryers, solar cookers, solar street lights, solar pumps, solar PV power plants, etc. These technological systems convert the energy of solar radiation into useful applications.

India is a growing economy and it has a wide potential for the application of these systems. India has been putting its best effort, into transferring its fossil fuel-based technology into renewable energy-based technology since the early times. A few years back in January 2010, Indian governments launched a National Solar Mission (NSM) to enhance and boost solar energy-based technology. This mission aimed to increase the use of solar energy to fulfill the country's energy needs [13]. Earlier under NSM India had set the target of achieving 20 GW of solar power now this target has been revised to 100 GW. India is enthusiastically well following the Paris agreement to reduce the emission intensity of its GDP by 33 to 35 % by the year 2030 from the year 2005. It is expected that India will achieve about 40 % of the cumulative installed capacity of electric power from non-fossil-based energy resources by the year 2030. From April 2014 to January 2021, the installed solar energy capacity increased about 15 times and India stood at 5$^{th}$ rank globally in solar power capacity. The various major ongoing schemes under NSM are as follows [14]:

a) The scheme for the development of solar parks and ultra-mega solar power projects.
b) The scheme for setting up over 300 MW of grid-connected solar PV power projects by Defence establishments under the Ministry of Defence and Para Military Forces with viability gap funding under phase-II and III.
c) The scheme of installation of grid-connected solar projects and various off-grid applications for 100 % solarization of Konark Sun Temple and Konark Town.
d) The solar power project of 20 $MW_{ac}$/50 $MW_P$ at Phyang, Leh, and 1 MW Solar-Wind hybrid plant at Nyoma under the Prime Minister Development Package.
e) The pilot-cum-demonstration project for the development of grid-connected solar PV power plants on the canal banks and canal tops.

f) The scheme for setting up 1000 MW of grid-connected solar PV power projects by Central Public Sector Units and government organizations under various central, and state schemes, self-use or third-party sales, and merchant sales with viability gap funding under phase II of Jawaharlal Nehru National Solar Mission.

g) The scheme of Central Public Sector Undertakings phase II for setting up 12000 MW grid-connected solar photovoltaic (PV) power projects by Central and State Public Sector Units, and government organizations, with viability gap funding support for self-use or use by government entities, either directly or through distribution companies.

h) The scheme for solarisation of the Sun Temple of Modhera Town in Mehsana district, Gujarat.

i) The scheme for grid-connected rooftop and small solar power plants program.

j) The scheme of grid-connected rooftop and small solar power plants program phase-I.

k) The scheme of off-grid and decentralized solar PV applications program.

l) The scheme of Pradhan Mantri Kisan Urja Suraksha Evam Utthaan Mahabhiyaan.

m) The scheme of off-grid and decentralized solar PV applications phase-III.

n) The scheme of Atal Jyoti Yojana phase-II.

o) The scheme of off-grid and decentralized concentrated solar thermal technologies for community cooking, process heat, space heating, and cooling applications in industrial, institutional, and commercial establishments.

p) The scheme of the solar off-grid program in Ladakh.

q) The scheme for green energy corridors.

## 1.4 Solar energy-active and passive systems

There are two major arrangements of solar energy systems found based on their applications. In the case of active systems, there is a need for mechanical energy in the form of pumps to transport some type of working fluid inside of the loop. While passive systems do not require mechanical energy to transport the working fluid inside the loop. These systems are driven by the natural circulation phenomenon. When the temperature of the working fluid increases then its density decreases and due to a decrease in density, the working fluid is able to transport inside of the loop of the solar system. The difference in densities of the working fluid is the main driving force for its transportation. Generally, it has been observed that small-capacity solar systems are designed for passive systems in residential applications, and medium, as well as large systems, are designed for active systems for commercial and industrial applications [15].

## 1.5 Solar water heating systems and their classifications

### 1.5.1 Historical background

The heating of water from solar radiation is not a new technique it has been happening for many years in various places around the world. People were practicing it by filling water into black-painted tanks and exposing it to solar radiation. Then this stored water in the tank gets heated through solar radiation. This prepared hot water was utilized for bathing purposes. The first patented design of the solar water heating (SWH) system was commercially manufactured in the USA under the name of "Climax Solar Water Heater" in the year 1891 as shown in Figures 1.5 (a) & (b) [16]. After this sequential number of patents were filed in the USA for the basic design mechanism of the SWH system. Further, a detailed study of integrated collector-type storage of the SWH system was done by F.A. Brooks in the year 1936 at the University of California Agricultural Experimental Station, USA [17]. In Japan, also many patents related to the primary design of the SWH system were filed in a similar duration of time [18]. In 1947, Yamamoto presented the first Japanese design of a solar energy-based water heating system. Later in the 1950s a stainless steel type of commercialized design of the SWH system, as shown in Figure 1.5 (c), had been introduced, and based on this design many units were sold in Japan [19,20].

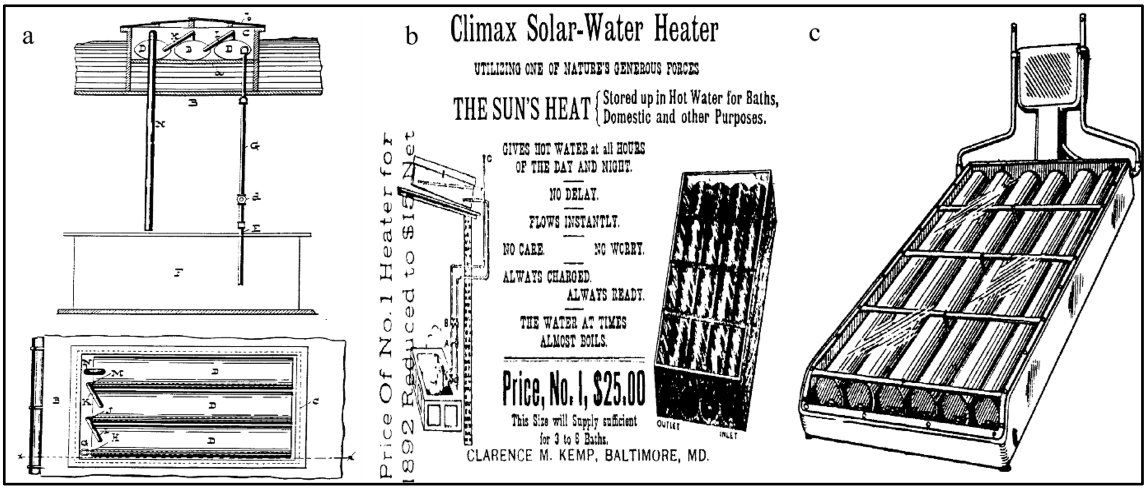


**Figure 1.5. (a)-Kemp's patent for the climax solar-water heater, (b)-Climax solar water heater, (c)-Stainless steel pipe type solar water heater [18]**

### 1.5.2 Working principle of solar water heating system

Solar energy coming in the form of solar radiation is converted into heat energy by the application of solar collectors. The transfer of heat from the sun in the form of solar radiation takes place through the radiation mode of heat transfer. When solar radiation falls on the surface of the collectors then its radiative energy is transferred into heat energy for heating incoming water from the inlet side of the collector. The collectors contain the absorber plate for capturing of radiative heat energy of solar radiation. The material of the absorber plate is generally chosen of high thermal conductivity such as copper with a suitable coating to maximize the absorption and minimize the emissions from the collector. The heat transfer into water takes place according to the conduction and convection modes of heat transfer. After getting heat energy from the collector's water becomes hot and advances towards storage tanks. The storage tanks store the hot water and this hot water is further advanced toward the utility points when needed. There are mainly two types of systems in use i.e. forced and natural circulation. In forced circulation, a pump is required and the same is not required in natural circulation. In the case of natural circulation, flow is maintained due to the density difference of circulating water in the loop. In both types of arrangements, the storage tank is located on the upper side of the circulation channel. Generally, the forced circulation system is preferred in cold climatic countries, and natural circulation in warm climatic countries.

The performance of the SWH system is evaluated by the term of a solar fraction. It describes the amount of renewable energy that displaces conventional energy for water heating. The performance is also dependent on some environmental and design factors such as the geographical location of the facility, the amount of solar radiation striking the collector, the type of collector (i.e. glazed, unglazed, or evacuated tube), the area of the collector, the efficiency of collector, solar tracking mode (i.e. fixed, one-axis, two-axis), the slope of collector, groundwater temperature and the azimuth of the collector. The layout diagram of the natural circulation SWH system has been depicted in Figure 1.6.

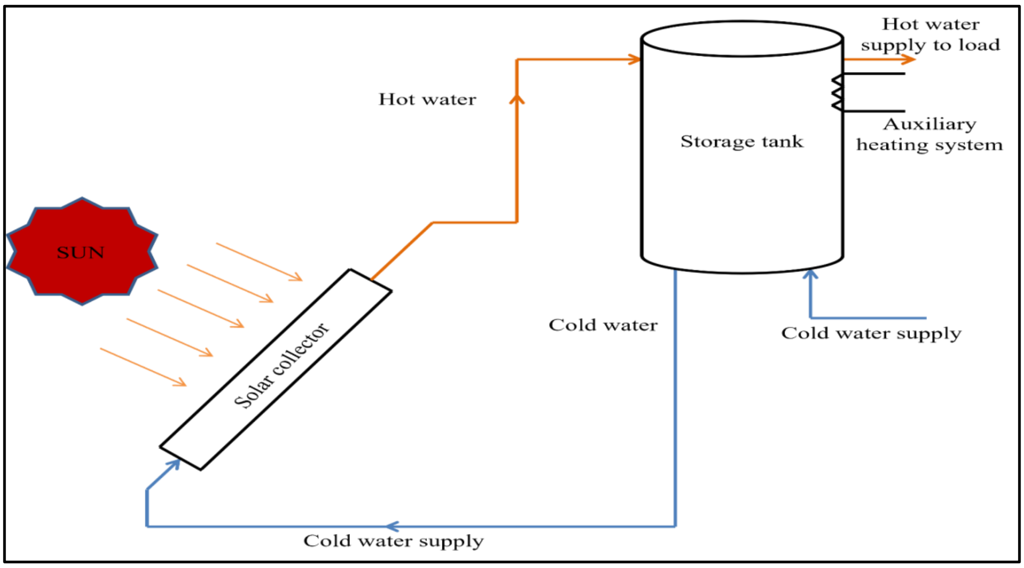


**Figure 1.6. Natural circulation SWH system**

### 1.5.3 Components of the SWH system

The major components of SWH systems are solar collectors, storage tanks, auxiliary heating systems, and balance of system as shown in Figure 1.7.

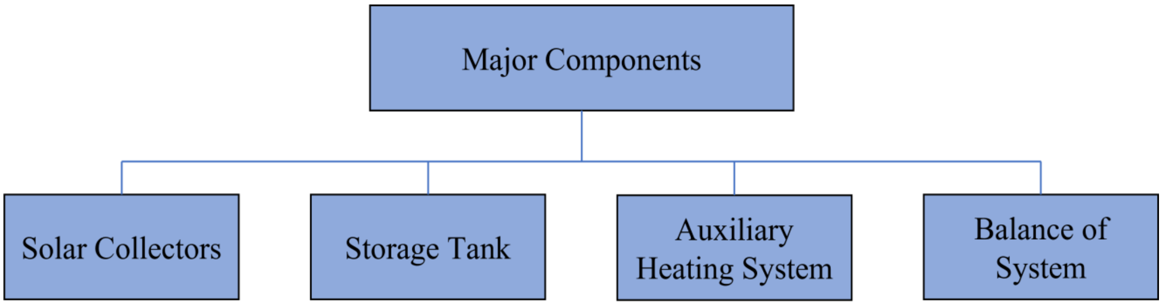


**Figure 1.7. Components of the SWH system**

- *Solar Collectors*

The main function of solar collectors is to convert the solar energy of incident solar radiations into heat energy. This heat energy is utilized for heating incoming water circulated inside the loop of the SWH system. The collectors should be efficient in energy conversion and must be durable. It is also desirable that it should be capable of withstand the variations in ambient temperature along with resistance to the leakage of any part of the system. The collectors contain the absorber plate of high thermal conductivity generally made of copper material. This absorber plate receives solar radiation and converts its solar energy into heat energy for the circulated water. The circulated water inside of tubes gets heated through the conduction and convection phenomenon of heat transfer. The whole arrangement of the absorber plate is fitted inside of the corrosive resistant casing such as aluminum along with the toughened glass cover of high transmission coefficient (i.e. approx.1). To prevent heat losses, thermal insulation must be provided for the collectors. Generally, glass wool or mineral wool is recommended as insulation materials. There are mainly three types of solar collectors that are frequently used for SWH systems namely, unglazed flat-plat liquid collectors, glazed flat-plat liquid collectors, and evacuated tube collectors, as shown in Figures 1.8 (a), (b), and (c). In unglazed and glazed flat-plate liquid collectors, the absorber plate is integrated with pipes of copper for heating circulating water inside of the transparent cover. When solar radiation falls on the absorber plate its heat is transferred to the water flowing inside the tubes. To minimize the losses and improve efficiency, the absorber plate and integrated tubes are enclosed in a transparent cover with effective insulations. In evacuated tube collectors, the absorber plate and the integrated copper tubes are fitted inside vacuum-sealed evacuated glass tubes. The evacuated tube collectors have the least heat transfer losses in comparison to unglazed and glazed flat-plate liquid collectors.

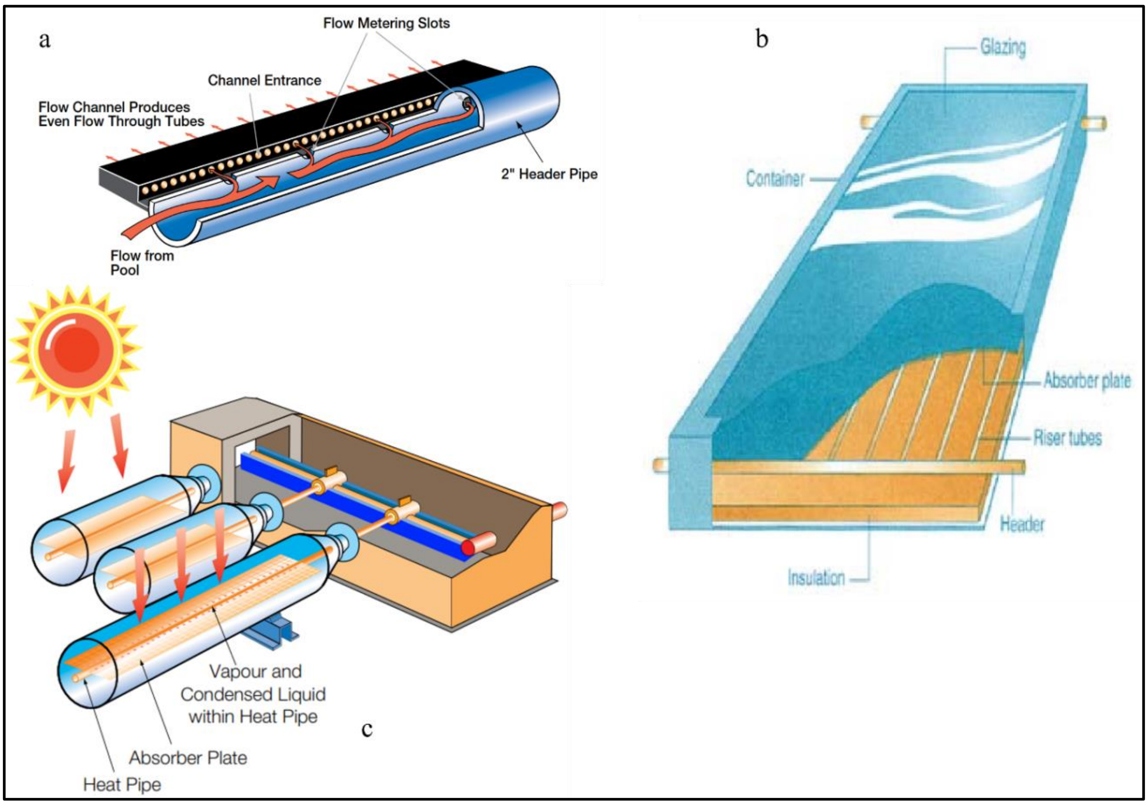


**Figure 1.8. (a) Unglazed liquid flat-plate collector, (b) glazed liquid flat-plate collector, (c) evacuated tube collector [21]**

- *Storage Tanks*

The SWH system contains a storage tank for storing hot water prepared from solar collectors. The storage of hot water in the tanks is required for domestic and commercial applications only. During off-sunshine hours, when hot water is needed by the utility points then this demand for hot water is fulfilled through the stored hot water from the storage tank. The number of storage tanks depends on the storage capacity and collector area of the SWH system. While, in the case of industrial applications, there is no need to store hot water so the storage tank is not generally required. The most common materials used for the production of storage tanks are galvanized iron, mild steel, stainless steel, and copper. More precisely the material for the storage tank should be chosen according to the water quality of the service region so that corrosive and scaling demerits must be minimized. It is also recommended that proper insulation must be provided to prevent convective heat losses to the surrounding atmosphere. Glass wool insulation is commonly used for this purpose. The line diagram of the storage tank of the natural circulation SWH system has been depicted in Figure 1.6.

- *Auxiliary Heating System*

The auxiliary heating system is the backup system of the SWH for heating water if due to rainy or cloudy seasons, the proper solar radiations are not available. The electrical heating element is generally provided in a storage tank for making auxiliary heating arrangements. In some cases, the auxiliary heating arrangement is not provided in the storage tanks rather, this is provided in the utility line or in the bypass line of the storage tank. The schematic arrangements of auxiliary heating arrangements for in tank, utility line, and bypass line around the storage tank are shown by A, B, and C points respectively in Figure 1.9.

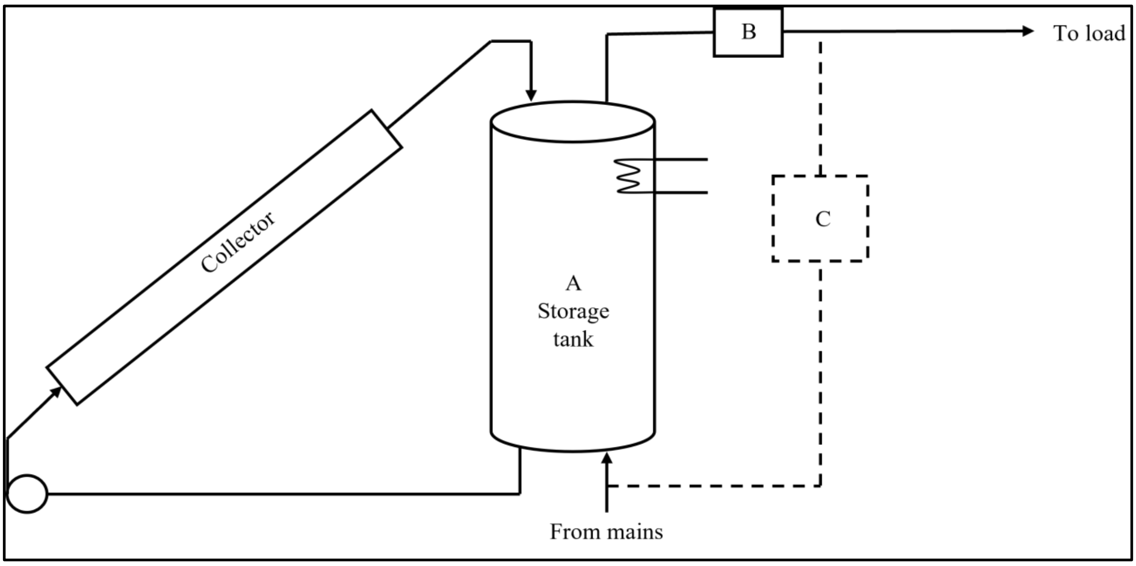


**Figure 1.9. Auxiliary heating arrangements**

- *Balance of System*

The balance of the system is the additional components used for smoothening the operations of the SWH systems. These components are the support structure of the solar collectors, liquid handling units (i.e. pumps, valves, strainers, thermal expansion tanks), controllers, freeze protection systems (i.e. heat exchanger), overheating protection systems, etc. These components are essential in the loop to regulate the smooth and safe operations of SWH systems.

### 1.5.4 Classification of the SWH system

The SWH system can be classified in many ways. The most common classification based on system configuration and its application has been presented in Figure 1.10.

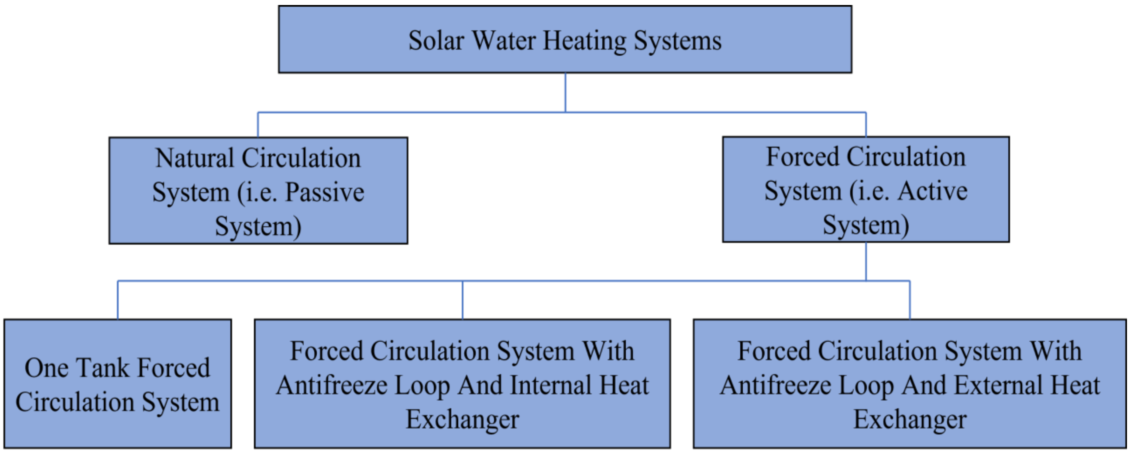


**Figure 1.10. Classification of SWH systems**

- *Natural and Forced circulation SWH system*

In the case of a natural circulation SWH system, the storage tank is situated above the collect bank and auxiliary heating is added to the above side of the storage tank for maintaining the desired outlet temperature of hot water. Here, the water circulates in the loop of the system due to the difference in the density of water. This density difference is created due to the addition of solar energy in the form of heat inside the solar collectors. This type of SWH system is accomplished by producing hot water of about 60 ℃ and it is best suited for domestic applications. This type of system is also recognized as the Thermosiphon SWH system. While, in the case of the forced circulation SWH system, these systems differ in the ways that they require mechanical energy in the form of electric pumps for the circulation of water inside the loop, a thermostat control device, and a check valve. A thermostat device is used for control of water flow inside the loop. This device operates the electric pump for on-and-off situations through the temperature difference of water in the storage tank. The check valve prevents the reverse flow of water in the loop. This type of system is capable of handling a large volume of water and it is best suited for commercial applications. The schematic arrangements of natural circulation and forced circulation systems have been presented in Figure 1.11 (a) and (b).

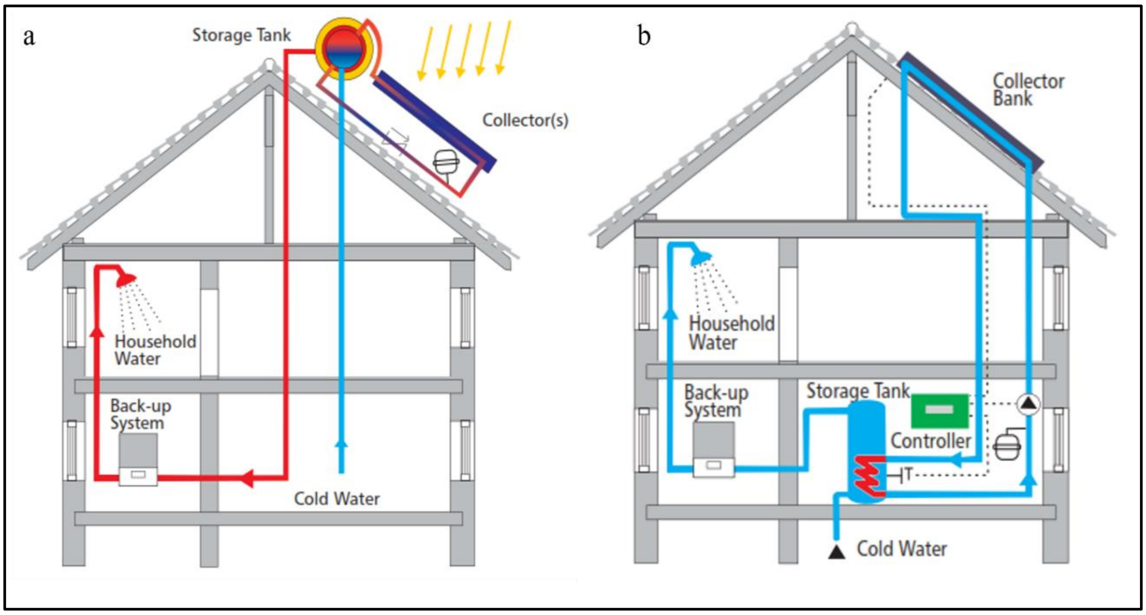


**Figure 1.11. (a) Natural circulation, and (b) Forced circulation SWH systems [22]**

- *Direct and Indirect SWH system*

The direct and indirect SWH system is categorized based on the heat exchanger utilized by the circulation loop. The direct SWH system does not require any type of heat exchanger in the circulation loop as shown in Figure 1.8 (a). The indirect SWH system contains the heat exchanger in the circulation loop as shown in Figure 1.9 (a) and (b). Generally, heat exchangers are employed in the SWH system, when it is used in cold climatic regions. Because there is a chance of freezing of water inside of circulation loop. To prevent the freezing of water it is necessary to use some type of antifreeze heat transfer fluid (i.e. ethylene glycol-water solution, and propylene glycol-water solution) to circulate inside the loop and to perform the heat transfer through the heat exchanger between water and heat transfer fluid. The storage tanks may be chosen according to the system design for a single-tank or two-tank system. The heat exchanger may be incorporated inside or outside of the storage tank as shown in Figure 1.12 (a) and (b).

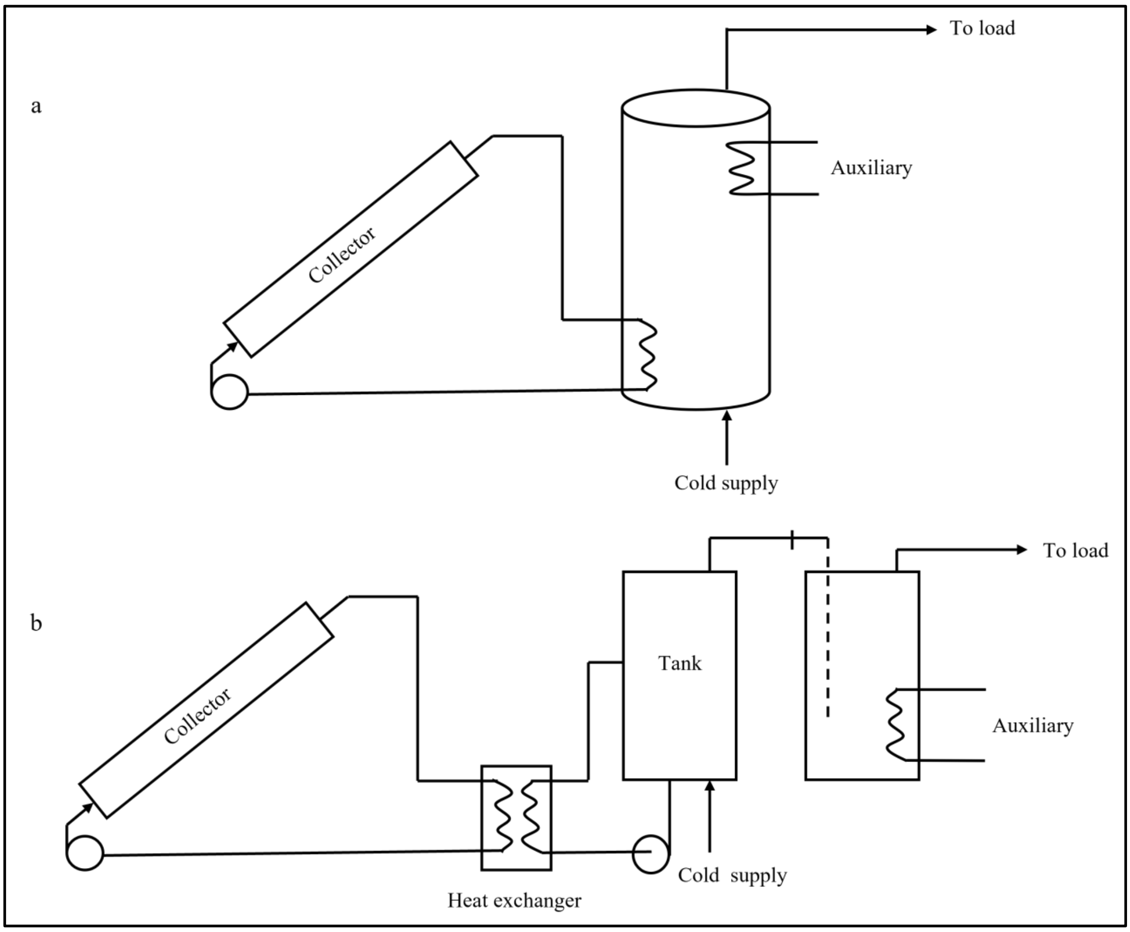


**Figure 1.12. (a) Internal heat exchanger, (b) External heat exchanger**

- *SWH system with different collectors*

The SWH system may also be categorized based on the use of solar collectors. Generally, the SWH system uses unglazed liquid flat-plate collectors, glazed liquid flat-plate collectors, and evacuated tube-type solar collectors. The unglazed and glazed liquid flat-plate collectors are recommended for low-temperature applications like swimming pool heating. While, an evacuated tube-type SWH system is recommended for high-temperature applications like domestic hot water, space heating, and process heating in the temperature range of 60 - 80 °C.

## 1.6 Limitations of the SWH system

It has been observed that many studies and research work have been carried out to improve the performance of SWH systems around the world. The results and conclusions of these studies have made significant modifications to the design of SWH systems over the last decade. Due to these modifications, the SWH system has gained much popularity in now these days. But still, SWH systems are not as popular as should be because of some limitations as listed here,

- The SWH systems have a low thermal efficiency during off-sunshine hours. Even if the storage tank is well insulated then the makeup hot water is also added by the auxiliary heating arrangement.
- During sunshine hours only sensible heat is stored in the water of the storage tank. So that water can be able to store heat up to its specific heat. The additional amount of heat generated by collector panels could not be stored for off-sunshine hours.
- The mass flow rate of water in the case of natural circulation systems cannot be altered because it is driven by the density difference of water when heated. So, these types of systems cannot be used for large-capacity applications.
- The total heat generated by the solar panels is not transported into the water circulating inside the loop due to conduction and convection heat losses.
- The total incident energy of solar radiation is not converted into the complete heat energy of water.
- There is a chance of freezing of water inside of pipe networks in cold climatic regions during off-sunshine hours even after the use of antifreeze solution along with a heat exchanger.

- The overall weight of the unit is high due to the use of metallic components such as stainless-steel storage tanks and support structures.
- The adverse quality of groundwater (i.e. hard water, saline water, acidic water, alkaline water, and water with high turbidity) makes a significant impact on the operational flow in the circulation loop of the SWH system.

### 1.7 Advancements of the SWH system

Many studies have been performed, as well as going on the path of improving the thermal efficiency of the SWH system around the globe. Such as Canbazoglu et al. [23] examined the impact of phase change material (PCM) when it is incorporated inside the storage tank of the SWH system. The authors found that the storage tank filled with PCM is capable of giving better thermal performance about 2 to 3 times more than a conventional storage tank. Regin et al. [24] calculated the effect of storage tanks filled with PCM in the spherical ball shape. The authors applied the enthalpy method for their study and found that to investigate the impact of PCM-filled storage tanks the accurate phase transforming temperature of PCMs should be known. The study of a storage tank filled with spherical balls of PCM is also carried out by Reddy et al. [25]. The authors investigated two types of PCM balls namely stearic acid PCM balls and paraffin wax PCM balls. The authors found that the PCM balls of 38 mm diameter have a significant impact in enhancing the enactment of the storage tank. Fazilati and Alemrajabi [26] also examined the performance of spherical ball-shaped PCM encapsulated inside the storage tank. The authors utilized paraffin wax as PCM balls and found that the energy storage capacity of the tank was improved by 39 % along with a 16 % increase in exergy efficiency. Huang et al. [27] examined experimentally the thermal enactment of the storage tank by application of sodium acetate trihydrate PCM balls. The authors found that the lower position of PCM balls is preferred along with the 0.42 $m^3$/h inlet flow rate of water. Bazri et al. [28] have developed an evacuated tube type of storage tank in which they applied multiple layers of PCMs to enhance thermal performance. The authors found that their PCM-embodied evacuated tube SWH system has better thermal performance in comparison to conventional storage tanks. Dadollahi and Mehrpooya [29] have investigated the charging phenomenon of high-temperature PCMs for storage tanks. The authors identified that the ratio of surface area to volume of PCMs plays an imperative role in the charging of PCMs. If this ratio is high then the charging time of PCMs in the tanks will be less. Bouhal et al. [30] have explored the new design model of the PCM embodied storage tank. The authors found that the complete melting time of PCMs inside of storage tank is 2.5 h. If the number of PCMs increases in quantity then it will lead to a decrease in the melting quantity of PCMs and an increase in heat loss takes place through the storage tank. Wang et al. [31] have studied the application of PCMs for SWH systems in the ways of structural analysis and methodological point of view. The authors found that PCMs are suitable and recommended for applications. Sadhishkumar and Balusamy [32] have studied the SWH system with PCM and without PCM for domestic applications. The authors found that by application of PCMs, the efficiency of the SWH system is increased from 36 % to 47 %. Teamah et al. [33] have presented a study of a storage tank containing PCMs in vertical bars. The authors calculated the benefits of PCMs through the performance parameter of the solar fraction. J. Zhao et al. [34] have analyzed the energy storage of solar heat storage tanks incorporated with PCMs. The authors found that about 34 % more energy is stored in PCM storage tanks in comparison to ordinary storage tanks. L. Xie et al. [35] have presented a review study on the application of PCMs in the water storage tank. The authors investigated various published kinds of literature concerning

PCM applications. The author's study suggested the practical application of PCM-based storage tanks for solar thermal systems. M. Mofijur et al. [36] have also presented a study on the application of PCMs in solar thermal systems for storing latent heat in various solar systems. The author's study suggests a future pathway of research in the field of energy storage through the PCMs for various solar thermal technologies. A. K. Pandey et al. [37] also have investigated the recent advancements of PCM applications in solar thermal systems. The author's study suggests the potential solar thermal technologies to which PCMs could be applicable. G. Murali et al. [38] have investigated experimentally the effect of paraffin wax as PCM for a storage tank of thermosyphon SWH system in real weather conditions. The authors found that by application of PCMs the stratification number, thermal efficiency, and charging efficiency of storage tank is improved significantly. E. Douvi et al. [39] have presented a review study associated with the application of PCMs for the storage of latent heat for the domestic hot water system. The authors also addressed many current technologies in which various PCMs are successfully incorporated along with the current challenges of PCMs for encapsulation inside the storage tank of the SWH system. Z. Wang et al. [40] have presented a review study depicting of application of PCMs for the SWH system. The authors study demonstrates the technical and economical aspects of PCMs application for the SWH system. The author's study focused on energy efficiency and the reduction of fossil fuel consumption through the SWH systems. S. Faisalahmed et al. [41] have presented a review study aimed to demonstrate the latest advancements in the SWH systems. The results of authors study depicts the recent technological advancements of storage tanks and solar collectors of the SWH systems.

## 1.8 Method of improvement

It is evident from the above discussion that the application of PCMs in the storage tank of the SWH system is a well-proven method for improving the thermal efficiency of the unit. The PCMs are capable of storing latent heat during the daytime when these are incorporated inside the storage tank of the SWH system. And when heat is required during off-sunshine hours, these provide heating action to the water. The PCMs are capable of exchanging heat energy with water in several thermal cycles. These are generally kept inside metallic containers in submerged conditions of the water. When the temperature of the water around these containers rises from the melting temperature of PCM, then it becomes melted inside of these containers and the latent heat is stored in it. And when the temperature of the water goes down well below from solidification temperature of PCM then the heating action of water by PCM takes place through the transfer of heat from PCM to water.

## 1.9 Objectives of present research work

The objectives of the present research work are given as:

- To exhibit the viability and benefits of the SWH system for the domestic sector based on a simple payback period (SPP), equity payback period (EPP), internal rate of return (IRR), and modified internal rate of return (MIRR).
- To investigate the comparative viability and benefits of the SWH system for domestic, commercial, and industrial sectors.
- To demonstrate the environmental benefits in terms of greenhouse gas emission reduction potential.
- To identify the suitable PCMs for application in the storage tank of the SWH system.

- To investigate the suitable container material for encapsulation of PCM inside of container material in the storage tank of the SWH system.

### 1.10 Motivation of the presented research work

It has been observed from the literature review that India has a great potential for solar radiation throughout the year. At the same time, we are facing energy crises in several parts of the country. To curb the energy crises we have to adopt solar energy-based technologies like SWH systems for the heating of water. It is not a good deal to heat the water from fossil-based technology like electric geysers. So this type of simulation study is very important for our country because it exhibits the benefits of the SWH systems in different geographical regions in different sectors of the country. This study of the SWH system is very rare for the different geographical regions of India for the different sectors like residential, commercial, and industrial. Through the study, financial parameters can be investigated in detail. With the help of these parameters, a decision to adopt SWH technology for the heating of water can take place in the residential, commercial, and industrial sectors of India. Apart from the financial parameters, the study also explains the environmental benefits of using SWH technology in the form of mitigation of harmful GHG emissions. In addition to these aspects, presenting the probable solution for the low thermal performance of the SWH systems in the form of PCMs was the main driving force to present this research work.

# Chapter 2: Mathematical formalism and Simulation details

This chapter presents details of the mathematical analysis and simulation technique used for this research work. The mathematical analysis includes formulations for the solar collector, storage tank, and heat exchanger. The chapter also describes the financial and environmental formulations of the SWH system. The discussed simulation technique is specifically devoted to the presented research work. These are covered in the following subsections,

## 2.1 Energy balance analysis

### 2.1.1 Solar collector

The overall energy balance of the solar collector is presented in Figure 2.1 as,

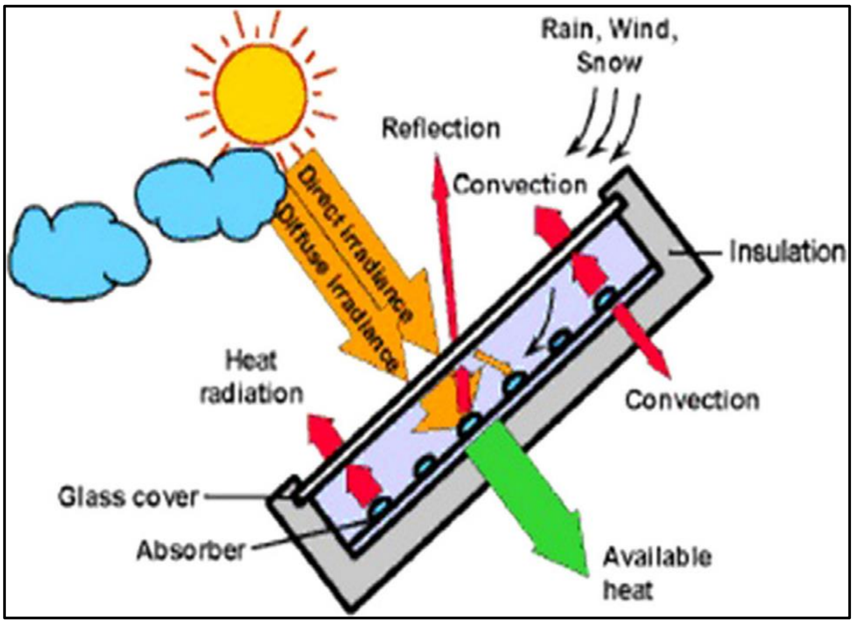


**Figure 2.1. Energy balance of solar collector [15]**

The overall useful energy balance of the solar collector at a steady state is expressed as [15,42],

$$Q_u = Q_i - Q_l \tag{2.1}$$

here, $Q_u$ is the useful energy flux in W, $Q_i$ is the incident energy flux in W, and $Q_l$ is the heat loss from the solar collector in W.

The incident solar energy absorbed by the collector is estimated as,

$$Q_i = A_c I \tau \alpha \tag{2.2}$$

here, $A_c$ is the area of the solar collector in m$^2$, $I$ is the total solar radiation on the surface of the collector in W/m$^2$, $\tau$ is the transmittance of the collector, and $\alpha$ is the absorptivity of the collector.

The heat loss from the solar collector to the atmosphere is estimated as,

$$Q_l = Q_{l,top} + Q_{l,back} + Q_{l,edge} \tag{2.3}$$

$$Q_l = A_c U_{l,top}(T_c - T_a) + A_c U_{l,back}(T_c - T_a) + A_c U_{l,edge}(T_c - T_a) \tag{2.4}$$

It is assumed that heat loss from the solar collector takes place from the top, back, and edges of the collector as shown in equation (2.3). In equation (2.4), $T_c$ is the collector temperature (i.e. mean temperature of the plate) in °C; $T_a$ is the ambient temperature in °C; $U_{l,top}$ is the heat loss coefficient of the top side of the collector in W/m$^2$ K, it is the function of the number and properties of the glass cover and ambient temperature; $U_{l,back}$ is the heat loss coefficient at the backside of the collector in W/m$^2$ K, it is the function of the thickness and thermal conductivity of the insulation; $U_{l,edge}$ is the heat loss coefficient from the edges of the collector in W/m$^2$ K.

Thus, the useful energy delivered by the collector can be rearranged in the form as,

$$Q_u = A_c[I\tau\alpha - U_l(T_c - T_a)] \tag{2.5}$$

It is difficult to measure the correct mean temperature of the collector plate $T_c$. So, equation (2.5) is modified in terms of collector inlet fluid temperature $T_{fi}$ through the application of collector heat removal factor $F_R$ as,

$$Q_u = A_c F_R \left[ I\tau\alpha - U_l \left( T_{fi} - T_a \right) \right] \tag{2.6}$$

The above equation (2.6) is also known as the Hottel-Whillier-Blis equation. The collector heat removal factor $F_R$ is defined as the ratio of heat delivered to the working fluid to the heat in the condition that the unified temperature of the collector plate equals the inlet fluid temperature. Since the useful energy delivered can also be expressed as,

$$Q_u = C_P \dot{m} \left( T_{fo} - T_{fi} \right) \tag{2.7}$$

here, $C_P$ is the specific heat of the working fluid of the solar collector, $\dot{m}$ is the mass flow rate of the working fluid, $T_{fo}$ is the collector outlet fluid temperature. From equations (2.6) and (2.7), the value of $F_R$ can be calculated as,

$$F_R = \frac{C_P \dot{m} \, (T_{fo} - T_{fi})}{A_c [I\tau\alpha - U_l (T_{fi} - T_a)]} \tag{2.8}$$

The solar collector efficiency can be expressed as the ratio of useful energy delivered by the collector to the incident solar radiation on the surface of the solar collector during a specified time. It is expressed by the equation (2.9) as,

$$\eta = \frac{\int Q_u dt}{A_c \int I dt} \tag{2.9}$$

The solar collector can be characterized using several design parameters so that the equation (2.9) can be simplified as,

$$\eta = \frac{Q_u}{A_c I} = \frac{I\tau\alpha - U_l (T_c - T_a)}{I}$$

$$\eta = \tau\alpha - U_l \frac{T_c - T_a}{I}$$

$$\eta = F_R\tau\alpha - F_R U_l \frac{T_{fi} - T_a}{I} \quad (2.10)$$

The variation of the solar collector efficiency with the operating temperature may be linear or nonlinear, it depends on the characteristics of the collector. These can be presented as,

For a linear relationship

$$\eta = \eta_o - U_l \frac{T_c - T_a}{I} \quad (2.11)$$

For a nonlinear relationship

$$\eta = \eta_o - U_{l1} \frac{T_c - T_a}{I} - U_{l2} \frac{(T_c - T_a)^2}{I} \quad (2.12)$$

here, $\eta_o$ is the optical efficiency of the collector, $U_{l1}$ and $U_{l2}$ are time-dependent heat loss coefficients. It has been found that the efficiency of the solar collector decreases with the rise in temperature of the collector plate and the decrease in ambient temperature along with a decrease in solar radiation. The variations of the efficiency with the combined factor of $\frac{T_c - T_a}{I}$ for solar collectors including unglazed panels, glazed black absorbers, glazed selective absorbers and evacuated tubes are presented in Figure 2.2. The evacuated tubes are found to have stable efficiency in the range of 55–70%, while the efficiency of the unglazed panels drops considerably from 90% to 0% at low $\frac{T_c - T_a}{I}$ [15].

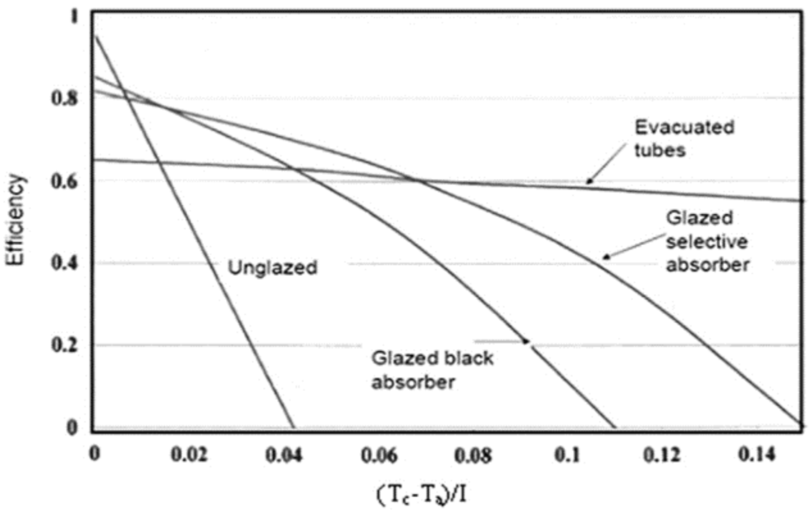


**Figure 2.2 Variations of the efficiency with the combined factor of $(T_c - T_a)/I$ for the solar collectors [15]**

### 2.1.2 Heat exchanger

When a heat exchanger is used to prevent the freezing of water in the circular loop between the solar collector and storage tank, as shown in Figure 2.3, then it reduces the performance of the solar system. The performance of the solar system is affected by the term of effectiveness of the heat exchanger ($\varepsilon$). The effectiveness of a heat exchanger is the ratio of the actual heat exchange rate to the maximum possible heat exchange rate. The reduced useful energy due to the employment of a heat exchanger in the circular loop is estimated as [15,42],

$$Q_u = \varepsilon(C_p\dot{m})_{min}(T_{fo} - T_{si}) \tag{2.13}$$

here, $(C_p\dot{m})_{min}$ is the minimum of $C_{pc}\dot{m}_c$ and $C_{ps}\dot{m}_s$. Here, $C_{pc}\dot{m}_c$ is the product of specific heat and mass flow rate of collector fluid. The $C_{ps}\dot{m}_s$ is the product of specific heat and mass flow rate of the storage tank fluid (i.e. water). $T_{fo}$ is the collector outlet fluid temperature and $T_{si}$ is the heat exchanger inlet fluid temperature.

From equations (2.6) and (2.7) of collector analysis, the useful energy and collector outlet fluid temperature could be established as,

$$Q_u = A_c F_R \left[ I\tau\alpha - U_l \left( T_{fo} - \frac{Q_u}{C_{pc}\dot{m}_c} - T_a \right) \right] \tag{2.14}$$

here, $T_a$ is the ambient temperature in °C. From equations (2.13) and (2.14), the useful energy delivered to the storage tank could be expressed by using an exchanger heat removal factor ($F'_R$) as,

$$Q_u = A_c F'_R [I\tau\alpha - U_l(T_{si} - T_a)] \tag{2.15}$$

$$F'_R = \frac{F_R}{\frac{A_c F_R U_l}{C_{pc}\dot{m}_c}\left(\frac{C_{pc}\dot{m}_c}{\varepsilon(C_p\dot{m})_{min}} - 1\right) + 1} \tag{2.16}$$

This indicates the reduction in heat output due to the employment of a heat exchanger. In other words, the ratio $F_R/F'_R$ represents the required increase in area with a heat exchanger for achieving the same energy output as in the case without a heat exchanger.

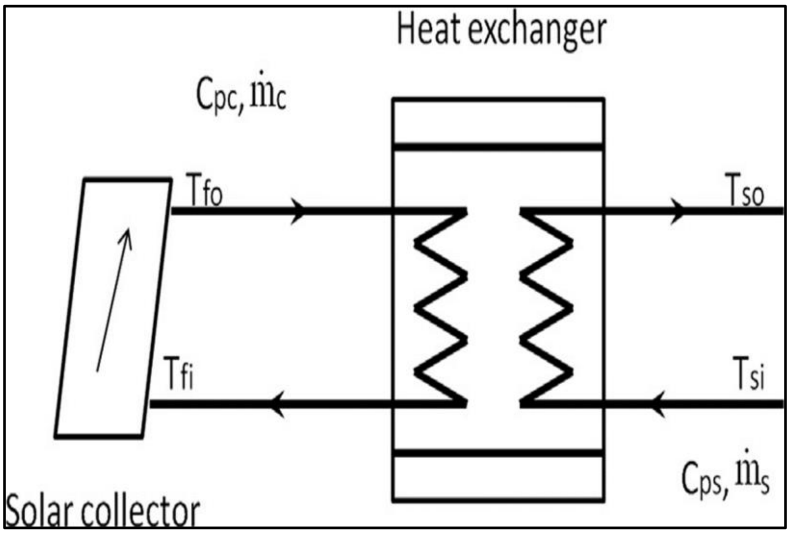


**Figure 2.3 Energy balance of heat exchanger [15]**

### 2.1.3 Water storage tank

The rate of change in internal energy of the storage tank filled with water for fully mixed with a unified temperature is expressed as [15,42],

$$C_{P,tk}\frac{dT_{tk}}{dt} = Q_u - Q_L - Q_{l,tk} \tag{2.17}$$

here, $Q_L$ is the heat load that is estimated as,

$$Q_L = C_P \dot{m}_w (T_r - T_w) \tag{2.18}$$

here, $C_P$ is the specific heat of the water in J/kg K, $\dot{m}_w$ is the mass flow rate of water in kg/s, $T_r$ is the required hot water temperature in °C, $T_w$ is the cold-water temperature in °C.

The $Q_{l,tk}$ is the loss of heat from the storage tank and it is estimated as,

$$Q_{l,tk} = UA_{tk}(T_{tk} - T_a) \tag{2.19}$$

In the above equation (2.19), $U$ is the heat loss coefficient for the storage tank in W/m$^2$ K, $A_{tk}$ is the area of the storage tank in m$^2$, $T_{tk}$ is the temperature of the hot water of the storage tank in °C, $T_a$ is the ambient temperature in °C.

If the water in the storage tank is not fully mixed (i.e. stratified as in the case of a passive system) then the storage tank can be divided into several layers and the energy balance equations can be established for each layer. As a result, the water temperature of the storage tank can be estimated by integrating equation (2.17) as,

$$T'_{tk} = T_{tk} + \frac{dt}{C_{P,tk} m_{tk}}\left(Q_u - Q_L - Q_{l,tk}\right) \tag{2.20}$$

From the above equation (2.20), the final temperature of water in the storage tank $T'_{tk}$ can be calculated for an initial value of water temperature $T_{tk}$ for the specified time difference of $dt$.

## 2.2 Financial feasibility analysis

### 2.2.1 Simple payback period

The simple payback period (SPP) is the number of years it takes for the cash flow (excluding debt payments) to equal the total investment (which is equal to the sum of the debt and equity) it is calculated as [21],

$$SPP = \frac{C-IG}{(C_{ener}+C_{capa}+C_{RE}+C_{GHG})-(C_{O\&M}+C_{fuel})} \quad (2.21)$$

here, C is the total initial cost of the project, IG is the incentives and grants, $C_{ener}$ is the annual energy savings or income, $C_{capa}$ is annual capacity savings or income, $C_{RE}$ is an annual renewable energy production credit income, $C_{GHG}$ is the GHG reduction income, $C_{O\&M}$ is a yearly operation and maintenance costs incurred by the clean energy project, and $C_{fuel}$ is an annual cost of fuel or electricity.

### 2.2.2 Equity payback period

The equity payback period (EPP) is also termed as a year to positive cash flow $N_{PCF}$, it is the first year that the cumulative cash flows for the project are positive. It is calculated by solving the following equation for $N_{PCF}$ as [21],

$$0 = \sum_{n=0}^{N_{PCF}} \widetilde{C_n} \quad (2.22)$$

here $\widetilde{C_n}$ is the after-tax cash flow in year n.

### 2.2.3 Internal rate of return

The internal rate of return (IRR) is the discount rate that causes the Net Present Value (NPV) of the project to be zero. It is calculated by solving the following equation for the IRR as [21],

$$0 = \sum_{n=0}^{N} \frac{C_n}{(1+IRR)^n} \tag{2.23}$$

here, $N$ is the project life in years, and $C_n$ is the cash flow for year n ( i.e. $C_0$ is the equity of the project minus incentives and grants, this is the cash flow for year zero). The pre-tax IRR is calculated using pre-tax cash flows, while the after-tax IRR is calculated using the after-tax cash flows.

## 2.3 Environmental analysis

### 2.3.1 Sky Temperature

It is required to quantify radiative transfer exchanges between a solar collector and the sky. The sky long-wave radiation is radiation originating from the sky at wavelengths greater than 3 μm. An alternative variable intimately related to sky radiation is the sky temperature, $T_{sky}$, which is the temperature of an ideal blackbody emitting the same amount of radiation. Its value in °C is computed from sky radiation $L_{sky}$ through as [21],

$$L_{sky} = \sigma(T_{sky} + 273.2)^4 \tag{2.24}$$

here, σ is the Stefan-Boltzman constant ($5.669\times10^{-8}$ (w/m$^2$)/K$^4$). The radiation of the sky varies according to the presence and absence of clouds. In the absence of clouds, the radiation of a clear sky is expressed by the Swinbanks equation as,

$$L_{clear} = 5.31 \times 10^{-13}(T_a + 273.2)^6 \tag{2.25}$$

here, $T_a$ is the ambient temperature in °C. For the cloudy sky, it is assumed that clouds are at a temperature of $(T_a - 5)$ and with an emittance of 0.96. This term $(T_a - 5)$ of difference in ambient temperature is considered to take care of the loss of radiation due to the presence of clouds. Moreover, it is a corrective term for the estimation of the loss of radiation in the presence of clouds. Under cloudy conditions, the flux of radiation received by the earth's surface is significantly modified. Because the liquid water and ice absorb and emit longwave radiation more efficiently than water in the vapor phase of the clouds. So, the sky radiation in the cloudy condition is expressed as [21],

$$L_{cloudy} = 0.96\sigma(T_a + 273.2 - 5)^4 \tag{2.26}$$

The actual sky radiation falls between the clear and cloudy values of radiation as,

$$L_{sky} = (1 - c)L_{clear} + cL_{cloudy} \tag{2.27}$$

here, c is the fraction of the sky covered by clouds. It is estimated as,

$$c = \frac{(K_d - 0.165)}{0.835} \tag{2.28}$$

here, $K_d$ is the diffuse fraction and it is calculated from the monthly average clearness index $(\overline{K}_T)$ using the Collares-Pereira and Rabl correlation as,

$$K_d = \begin{cases} 0.99 \ \ for\ K_r \le 0.17 \\ 1.188 - 2.272K_r + 9.473K_T^2 - 21.865K_T^3 + 14.648K_T^4 \ \ for\ 0.17 < K_r < 0.75 \\ -0.54K_T + 0.632 \ \ for\ 0.75 \le K_T < 0.80 \\ 0.2 \ \ for\ K_T \ge 0.80 \end{cases} \tag{2.29}$$

### 2.3.2 Tilted irradiance

The monthly average radiation in the plane of the collector ($\overline{H}_T$) is computed by using Liu and Jordan's isotropic diffuse algorithm for the SWH project model as [21],

$$\overline{H}_T = \overline{H}_b \overline{R}_b + \overline{H}_d \left(\frac{1+Cos\ \beta}{2}\right) + \overline{H}\rho_g \left(\frac{1-Cos\ \beta}{2}\right) \tag{2.30}$$

$$\overline{H}_T = \overline{H}_b \overline{R}_b + 0.5\ \overline{H}_d (1 + Cos\ \beta) + 0.5\ \overline{H}\rho_g (1 - Cos\ \beta) \tag{2.31}$$

The first term of the right-hand side of equation (2.31) represents solar radiation coming directly from the sun and depends only on collector orientation, site latitude, and time of year. It is a product of monthly average beam radiation ($\overline{H}_b$) and geometrical factor ($\overline{R}_b$). The second term represents the contribution of monthly average diffuse radiation, ($\overline{H}_d$) which depends on the slope of the collector β. The third term represents the reflection of radiation on the ground in front of the collector and depends on the slope of the collector and on-ground reflectivity $\rho_g$. The monthly average daily diffuse radiation ($\overline{H}_d$) is calculated from global radiation through the following equations.

When $W_s$ (sunset hour angle) < 81.4°

$$\frac{\overline{H}_d}{\overline{H}} = 1.391 - 3.560\ \overline{K}_T + 4.189\ \overline{K}_T^2 - 2.137\ K_T^3 \tag{2.32}$$

When $W_s$ (sunset hour angle) > 81.4°

$$\frac{\overline{H}_d}{\overline{H}} = 1.311 - 3.022\ \overline{K}_T + 3.427\ \overline{K}_T^2 - 1.821\ K_T^3 \tag{2.33}$$

The monthly average daily beam radiation ($\overline{H}_b$) is computed as,

$$\overline{H}_b = \overline{H} - \overline{H}_d \tag{2.34}$$

### 2.3.3 Cold water temperature

The temperature of cold water supplied by the ground piping system of the municipal corporation is used to calculate the energy needed to heat the cold water to the desired temperature. The diffused heat on the ground obeys the following equation of heat as [21],

$$\frac{\partial T}{\partial t} = \alpha \frac{\partial^2 T}{\partial z^2} \tag{2.35}$$

here, $T$ is the soil temperature, $t$ is the time, $\alpha$ is the thermal diffusivity of the soil, and $z$ is the vertical distance. For semi-infinite soil with a periodic fluctuation at the surface is expressed as,

$$T(0,t) = T_0 e^{i\omega t} \tag{2.36}$$

here, $T_0$ is the amplitude of the temperature fluctuation at the surface and $\omega$ is its frequency for the month $i$. The solution to the equation (2.36) is provided as,

$$T(z,t) = T_0 e^{-(1+i)z/\sigma} e^{i\omega t} \tag{2.37}$$

here, $\sigma$ is the spatial scale defined by as,

$$\sigma = \sqrt{\frac{2\alpha}{\omega}} \tag{2.38}$$

In other words, a seasonal fluctuation of amplitude $\Delta T$ at the surface will be felt at a depth $z$ with an amplitude $\Delta T(z) = \Delta T e^{-Z/\sigma}$ and with a delay of $\Delta t = z/\sigma\omega$. In the simulation model, the cold-water temperature is considered the same as the soil temperature at an appropriate depth. The model considered $\alpha = 0.52 \times 10\text{-}6\ m^2/s$ and z = 2 m, the assumed depth at which water pipes are buried. This leads to,

$$\sigma = 2.28 \text{ m} \tag{2.39}$$

$$\Delta T(z) = \Delta T(0) \times 0.42 \tag{2.40}$$

$$\Delta t = 51 \text{ days} \approx 2 \text{ months} \tag{2.41}$$

This theoretical model was compared with the experimental data of Toronto, Ontario, Canada [21]. And it is found that a factor of 0.35 would be better than 0.42 in the equation (2.40) and a time lag of *1* month gives a better fit than a time lag of *2* months. The presented model of water temperature calculation is capable for estimation of water temperature of any month i.e. the water temperature for month *i* is equal to the yearly average water temperature plus 0.35 times the difference between ambient and average temperature for month *i-1* (in addition the model also limits water temperature to *+1* in winter, so water does not freeze). The modification is necessary and methodologically acceptable given the coarseness of the assumptions made in the model.

### 2.3.4 Greenhouse gas emission reduction

The annual value of GHG emission reduction is estimated as [21],

$$\Delta_{GHG} = (e_{base} - e_{prop})E_{prop}(1 - \lambda_{prop})(1 - e_{cr}) \tag{2.42}$$

here, $e_{base}$ is the GHG emission factor for the base case, $e_{prop}$ is the GHG emission factor for the proposed case, $E_{prop}$ is the proposed case of annual electricity required, $\lambda_{prop}$ is the fraction of electricity lost for the proposed case, and $e_{cr}$ is the credit fee for GHG emission reduction.

## 2.4 Simulation details

### 2.4.1 Selection of software tool

Various simulation software tools like Photovoltaic Systems (PVsyst), Hybrid Optimization Model for electric renewables (HOMER), System Advisor Model (SAM), Renewable Energy Technologies Screen (RETScreen), PV*SOL Premium, Solar Pro, PV F-Chart, Solar Gis PV Planner, Helioscope, and Solarius PV have been studied for the simulation of SWH system. These software tools are frequently used by engineers and researchers for performance and viability analysis. Their comparative advantages and disadvantages are presented in Table 2.1.

**Table 2.1 Comparative advantages and disadvantages of the available software tools**

| Software tools | Advantages | Disadvantages |
| --- | --- | --- |
| PVsyst (Availability=Priced; 30-day trial version is free.) | Capable for indication of the weakness of proposed projects through the loss diagram. | The program screen is short. Shadow analysis is not good. The single-line diagram is not generating. |
| HOMER (Availability=Priced; 21-day trial version is free.) | Predict the performance of the project for different technologies. | The input data is required in detail. |
| SAM (Availability=free.) | User-friendly; Modules and inverters can be easily customizable. | Shading three-dimensional is not possible. |
| RETScreen (Availability=Priced; viewer mode is free.) | High accuracy in feasibility analysis, NASA database, high volume of the product database, sensitivity analysis, and | Projects cannot be saved in viewer mode. The shading analysis is not possible. |

| | | |
|---|---|---|
| | risk analysis. | |
| PV*SOL Premium (Availability=Priced; 30-day trial version is free.) | The high volume of the metrological database of 8000 climatic locations around the globe. | Sensitivity analysis is not produced. |
| Solar Pro (Availability=Priced; 30-day trial version is free.) | Three-dimensional shading is available. | Doing feasibility analysis is not easy as compared to other simulation software. |
| PV F-Chart (Availability=trial version is free.) | Provides detailed numerical and graphical output reports. | Advanced calculations are not supported. The shading analysis is not suitable. |
| Solar Gis PV Planner (Availability=Priced; 30-day trial version is free.) | A user-friendly web-based tool. Provides detailed outputs in the form of tables and graphs. | The tool is not suitable for financial analysis. |
| Helioscope (Availability=Priced; 30-day trial version is free.) | A user-friendly web-based tool. Provides detailed line diagrams. | Not suitable for financial and feasibility analysis. |
| Solarius PV (Availability=Priced; 30-day trial version is free.) | The tool has photographic simulation features. Numerical and graphical results can be easily exported. | Less user-friendly and feasibility analysis is not supported. |

It is observed from existing research work that RETScreen clean energy management software has the highest compatibility with the presented research work. The performance results of the comparative feasibility analysis of the various listed software tools also lead to choosing the RETScreen software to carry out the simulation work of the SWH system.

### 2.4.2 Simulation methodology

The simulated work of the SWH system of the presented study has been done through the RETScreen Expert Clean Energy Management Software. It is developed by the Ministry of Natural Resources Canada. It is the most widely applicable tool for evaluating the feasibility or pre-feasibility analysis of SWH projects around the world. It has the capability of analyzing the SWH system virtually and calculating its associated risk. This software tool is popular for evaluating the viability of SWH projects around the world among renewable energy professionals.

The simulation of the SWH project model contains six worksheets namely energy model (EM), solar resource and heating load calculation (SRHLC), cost analysis (CA), greenhouse gas emission reduction analysis (GHG analysis), financial analysis (FA), and sensitivity & risk analysis (SRA), as shown in Figure 2.4.

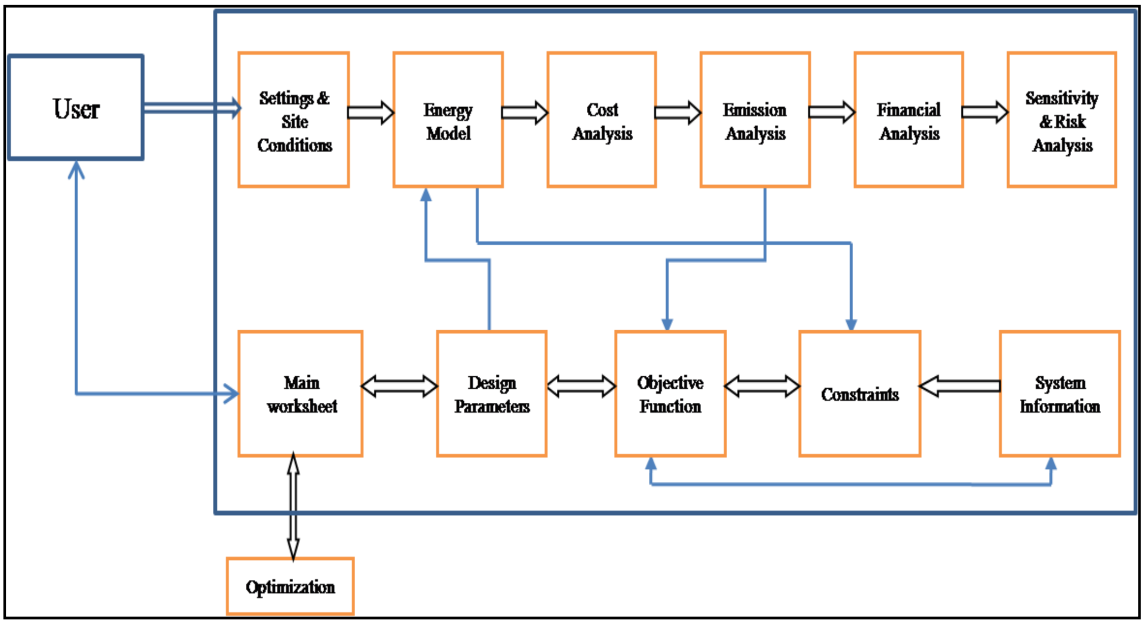


**Figure 2.4 Flow chart of the simulation model**

All these six worksheets are available in the SWH project workbook file. These worksheets are used step by step for the simulation of SWH projects as shown in Figure 2.4. The simulation starts with the selection of the location of the project and the type of facility required at that place. After this, the energy worksheet comes and it has input parameters like fuels & schedules, equipment, end-use, optimized supply, and summary. These input parameters must be completed according to the requirements of the SWH project. The monthly energy load required to heat the water to the desired temperature is calculated by the SRHLC worksheet. This worksheet also calculates the annual solar radiation on the tilted collector array for any orientation, using monthly values of solar radiation on a horizontal surface. The cost analysis includes initial costs (credits), annual costs (credits), and annual savings based on some input parameters of the simulation model like the type of unit, the number of collectors, storage capacity or solar collector area, heat exchanger, pump power, etc. The gross annual GHG emission reduction potential in terms of $tCO_2$ is analyzed by the worksheet of GHG analysis. This worksheet also calculates the equivalent of $tCO_2$ in terms of cars & light trucks not used, liters of gasoline not consumed, and barrels of crude oil not consumed, etc. The financial analysis worksheet mainly calculates the financial viability of the project in terms of pre-tax IRR-assets, SPP, and EPP at the rate of input parameters like inflation rate, project life, and debt ratio. The sensitivity and risk analysis worksheet evaluates the risk associated with the project based on any constraint of equity payback, pre-tax IRR-equity, and pre-tax IRR- assets with a range of sensitivity.

The optimization of the simulation model is also necessary for making the project feasible. It can be achieved if design parameters, objective functions, and constraints of the system are considered properly. The energy model must consider constraints and design parameters of the system based on the feedback of the alteration in the energy model. This feedback is used and kept until suitable financial viability in terms of payback periods or emission analysis is achieved. The process steps are repeated continuously till the optimization of the simulation model is achieved.

# Chapter 3: Feasibility study of the SWH system for domestic applications

Energy consumption reflects the socio-economic growth of any country in the present time. The energy derived from fossil fuels generates a large number of GHGs, which are the major cause of global warming [43]. The adverse effect of global warming is observed in almost every part of the globe. It is expected that global warming is likely to cause a 1.5 °C rise in the average surface temperature between 2030 and 2052 if the current rate of emissions continues [44]. Tackling the adverse impact of climate change is the biggest challenge to the concern of society worldwide. A possible solution is to exploit renewable-based technologies and replace them with fossil ones. Such technologies must be implemented through government policies and incentives around the world.

This chapter presents a detailed study of the feasibility analysis of the SWH system for application in the domestic sector. In this chapter, the environmental, technical, and financial viability of evacuated tube-type SWH systems at different geographical locations across seven cities in India have been analyzed in the subsequent sections.

## 3.1. Introduction

Among all renewable energy sources, solar energy is widely available in abundant and present in almost every part of the world. India being a tropical country is blessed with an abundant amount of solar energy. A good amount of solar radiation is available all across the country throughout the year. India receives about 5000 trillion kWh of solar radiation annually amounting to 4 - 7 kWh/m$^2$ daily average which is a good sign for implementing solar-based technology in a country like India. The record shows that solar energy has been utilized since the 18$^{th}$ century for heating water.

Since then, solar-based heating technology has grown to an advanced level, and a more sophisticated SWH system has been commercialized in the market. It should be noted that the SWH system can be operated in any climatic zone. It requires only solar radiation for heating water. It can heat water to 80 °C by the use of suitable collectors varying across different climatic zones. India has great potential for SWH systems. Under a realistic scenario, the demand for the SWH system according to facility type is presented in Table 3.1.

**Table 3.1: Potential of the SWH system in cumulative million $m^2$ [45]**

| **Facility Type** | **2010** | **2013** | **2017** | **2022** |
|---|---|---|---|---|
| Residential | 2.58 | 4.25 | 7.68 | 15.74 |
| Commercial/Institutional | | | | |
| • Hotels | 0.19 | 0.35 | 0.61 | 0.97 |
| • Hospitals | 0.10 | 0.17 | 0.27 | 0.43 |
| • Others | 0.18 | 0.27 | 0.39 | 0.52 |
| Industry | 0.19 | 0.33 | 0.57 | 1.05 |
| **Total** | **3.24** | **5.37** | **9.52** | **18.70** |

It is evident from Table 3.1 that the residential sector is the largest sector contributing 84 % of the cumulative installations by the year 2022. The percentage share of the different sectors is shown in Figure 3.1.

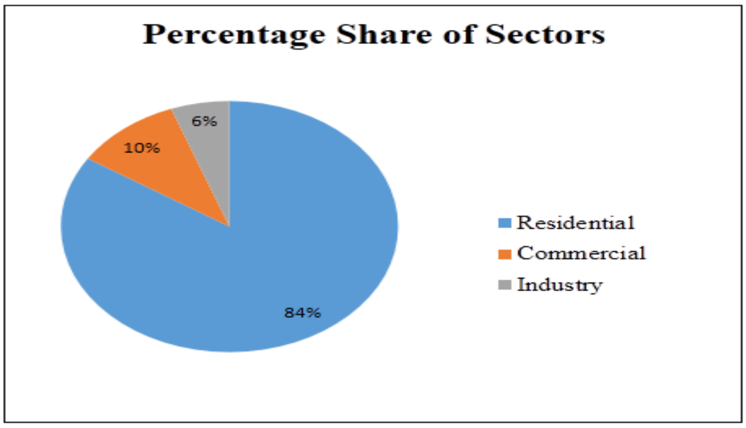


**Figure 3.1. Expected share of sectors in solar water heating installation (Yr. 2022)**

It can be also observed from Table 3.1 that for the years 2010, 2013, and 2017 the residential sector is the largest among all for the potential installation of SWH systems. It indicates that greater emphasis must be given to the residential sector for the installation of SWH systems. The gross potential for the SWH system has been estimated by the Ministry of New and Renewable Energy department to be 140 million $m^2$ of collector area [45]. Of this 40 million $m^2$ has been estimated as the realizable techno-economic potential at this stage. A total of 3.53 million $m^2$ of collector area has so far been installed in the country for SWH, of which about 1.55 million $m^2$ has been installed since 2005 - 06. A target of 5 million $m^2$ has been set for the 11th Plan (2007 - 12) and a goal of 20 million $m^2$ for 2020. Recently, the National Solar Mission has been announced, and as per the mission, the deployment of the SWH system has been divided into three phases. The target of 7 million $m^2$ has been set for phase I i.e. FY. 2010-13, 15 million $m^2$ for phase II i.e. FY. 2013-17, and 20 million $m^2$ for phase III covering the period FY. 2017-22 [46,47]. The Price and demand for electricity in India are increasing gradually as more developing activities are taking place. It is also important that grid-connected electrical energy must be maximized by production industries to improve economic growth. The use of electric geysers to heat water for domestic purposes is not reasonable at all, knowing that lots of electrical energy is consumed. It is evident that a 100 L capacity SWH system can replace an electric geyser of 2 kW capacities, for residential use and may save up to 1500 units of electricity annually depending upon the location of the SWH. While in some parts of the country where the hot water requirement is for 9 months or more, the SWH system may save about 1400 - 1500 units of electricity. The use of 1000 SWHs of 100 liters capacity each can contribute to a peak load shaving of approximately 1 MW while one SWHS of 100 liters capacity can prevent the emission of up to 1.5 tons of $CO_2$ per year [47]. The SWH system has great potential for the reduction of greenhouse emissions in large amounts. It must be undertaken by the Clean Development Mechanism (CDM). The annual Certified Emissions Reductions (CERs) potential of solar water heaters in India could theoretically reach 27 million tonnes. Houri [48] investigated the current status and future prospects of the SWH system in Lebanon. The author found that the most advanced evacuated tube technology has a payback period of fewer than 9 years at the current market price with the help of RETScreen analysis. Purohit and Michaelowa [49] have done a detailed study of CDM potential by using the SWH system in India. The authors study indicates that there is a vast theoretical potential for $CO_2$ mitigation through the use of the SWH system in India. Gastli and Charabi [50] have investigated the potential of SWH in Oman by considering a case study of the Seeb district through the RETScreen. The result showed 335,431 MWh of energy saving was achieved which was equivalent to power produced annually by a 38.3 MW generator. The payback period obtained was between 7 to 10 years. Stevanović and Pucar [51] have done a financial analysis of Serbia for the possibility of SWH systems through RETScreen. The authors' study suggested that the payback period would be high if no subsidy was provided by the government. The payback period would be between 7.6 to 8.3 years if a 25 % subsidy was offered by the government. The same would be between 5.5 to 6 years at a 50 % subsidy by the government. The lifetime emission reduction would be 31 - 34 $tCO_2$. Rehman and Sulaiman [52] have evaluated the optimum selection criteria for domestic SWH in Saudi Arabia based on the techno-economic aspects of the evacuated tube and glazed solar collectors. Yasin [53] has analyzed technical and financial assessments of glazed and evacuated tube solar collectors for domestic water heating applications in Palestine. Both types of collectors were found suitable for the Palestinian climate. It was also concluded that effective $CO_2$ mitigation would be achieved if 65 % of the Palestine family used the SWH system. M. Bentaher et al.

[54] have developed an SWH system model for the Middle East and North African regions. The authors simulated their model through the environmental data of these regions for flat plate and evacuated tube-type collectors. The authors found that for all selected regions the value of the solar fraction is 60 % and 83 % for flat plate and evacuated tube-type collectors respectively. M. Hazami et al. [55] have investigated the domestic model of the SWH system through the TRNSYS simulation model. The authors evaluated various parameters of viability like thermal energy savings, SPP, life cycle savings, GHG emission reduction, etc. The authors found that the application of the SWH system in the domestic sector of Tunisia will be feasible and beneficial. M. Sadiq [56] has analyzed the cost benefits of using SWH systems in Islamabad Pakistan. The author depicts that if SWH systems were used then it would replace electric power and natural gas at the cost of 430.95 Euros and 67.81 Euros of energy cost per annum per household. J. Kaldellis et al. [57] have suggested decreasing of import of fossil fuel by techno-economical and cost-benefit analysis for hot water production from the domestic SWH system in Greece. The author's study conclusion indicates the successful feasibility and viability of SWH systems along with scenarios of the current potential of the solar collectors market in Greece. T. Cruz et al. [58] have performed a technical and economical feasibility study of the domestic SWH system in Brazil through the RETscreen simulation tool. The authors found that economic feasibility is greatly dependent upon certain parameters like equipment cost, family size, and alternative energy cost for hot water requirements in Brazil. The authors also found that the south region of the country is the best site and the southeast region is the best economical site for SWH systems. P. Veerabonia and G. Yesuratnam [59] have presented a study on the opportunities and challenges in the application of SWH systems in the country of India. The authors demonstrated the

potential areas for the application of the SWH systems in the residential, commercial, and industrial sectors in the country. M. Raisulislam et al. [60] have also presented an economic analysis study of applications of the SWH systems. The results of the economic analysis indicate the advantages of applications of the SWH systems.

India with a population of 1.4 billion having an average household size of between 5 - 7 people is highly dependent on electricity for water heating. The water heating requirement varies across regions. Hot water is generally required between 4 - 9 months which varies across regions. The electricity production typically 80 % in the region is highly fossils based. The dependency on electricity for hot water requirements creates high pressure on the power grids. There were 888.34, 922.18, 960.90, 928.14, and 910.02 million tonnes of $CO_2$ emissions during the successive financial years of 2016 – 17, 2017 – 18, 2018 – 19, 2019 – 20, and 2020 - 21 from the power sector [61]. Being located in the tropical region there is a tremendous potential to shift from fossils to renewable-based technologies. The region provides an attractive option for solar power firms across the world for large-scale investment. Many large and small-scale manufacturers are coming and have shown interest in solar projects. Despite that, there are many constraints viz. social, economic, geographical, political, financial, and technological to the adoption of SWH technology and providing interference for its proper growth. The solar resource varies across regions, where the potential is very high in some regions with some relatively low. The Indian household is skeptical about SWH technology because of a lack of awareness and benefits associated with it. People are hesitant to adopt these technologies because of the unreliability and uncertainty related to payback. The SWH system is costly and can only be afforded by the affluent. It is practically out of reach of the common masses without government incentives. The government is willing to encourage such micro-scale installation because such projects have large GHG emission reduction potential. On one hand, it reduces the dependence on grid electricity, and on the other, it would be beneficial for achieving emission reduction targets. The study related to the environmental benefits of such installation, the $CO_2$ mitigation potential, energy-saving, and techno-economic feasibility is not available in the public domain. In a time when electricity prices are highly subsidized, and also due to the lack of such type of comprehensive study, the government seems a little reluctant to provide a financial incentive to such micro-scale projects. This chapter provides insight into the benefits of using the domestic SWH system at various sites in India. The chapter reveals the various environmental, technical, and economic aspects of using the SWH system for Indian climatic conditions.

## 3.2. Selection of locations

To demonstrate the benefits of the SWH system in different sites, seven cities have been selected from different geopolitical zones of India. The climate data locations of all selected cities are shown in Table 3.2.

**Table 3.2: Selected cities for simulation modeling (Source: NASA database)**

| City | Latitude (°N) | Longitude (°E) | Elevation (m) |
|---|---|---|---|
| Shimla | 31.11 | 77.16 | 1770 |
| Delhi | 28.58 | 77.2 | 216 |
| Hyderabad | 17.45 | 78.47 | 545 |
| Guwahati | 26.1 | 91.58 | 54 |
| Pune | 18.53 | 73.85 | 559 |
| Indore | 22.72 | 75.8 | 567 |
| Bangalore | 12.97 | 77.58 | 921 |

### 3.2.1. Shimla

The city of Shimla is located at 31.11 °N and 77.16 °E. It is a cold climatic city and receives a good amount of solar radiation approx. 5.28 kWh/$m^2$/day. Hot water is required at least 9 months a year. Out of the total number of days around 20 - 25 days remain foggy/cloudy/rainy when some kind of backup is needed. Shimla has good potential for SWH systems as almost 83.2 % of the households are under permanent construction.

### 3.2.2. Delhi

The city of Delhi located is at 28.58 °N and 77.2 °E and falls under a composite climate. It receives a good amount of solar radiation about 5.25 kWh/$m^2$/day. In Delhi, almost 91.7 % of the households are in permanent construction of apartment buildings, which is favorable for installing SWH systems. Hot water is required for 4 - 5 months a year. Being the capital of the country, the residential sector has grown at a very fast pace in the city and the requirement for hot water is continuously increasing. Other than bathing, hot water is also required for utensil scrubbing, washing machines, hand washing, etc.

### 3.2.3. Hyderabad

The city of Hyderabad is located at 17.45 °N and 78.47 °E. It falls under a composite climate and receives solar radiation of about 5.0 kWh/$m^2$/day. Hyderabad has developed into a major hub of the IT industry in India. In the city, about 86 % of the households are of permanent construction which is suitable for installing SWH systems. The hot water requirement in the city is 9 months or above in a year.

### 3.2.4. Guwahati

The city of Guwahati is located at 26.1 °N and 91.58 °E. The climate of city falls under a warm-humid climate and receives a plenty amount of solar radiation about 4.69 kWh/$m^2$/day. In the city, almost 33 % of the households are of permanent construction. The average demand for hot water for residential purposes is 9 months a year.

### 3.2.5. Pune

The city of Pune is located at 18.53 °N and 73.85 °E. It falls under a warm-humid climate and receives solar radiation of about 5.52 kWh/m$^2$/day. In the city, almost 61 % of the urban households are permanent construction which is suitable for SWH systems in the city. The average demand for hot water for residential purposes is about 8 months a year.

### 3.2.6. Indore

The city of Indore is located at 22.72 °N and 75.8 °E. The city falls under a composite climate and receives solar radiation of about 5.17 kWh/m$^2$/day. In the city, about 66.6 % of the households are of permanent construction and have a good precursor for the installation of SWH systems in the city. The average demand for hot water in the residential sector is 5 - 6 months a year.

### 3.2.7. Bangalore

The city of Bangalore is located at 12.97 °N and 77.58 °E. The city falls under a temperate climate and receives a good amount of solar radiation about 5.32 kWh/m$^2$/day. In the city, almost 89.7 % of the households are in permanent construction which is a good sign for installing SWH systems. Hot water is required throughout the year.

## 3.3. Metrological data of selected locations

In this section, the metrological data like air temperature, wind speed, solar radiation, etc, of all seven cities are taken from the National Aeronautics and Space

Administration (NASA) database for the modeling of the SWH system. The metrological data of all seven cities are provided in Table 3.3.

**Table 3.3: Metrological data of all selected cities (Source: NASA database)**

| Metrological Parameters | Annual Values | | | | | | |
|---|---|---|---|---|---|---|---|
| | **Shimla** | **Delhi** | **Hyderabad** | **Guwahati** | **Pune** | **Indore** | **Bangalore** |
| Air temperature (°C) | 15.4 | 25.1 | 26.7 | 24.2 | 24.7 | 25.0 | 24.1 |
| Relative humidity (%) | 49.9 | 61.1 | 60.8 | 80.0 | 64.4 | 52.3 | 68.6 |
| Daily solar radiation-horizontal ($kWh/m^2/d$) | 5.28 | 5.25 | 5.00 | 4.69 | 5.52 | 5.17 | 5.32 |
| Daily solar radiation-tilted ($kWh/m^2/d$) at latitude | 5.90 | 5.74 | 5.18 | 5.17 | 5.77 | 5.53 | 5.43 |
| Atmospheric pressure (kPa) | 82.4 | 98.2 | 94.4 | 98.1 | 94.3 | 95.7 | 92.6 |
| Wind speed at 10 m (m/s) | 2.4 | 2.4 | 2.8 | 0.9 | 1.8 | 3.9 | 1.9 |
| Earth temperature at 0 m (°C) | 14.6 | 25.9 | 26.8 | 23.2 | 24.6 | 26.6 | 25.1 |
| Heating-degree days (at18°C) | 1486 | 220 | 0 | 37 | 0 | 0 | 0 |
| Cooling- degree days (at 10°C) | 2238 | 5524 | 6078 | 5191 | 5369 | 5468 | 5149 |
| Supply water temperature - minimum (°C) | 12 | 21.3 | 24.9 | 21.5 | 23.1 | 22.6 | 23.1 |
| Supply water temperature- maximum (°C) | 18.3 | 28 | 28.9 | 25.8 | 26.5 | 27.6 | 25.5 |

Among all the meteorological parameters, the daily solar radiation on the horizontal surface and tilted at the latitude surface are the most essential parameters for the energy generated at the collectors. The monthly variation of the daily solar radiation on the horizontal surface of all seven cities is provided in Figure 3.2. The modeling worksheet also provides the facility to calculate the monthly variations of solar radiation at the tilted surface. It has been calculated from the worksheet that the annual solar energy produced at the tilt angle of the latitude of each geographical location, has the maximum value which is very evident from Figure 3.3. This is very essential as the tilted angle at latitude orientation will transfer the maximum amount of solar radiation to the water.

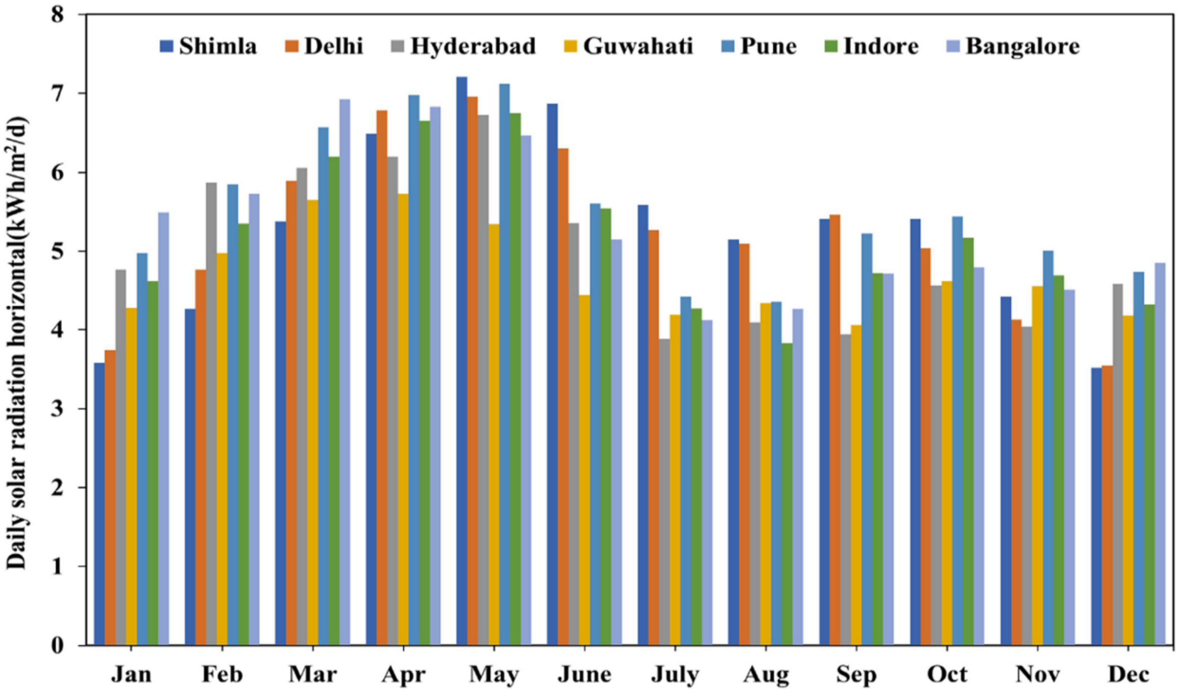


**Figure 3.2. Daily solar radiation of all selected cities (Source: NASA)**

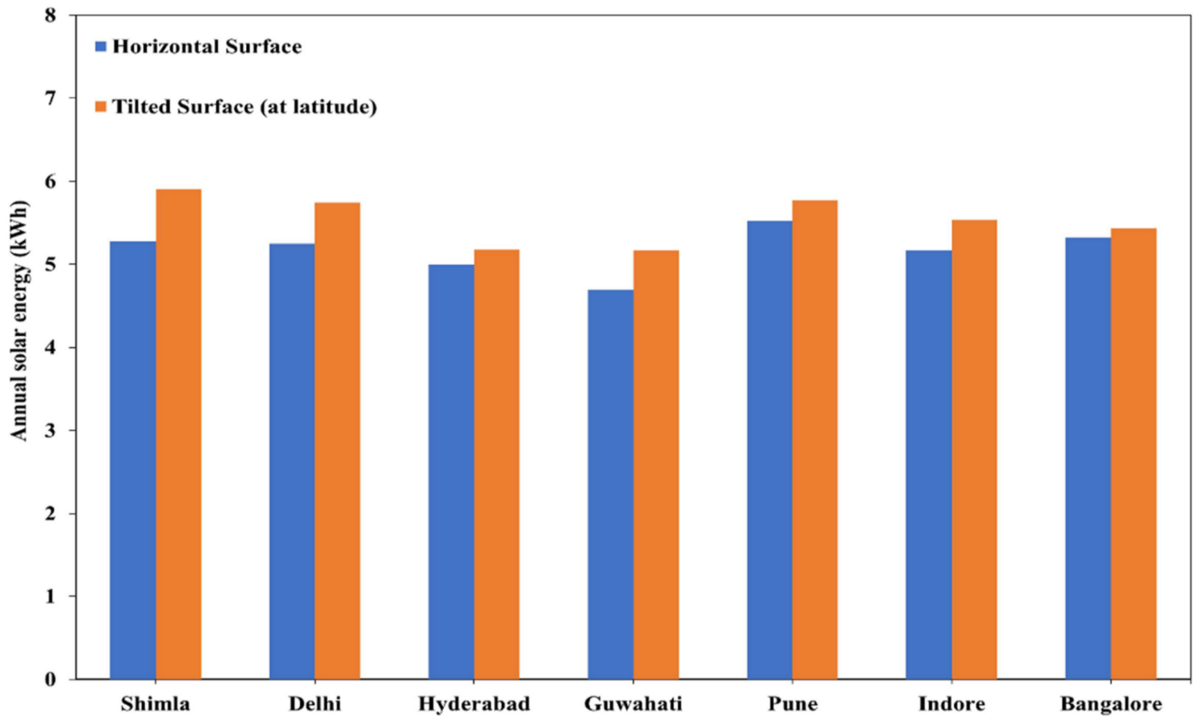


**Figure 3.3. Annual average solar radiation at the selected cities**

### 3.4. Simulation parameters

In this section, technical and economic parameters for the simulation model have been presented. These input parameters are used to find the optimum locations for installing the SWH system with the minimum associated cost of the project. The model provides flexibility to identify sites of the project with an associated cost. This type of analysis is very important to find the project viability at a different geographical location anywhere around the globe. The technical term indicates the technical specifications of the components like type (glazed, unglazed, and evacuated), manufacturer, and model of the SWH system. The economic term indicates financial indices like SSP, EPP, IRR-equity, and MIRR-equity. The input parameters for the basic scenario model (1) are presented in Table 3.4.

**Table 3.4: Energy model input parameters for the basic scenario model (1)**

| Input Parameters | Values |
|---|---|
| The average number of people per house | 7 |
| Occupancy rate (%) | 100 |
| Daily hot water usage estimate(L/day) | 420 |
| Hot water temperature(°C) | 60 |
| Solar tracking mode | Fixed |
| Slope | Latitude |
| Azimuth | 0 |
| Operating days per week | 7 |
| Solar water heater type | Evacuated |
| Miscellaneous losses (%) | 3 |
| Conventional fuel type | Electricity |
| Seasonal efficiency (%) | 90 |
| Electricity rate annual (USD/kWh) | 0.11 |
| Fuel cost escalation rate (%) | 5 |
| Discount rate (%) | 8 |
| Reinvestment rate (%) | 9 |
| Inflation rate (%) | 4 |
| Project life (years) | 25 |
| Debt ratio (% of the initial cost) | 0 |
| Initial grant (% of the initial cost) | 0 |
| Annual O&M cost (USD) | 0 |
| GHG emission factor for coal ($tCO_2$/MWh) | 1.26 |

The present study considered the number of people per house as seven in the different selected cities for the simulation of the domestic SWH system in India. Initially, no grant for purchasing domestic SWH is considered and further, the effect of the grant is studied in terms of SPP. The technical specifications of the selected SWH system for simulation purposes are presented in Table 3.5.

**Table 3.5: Technical specifications of the evacuated tube-type SWH system for all cities**

| | |
|---|---|
| Manufacturer | Thermomax |
| Model | MS 20 - TMO 500 |
| Gross area per solar collector ($m^2$) | 2.779 |
| Aperture area per solar collector ($m^2$) | 2.135 |
| Fr (tau alpha) coefficient | 0.578 |
| Fr UL coefficient ($W/m^2$)/°C | 1.05 |
| Temperature coefficient for Fr UL | 0 |

### 3.5. Result and discussion

The simulation output parameters of the basic scenario model (1) of all selected cities are summarized and presented in Table 3.6.

**Table 3.6: Simulation model output parameters of all selected cities**

| **Output Parameters** | **Values** | | | | | | |
|---|---|---|---|---|---|---|---|
| | **Shimla** | **Delhi** | **Hyderabad** | **Guwahati** | **Pune** | **Indore** | **Bangalore** |
| Number of collectors | 3 | 2 | 2 | 2 | 2 | 2 | 2 |
| Solar collector area ($m^2$) | 8.3 | 5.6 | 5.6 | 5.6 | 5.6 | 5.6 | 5.6 |
| Capacity (kW) | 4.5 | 3 | 3 | 3 | 3 | 3 | 3 |
| Storage capacity/solar collector area ($L/m^2$) | 23 | 23 | 23 | 23 | 23 | 23 | 23 |
| Storage capacity (L) | 150 | 100 | 100 | 100 | 100 | 100 | 100 |
| Initial cost ($USD/m^2$-aperture) | 635 | 635 | 635 | 635 | 635 | 635 | 635 |
| Energy saved (MWh) | 4.8 | 1.8 | 2.9 | 3.1 | 3 | 2.3 | 3.1 |
| Solar fraction (%) | 80.2 | 67.4 | 64 | 64.7 | 70.5 | 72.1 | 64.3 |
| Gross annual GHG reduction $tCO_2$/yr. | 6.8 | 2.5 | 4.1 | 4.4 | 4.2 | 3.3 | 4.4 |

| | | | | | | | |
|---|---|---|---|---|---|---|---|
| Gross GHG reduction $tCO_2$-25 yrs. | 169 | 63 | 102 | 109 | 105 | 81 | 110 |
| Barrels of crude oil not consumed | 15.7 | 5.9 | 9.5 | 10.1 | 9.8 | 7.6 | 10.2 |
| Simple payback period (yr.) | 7.8 | 14.8 | 9.2 | 8.6 | 8.9 | 11.5 | 8.5 |
| Equity payback period (yr.) | 6.5 | 10.9 | 7.4 | 7 | 7.2 | 8.9 | 7 |
| Pre-tax IRR-equity (%) | 17.6 | 9.7 | 15.3 | 16.3 | 15.8 | 12.5 | 16.4 |
| Pre-tax MIRR-equity (%) | 12.1 | 9.3 | 11.4 | 11.7 | 11.6 | 10.4 | 11.8 |

The variation of the solar collector area, number of collectors, and capacity of the project of all cities have been presented in Figure 3.4. It is evident from the figure that Shimla has the maximum value of the solar collector area, the number of collectors required, and capacity among all selected cities. This could be explained as Shimla being a cold climatic city among all selected cities and it has the maximum percentage of SWH system usage in the whole year. The other cities have lesser value being situated in the warm climatic region in comparison to Shimla city.

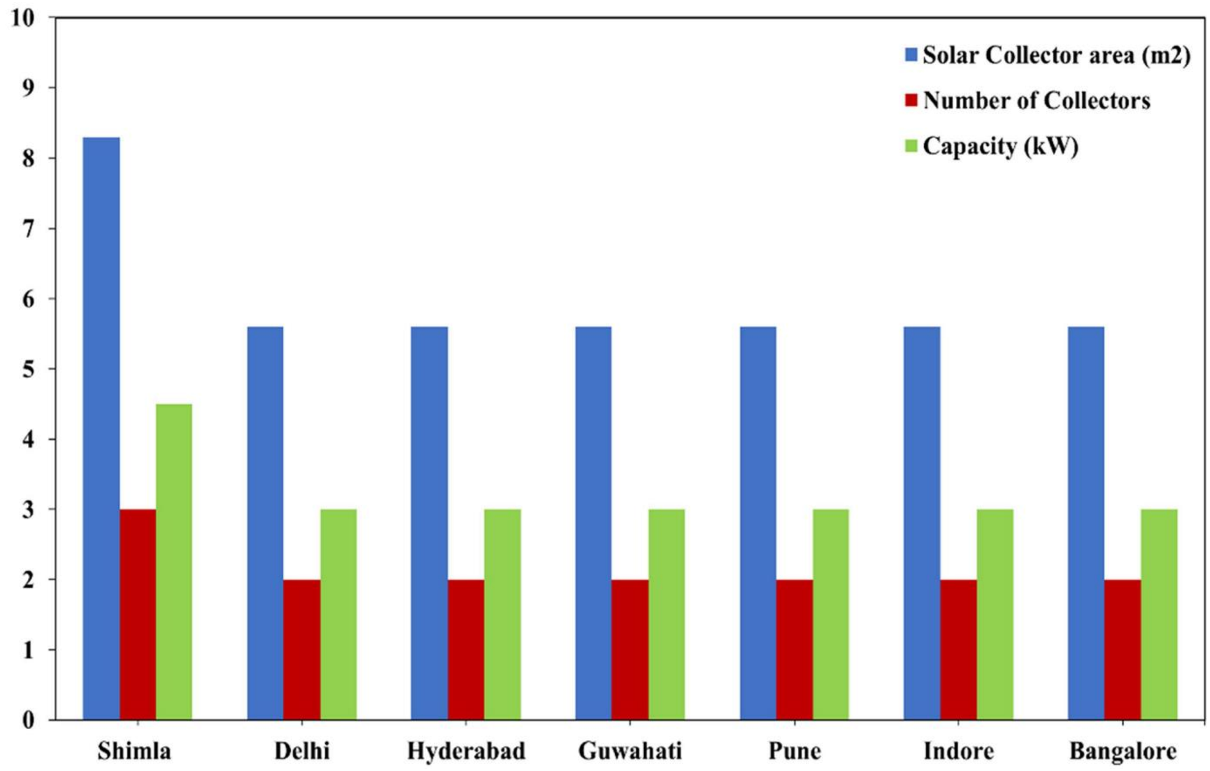


**Figure 3.4. Variation of solar collectors, number of collectors, and capacity at all cities**

### 3.5.1 Performance estimation analysis

The performance of the SWH system is evaluated by the term solar fraction. It is the ratio of energy delivered by the SWH to the total energy needed for the water heating service. If the solar fraction is 1 (100 %), it indicates that the SWH can provide the entire energy required by the heating system. The solar fractions of all cities have been calculated through the simulation model and presented in Figure 3.5. From the figure, it is evaluated that the maximum solar fraction for the evacuated tube type domestic SWH system is obtained for Shimla as 80.2 % and the minimum value is obtained for Hyderabad as 64 %. The second highest value is for Indore at 72.1 % followed by Pune at 70.5 %. Other cities like Delhi at 67.4 %, Guwahati at 64.7 %, and Bangalore at 64.3 %, these values are also satisfactory values of the solar fractions. It is also estimated that the value of solar fraction may be increased by increasing the value of the number of the collectors but if the number of collectors is increased the initial cost will also increase. To optimize the minimum cost for all cities, the number of collectors used is the same as suggested by the simulation model in this study. To meet the 100 % demand for hot water an auxiliary fuel is also needed.

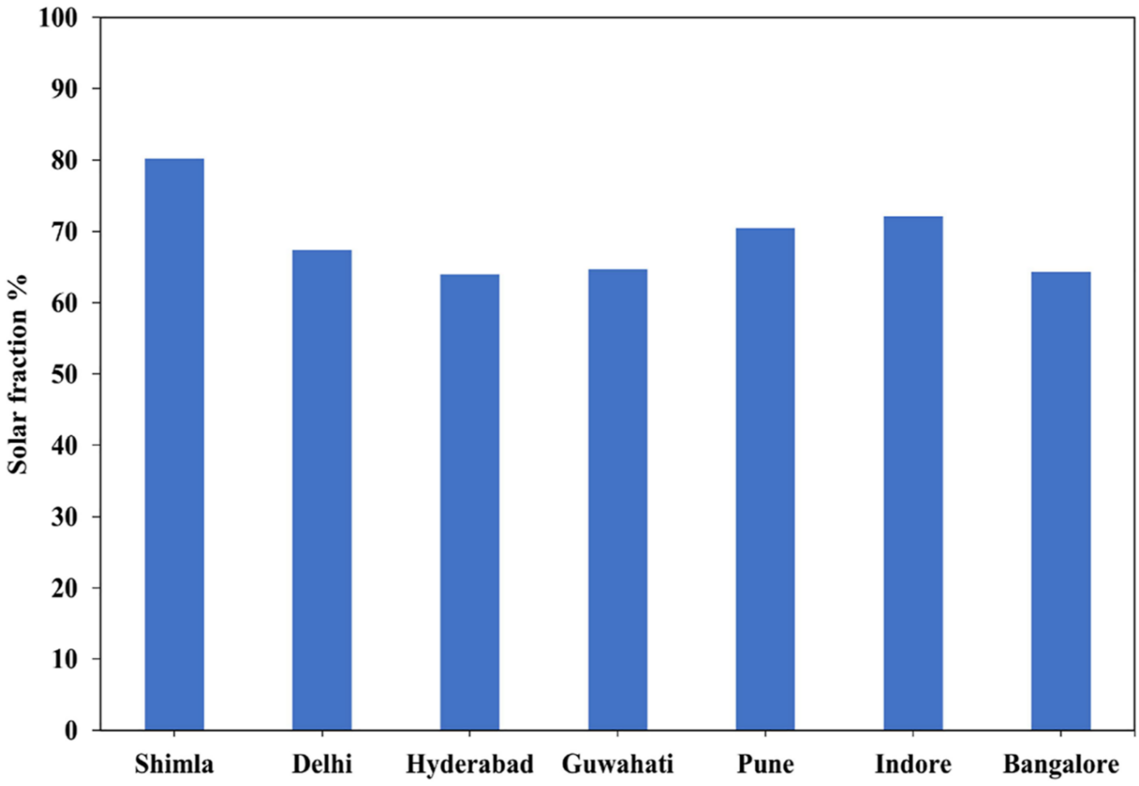


**Figure 3.5. Performance of evacuated tube-type domestic SWH system**

### 3.5.2 Energy saving analysis

The annual energy saving potential is a function of the solar fraction. The higher value of solar fraction represents a higher amount of energy savings. The annual energy-saving potential of the SWH system for all selected cities has been presented in Figure 3.6. The maximum value of energy savings is obtained for Shimla as 4.8 MWh followed by Guwahati and Bangalore having an energy saving of 3.1 MWh each. The least value of energy savings is obtained for Delhi as 1.8 MWh. Other observations of energy savings are of Hyderabad at 2.9 MWh, Pune at 3 MWh, and Indore at 2.3 MWh. The average energy-saving value of 3 MWh is obtained for installing evacuated-type domestic SWH systems in these selected cities. The variations in annual energy savings are observed due to the different values of solar fraction and the number of months the SWH systems are used in a year.

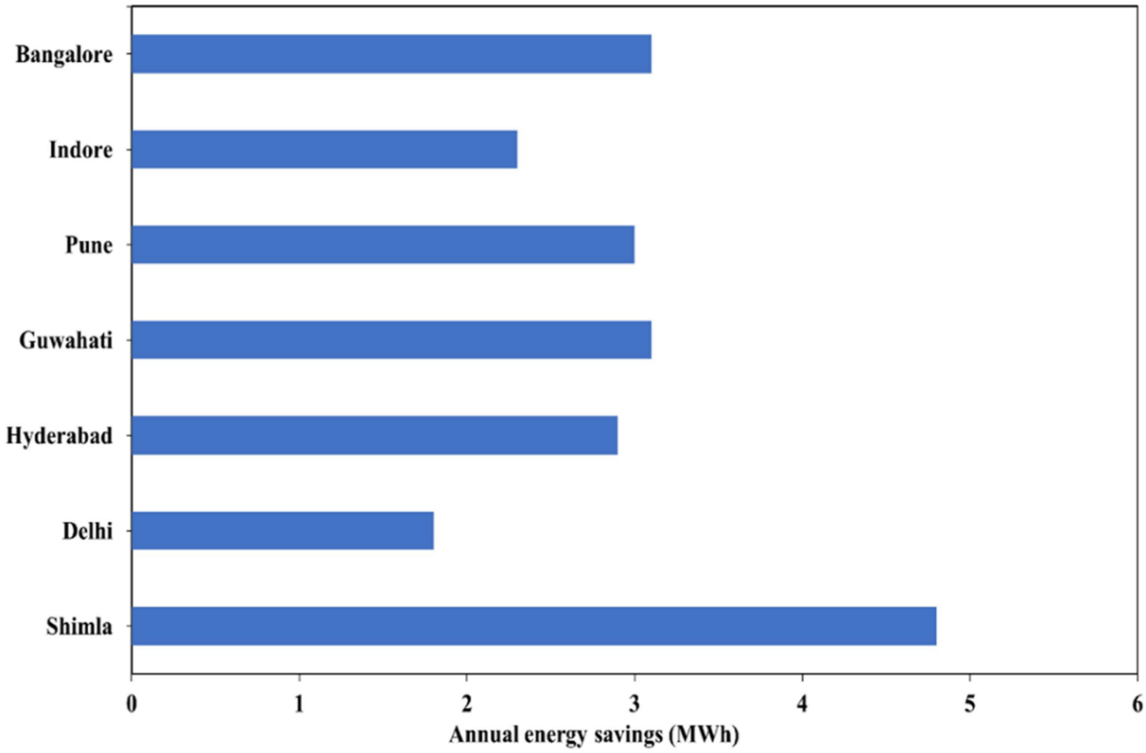


**Figure 3.6. Annual energy savings potential of the SWH system**

### 3.5.3 Greenhouse gas emission reduction analysis

The SWH technology does not emit any greenhouse gas (GHG) emissions. By application of this renewable energy technology to fulfill the hot water demand, a certain amount of GHG reduction is calculated here through the simulation model. The GHG emission reduction potential is a significant environmental phenomenon showing the benefits of the application of SWH projects in domestic sectors for curbing the effect of global warming. The simulation model facilitates the calculation of the GHG emissions on an annual basis and for the whole project duration. It is calculated in two terms namely the gross annual GHG emission reduction in the unit of $tCO_2$/year and the gross GHG emission reduction for the whole project life in the unit of $tCO_2$ – year for the 25 years of project duration. The gross annual GHG emission reduction presents the amount of emission reduction potential for a single year only while in the case of gross GHG emission reduction it is a cumulative value for the whole life of the project. In the present study, the gross annual GHG emission reduction potential of the SWH system for all selected cities is calculated here and shown in Figure 3.7.

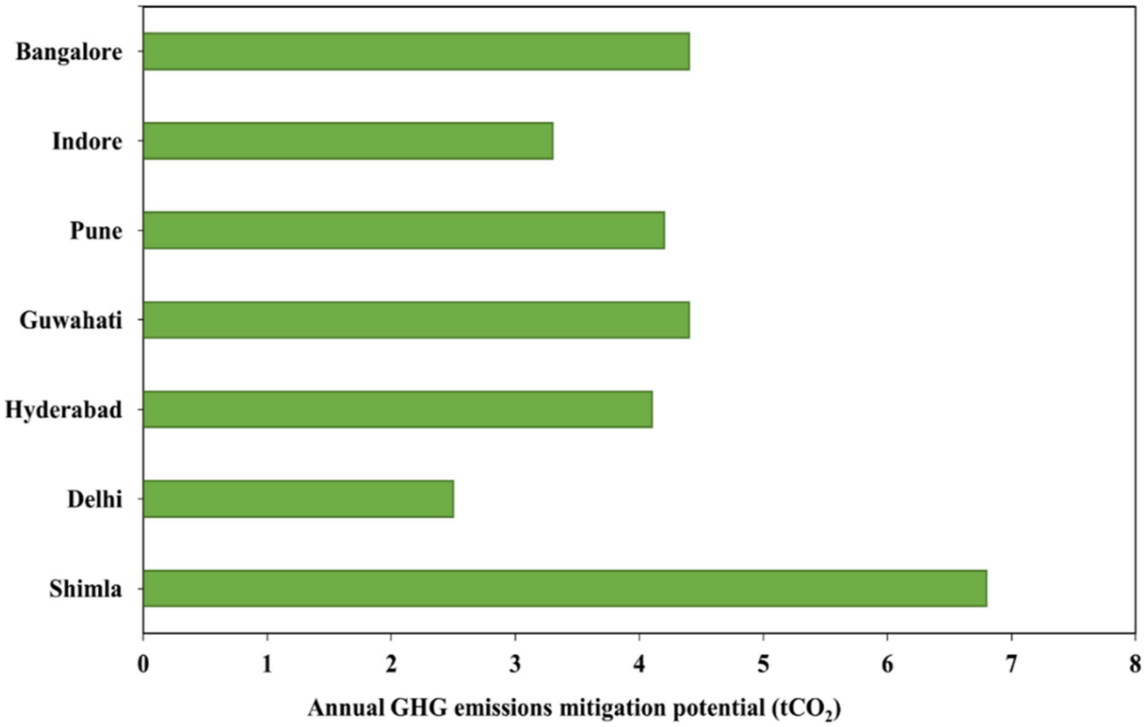


**Figure 3.7. Gross annual GHG emissions mitigation of the SWH system**

From the figure, it can be evaluated that the gross annual GHG emissions reduction potential of an evacuated tube SWH is found in the range of 2.5 $tCO_2$ to 6.8 $tCO_2$. The minimum value is found for Delhi at 2.5 $tCO_2$ and the maximum value is for Shimla at 6.8 $tCO_2$. The maximum value is followed by two cities namely Guwahati at 4.4

$tCO_2$ and Bangalore at 4.4 $tCO_2$. The next highest value is obtained for Pune at 4.2 $tCO_2$. The other values are Hyderabad at 4.1 $tCO_2$ and Indore at 3.3 $tCO_2$. The variation of gross GHG emission reduction in $tCO_2$ for the whole project life of 25 years for all selected cities is presented in Figure 3.8. It is observed that for all cities the gross GHG emission reduction is about 739 $tCO_2$ if the proposed SWH system project is implemented at the suggested locations.

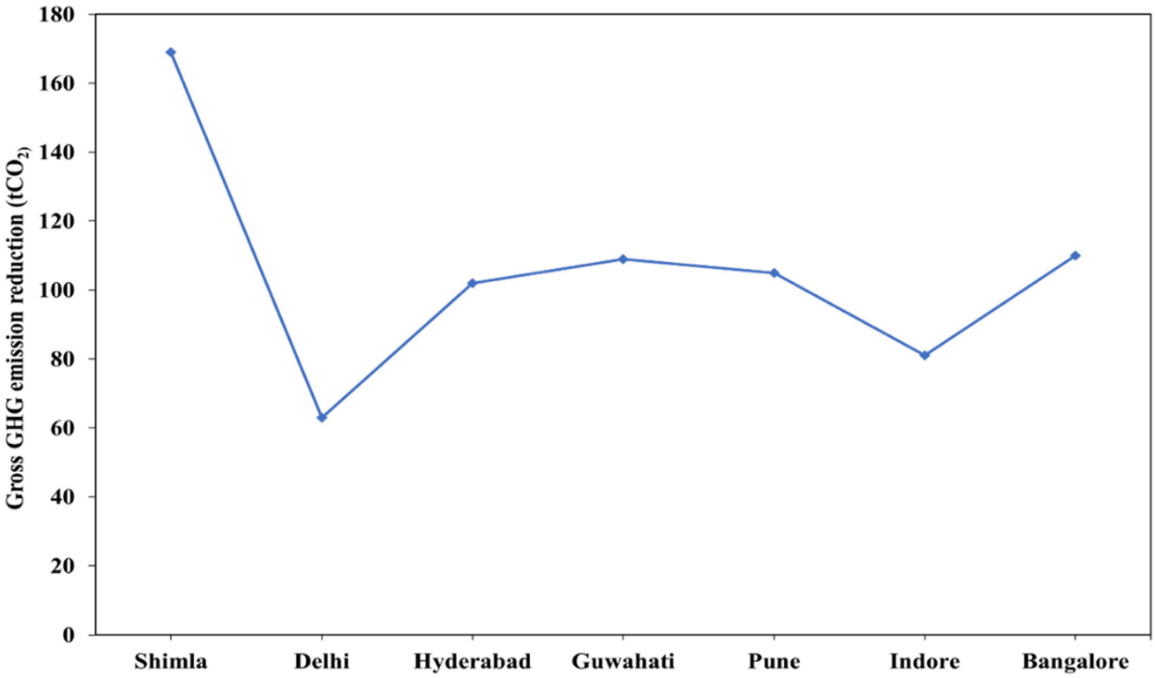


**Figure 3.8. Gross GHG emission reduction for 25 years of project life**

Here emission analysis of the simulation model is also presented in terms of gross annual GHG emission reduction in the form of barrels of crude oil not consumed, which is another important environmental criterion for SWH project analysis. These values of barrels of crude oil not consumed in all cities have been given in Figure 3.9.

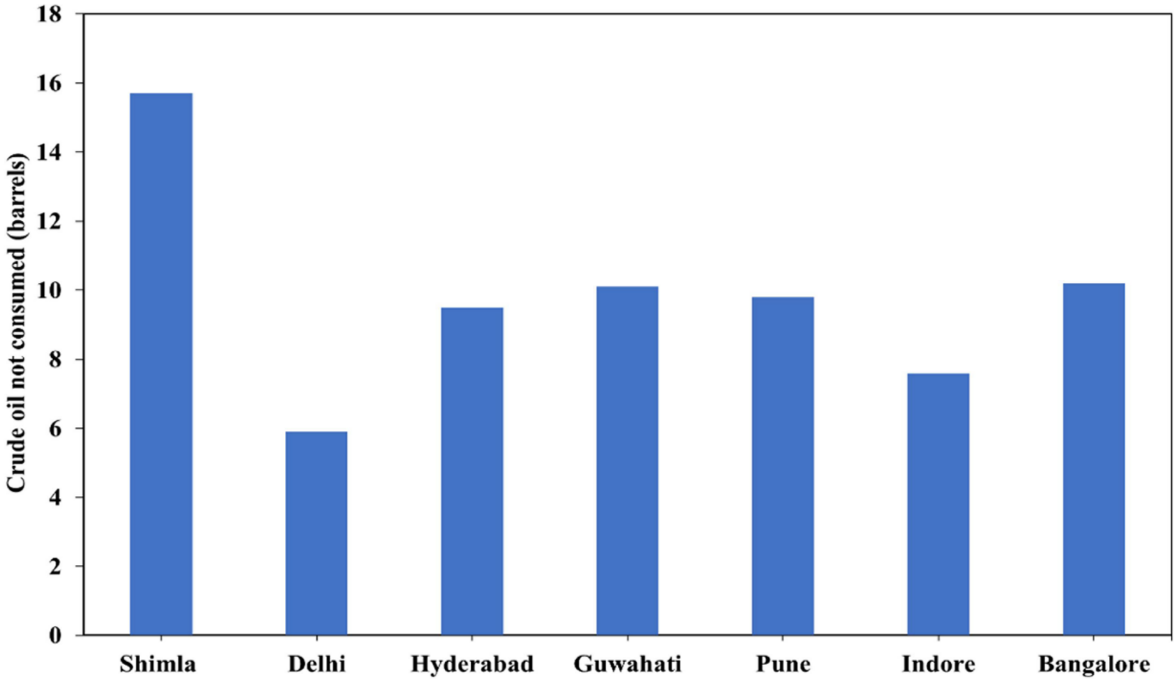


**Figure 3.9. Barrels of crude oil not consumed at various locations**

It is clear from the figure that the highest and the lowest values are for Shimla and Delhi respectively. The second highest value is obtained for Bangalore and the next for Guwahati. This variation in the quantity of crude oil not consumed is due to variations in the number of months the SWH system is used in a year according to the requirements at a particular geographical location.

### 3.5.4 Financial analysis

In this section, the financial viability analysis of installing SWH projects is analyzed in terms of SPP, EPP, IRR-equity, and modified internal rate of return (MIRR)-equity.

An SPP is calculated from cumulative cash flow graphs of the basic scenario model 1 without any incentives and grants. The cumulative cash flow graph of each city is presented in Figure 3.10. An SPP represents the length of time that it takes to recoup its own initial cost, out of the revenue or savings it generates. It is an indicator of how quickly the cost of an investment can be recovered. For example, in the case of the implementation of an SWH project, a negative payback period would be an indication that the annual costs incurred are higher than the annual savings generated. The other financial indicator of EPP is also evaluated here, which represents the length of time that it takes for the owner of a facility to recoup its initial investment in the form of equity of the project cash flows generated. The equity payback considers project cash flows from its inception as well as the leverage of the project, which makes it a better time indicator of the project than the simple payback. The SPP and EPP of all selected cities for installing of evacuated type domestic SWH system are presented in Figure 3.11. It can be observed from the figure that the maximum value of SPP and EPP is found for Delhi and the minimum value is found for Shimla. It is because Delhi has the least number of months of using the SWH system in a year while Shimla has the highest number of months of usage.

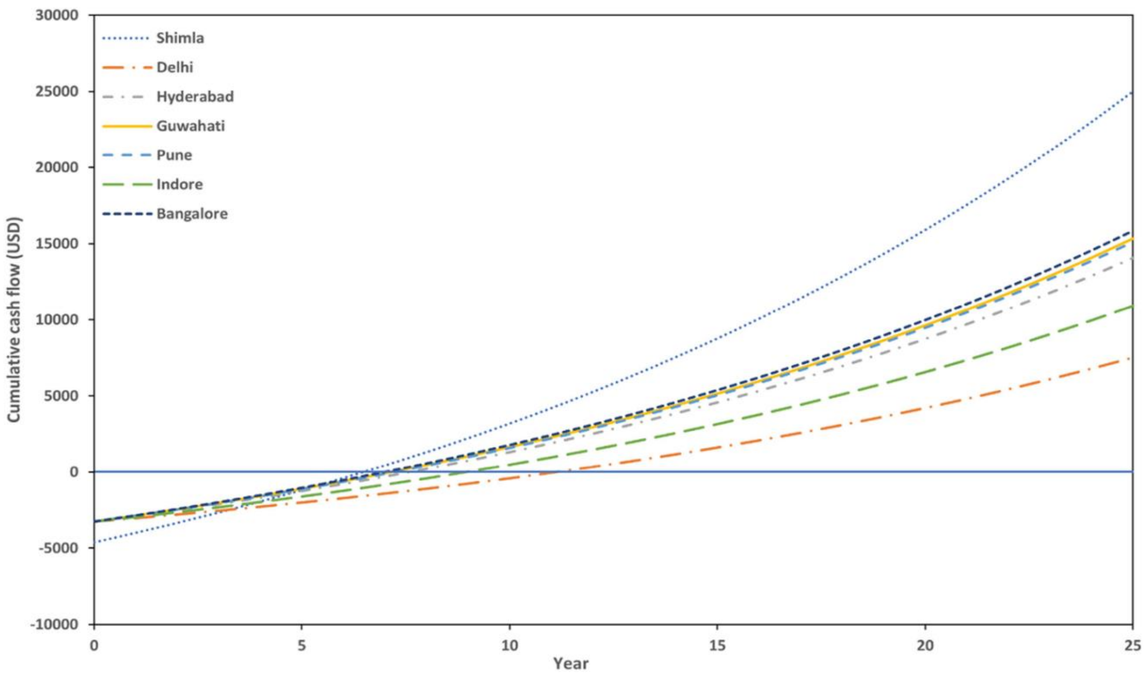


**Figure 3.10. Cumulative cash flow of each city**

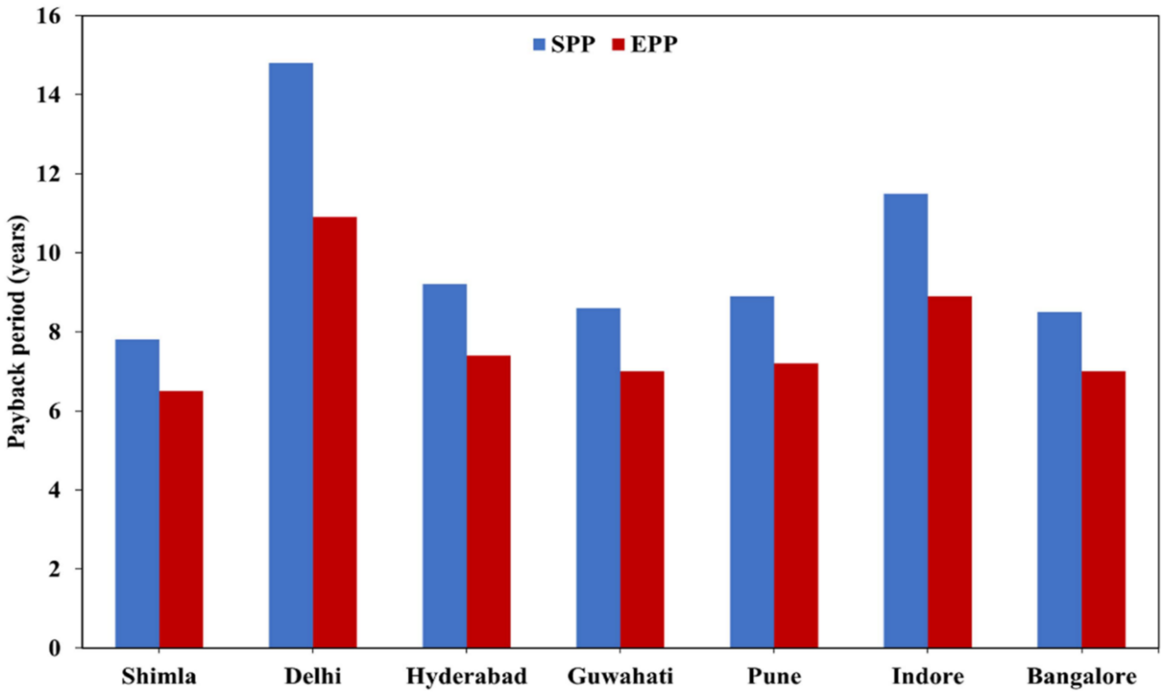


**Figure 3.11. Simple and equity payback periods of all selected cities**

The next financial indicators of IRR and MIRR on equity are also evaluated here, the IRR is the true interest yield provided by the project equity over its life before income tax. It is calculated using the pre-tax yearly cash flows and the project life. The MIRR on equity is the cost and profitability provided by the project equity over its life before income tax. It is calculated using the pre-tax yearly cash flows, the project life, the discount rate, and the reinvestment rate. The IRR and MIRR of all selected cities for installing the domestic SWH system are presented in Figure 3.12. It can be evaluated from the figure that the maximum value of IRR and MIRR was found for Shimla (i.e IRR=17.6 %, MIRR=12.1 %), and the minimum value was found for Delhi (i.e IRR=9.7 %, MIRR=9.3 %). This is because Delhi has the least number of months of SWH usage while Shimla has the maximum number of months of usage.

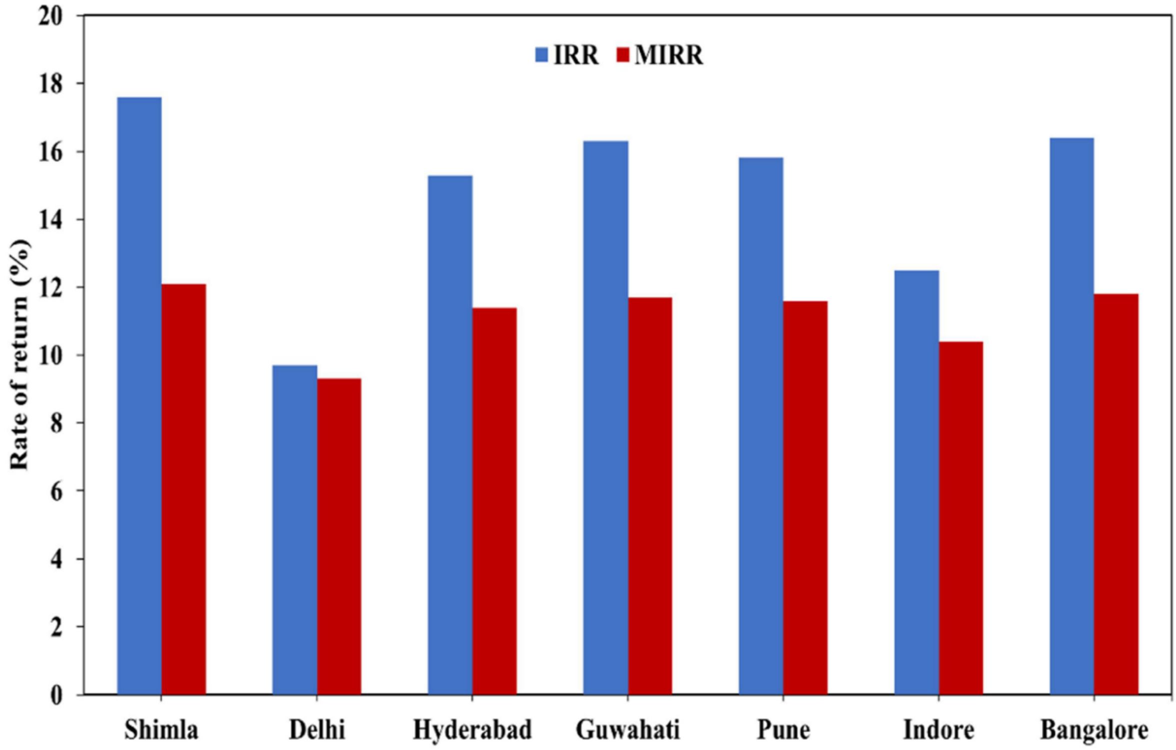


**Figure 3.12. Internal and modified internal rate of return of all cities**

### 3.5.5 Impact of incentives and grants on financial analysis

In this section, the impact of incentives and grants on financial analysis has been presented by considering one parameter of SPP. To demonstrate the effect on an SPP, three cities namely Delhi (i.e. 14.8 yrs.), Indore (i.e. 11.5 yrs.), and Hyderabad (i.e. 9.2 yrs.) have been considered. The study shows that these three cities have consecutively higher values of SPP as represented in Figure 3.13.

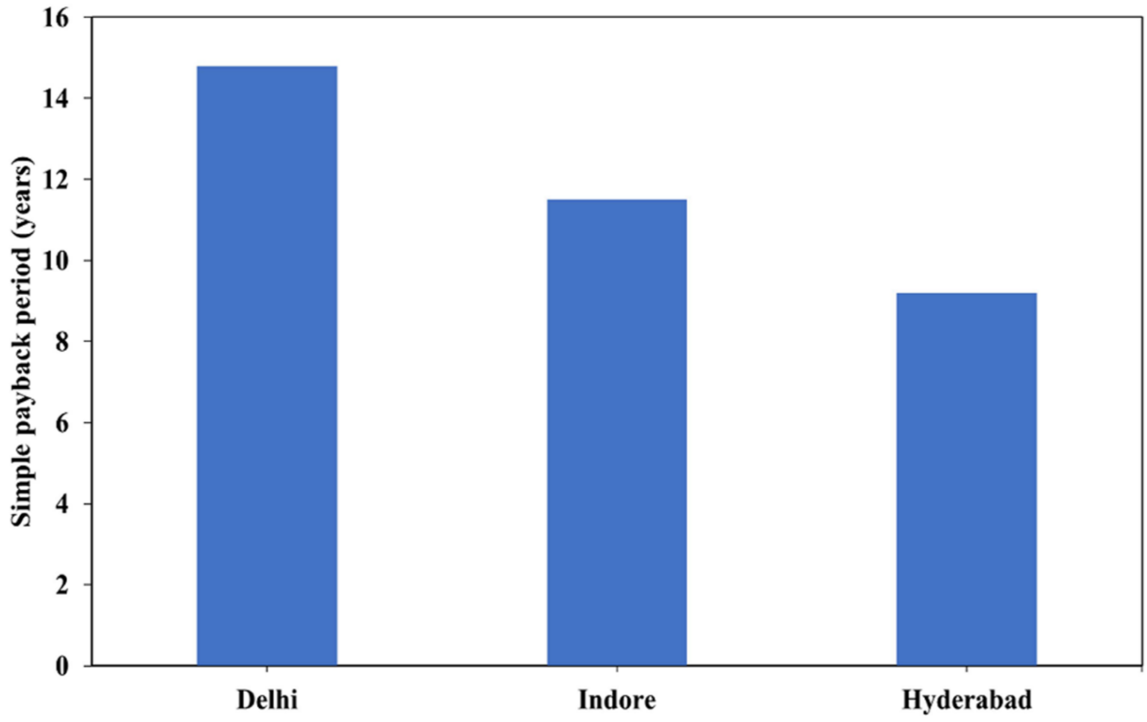


**Figure 3.13. SPP of three selected cities**

The incentive and grant at 0 %, 25 %, and 50 % of the initial costs are considered for the basic scenario model (1) and represented in Figure 3.14. It could be observed from the figure that SPP is decreasing as the grant is increasing. If the grant of 25 % of the initial cost is provided then the SPP of Delhi, Indore, and Hyderabad will be 11.1, 8.6, and 6.9 years respectively. Similarly, if the grant will be provided as 50 % of the initial cost, then the SPP of Delhi, Indore, and Hyderabad will be 7.4, 5.7, and 4.6 years respectively. So these values of incentives and grants will be advantageous for enhancing the popularity of SWH systems in the residential sector.

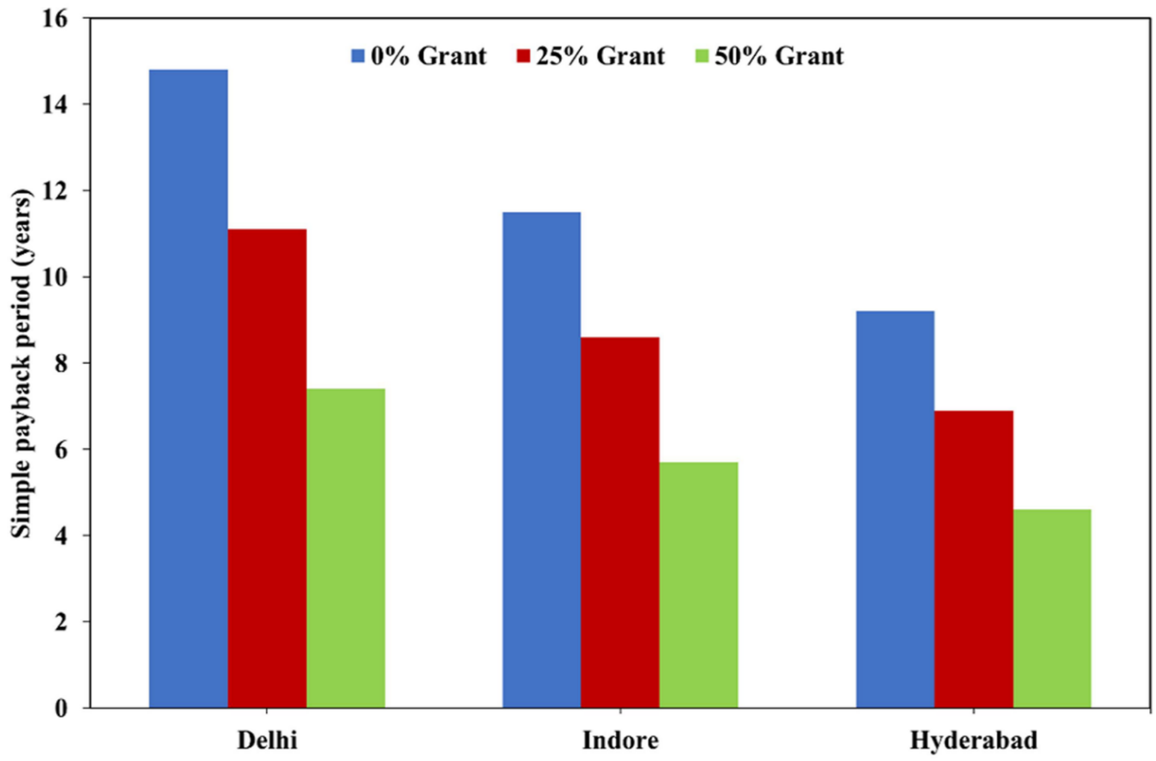


**Figure 3.14. Impact of incentives and grants on SPP**

### 3.6. Clean Development Mechanism Potential (CDM)

In the Kyoto Protocol (1997), the CDM was formulated to facilitate developed countries to purchase carbon credits savings for renewable energy projects in developing countries. It is observed that the need for this agreement arises because it is more expensive for developed countries to save carbon credit in their own countries in comparison to developing countries. For small-scale projects, the CDM executive board defined some guidelines as;

- The renewable energy project activities with a maximum output capacity equivalent of up to 15 MW.
- The energy efficiency improvement project activities reduce energy consumption by an amount equivalent to 60 GWh per year.

- The project activities whose emission reductions are less than 60 $ktCO_2$ per year.

The results obtained in the present study clearly indicating the SWH projects in India are good candidates for CDM approval.

# Chapter 4: Techno-comparative study of SWH system for residential, commercial, and industrial applications

This chapter evaluates the techno-comparative study for the viability of the SWH system applications in residential, commercial, and industrial sectors of India through the RETScreen Expert Clean Energy Management Software.

It has been found that a specific study related to the techno-comparative viability study of SWH system applications for residential, commercial, and industrial sectors for the Indian climatic region is very rare. This type of study is very essential for developing countries like India, to demonstrate the comparative benefits of SWH systems for residential, commercial, and industrial sectors. Hot water is also needed frequently for commercial and industrial applications, in a similar fashion to the residential sector. However, due to a lack of awareness of the benefits of the application of the SWH systems, these sectors have less number of installations in India. In this chapter, an attempt has been made to attract the attention of the government of India to make specific policies and regulations for the application of the SWH systems in commercial and industrial sectors.

The outcome of this chapter will exhibit the benefits in terms of financial indicators and environmental benefits of the application of SWH systems. The simulation modeling has been performed by considering the three different geographical locations of India, namely Leh, Amethi (Jais), and Ludhiana districts for residential, commercial, and industrial case studies respectively. The three different locations had been chosen to explain the applicability and performance in different climatic regions of India, the detailed analysis has been presented in the subsequent sections as,

## 4.1. Introduction

The hot water requirement is an important segment for residential, commercial, and industrial applications for all climatic regions of the world. In the case of the residential sector, hot water is utilized for bathing, cloth cleaning, dishwashing, etc. The commercial sector includes the application of hot water for schools, institutions, hotels, hospitals, office buildings, community kitchens, etc. In the case of the industrial sector, hot water is required by industries like food processing, rice milling, textile processing, pharmaceutical, pulp & paper, chemical, and auto component industries, etc. It has been observed that generally the hot water requirement is fulfilled by biomass fuels, kerosene oil, LPG, and electric geysers, which are not a good means according to price, health, and environmental issues as well as such types of fuels are limited in quantities in the whole world. So there is a need for alternative solar thermal energy technology for heating water called SWH.

The Global Status Report REN21 [62], shows that solar thermal technologies are getting attention broadly in all regions of the world to provide low-temperature heat for hot water, space heating, and drying. Large heat consumers such as industries, hospitals, hotels, and laundries are adopting solar thermal systems to meet their energy needs for high-temperature heat, steam, and refrigeration. It has been observed that by the end of the year 2018, residential, commercial, and industrial sectors in 130 countries benefited from solar heating and cooling systems. Glazed (flat plate and vacuum tube) and unglazed solar thermal systems combined provided around 396 TWh (1,426 PJ) of heat annually – equivalent to the energy content of 233 million barrels of oil. Globally, China is a world leader in the manufacturing of SWH systems and using them for heating water. Household in China uses about 10 % of SWH systems and they set a target to use about 30 % of households that will use the

SWH system by the year 2020. Other countries, like the European Union, Turkey, Japan, Israel, and India also have 12.3 %, 5.8 %, 4.1 %, 2.8 %, and 1.2 % users respectively of household SWH systems [63].

India is a developing country and its energy requirements are regularly expanding, it is very difficult to fulfill all energy needs alone from conventional sources of energy which are limited in quantities, in this viewpoint, renewable energy sources are much enough to provide an effective solution to fulfill the energy requirements of nation for an infinitely long period. Fortunately, India receives $5 \times 10^{15}$ kWh per annum of solar radiation with a daily average of 4–7 kWh/$m^2$. It can heat water from 60 °C to 80 °C by use of a suitable type collector at different climatic zones. The received annual solar radiation shows the large potential for SWH projects in residential, commercial, and industrial sectors. It has been estimated that the gross potential for SWH systems is 140 million $m^2$ of collector area, out of this 40 million $m^2$ has been estimated as the realizable techno-economic potential at this stage. The government of India has set a target of 7 million $m^2$ under the Jawaharlal Nehru National Solar Mission (JNNSM) by the end of the first phase of the Mission (2010-13) and a goal of 20 million $m^2$ by the end of the third phase of the Mission (2017 - 22) [64]. The sector-wise installed and functional percentage share of SWH systems till the year 2009 has been shown in Figure 4.1.

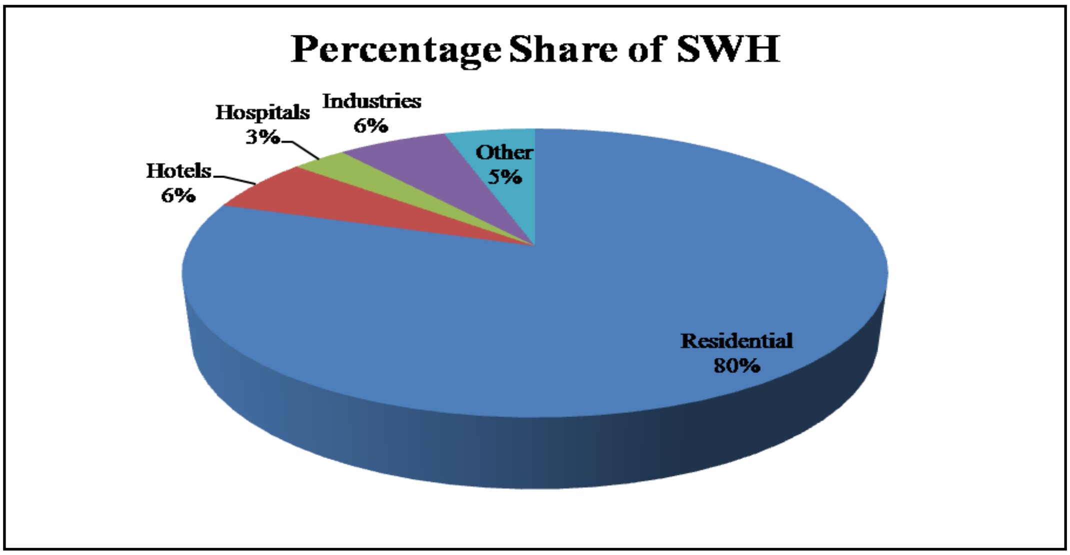


**Figure 4.1. Percentage share of SWH systems [63]**

It has been observed from the figure that the residential sector has an 80 % share of SWH systems, the commercial sector includes hotels and hospitals, and others have 6 %, 3 %, and 5 % respectively, and the industrial sector contains a 6 % share of SWH systems. The percentage of share shows that the residential sector is one of the largest sectors among commercial and industrial sectors in India. The residential sector is also the largest in the whole world. The installed and functional numbers of SWH systems in the form of collector areas till the year 2009 are also presented in Figure 4.2.

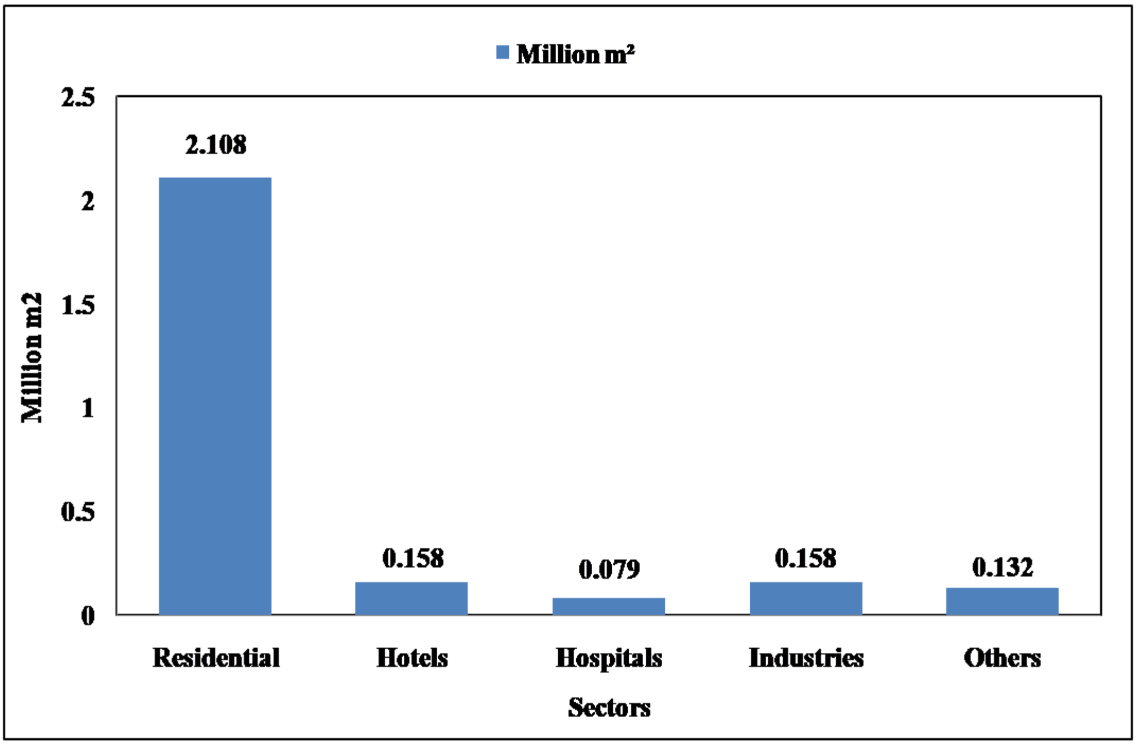


**Figure 4.2. Numbers of installed SWH systems till the year 2009**

The sector-wise installed capacity and future demand for SWH systems in India are also presented in Figure 4.3. It can be evaluated from the figure that the residential sector has the highest potential in comparison to the commercial sector (i.e. hotels, hospitals, and others including railway, defense & religious places, etc.) and industrial sector. The cumulative yearly installed capacity of residential SWH systems for the years 2009, 2010, 2013, and 2017 was 2.108, 2.58, 4.25, and 7.68 million $m^2$ respectively; and the future expected demand for the year 2022 is 15.74 million $m^2$ [63]. The cumulative yearly installed capacity of hotels for the years 2009, 2010, 2013, and 2017 was 0.158, 0.19, 0.35, and 0.61 million $m^{2,}$ and the future expected demand for the year 2022 is 0.97 million $m^2$ [63].

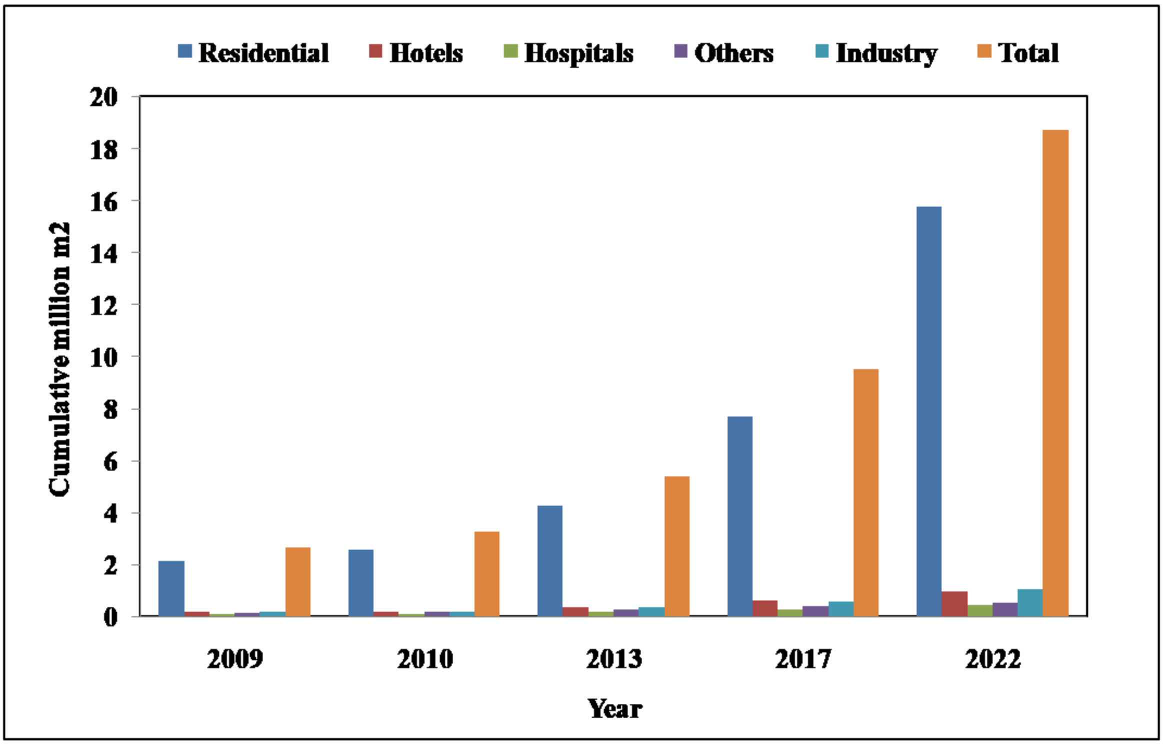


**Figure 4.3. Installed and potential SWH systems in India**

The cumulative yearly installed capacity of SWH systems for the hospitals for years 2009, 2010, 2013, and 2017 was 0.079, 0.10, 0.17, & 0.27 million $m^2$ and the future expected demand for the year 2022 is 0.43 million $m^2$ [63]. In this sequence, the cumulative yearly installed capacity for the others (i.e. railway, defense, and religious places, etc) of the SWH systems for the years 2009, 2010, 2013, and 2017 was 0.132, 0.18, 0.27 & 0.39 million $m^2$, and future expected demand for the year 2022 is 0.52 million $m^2$ [63]. The cumulative yearly installed capacity of SWH systems for the industrial sector for years 2009, 2010, 2013, and 2017 was 0.158, 0.19, 0.33, & 0.57 million $m^2$, and future expected demand for the year 2022 is 1.05 million $m^2$ [63]. The gross total demand including all sectors (i.e. residential, commercial, and industrial) for the years 2009, 2010, 2013, and 2017 was 2.63, 3.24, 5.37, and 9.52 million $m^{2,}$ and the expected demand for the year 2022 is 18.70 million $m^2$ [63]. The demand pattern shows that there is a regular increase in demand for the SWH systems for the coming years. There is a need for government policies for supporting SWH technology to sustain in all sectors of the economy. Especially there is a requirement of making effective policies, in favor of the consumer and the nation, for commercial and industrial sectors to enhance the installation of the SWH system throughout the country for the coming years.

There are many studies have been performed on the techno-comparative feasibility analysis of the SWH system around the globe at different climatic zones such as Chandrasekar and Kandpal [65] have done a detailed techno-comparative evaluation of the domestic SWH system for assessment of the potential for the Indian region. The authors have an estimated number of households who can invest in SWH systems based on the income, the capital cost of the SWH system, interest rate charged on the loan provided for the purchase of domestic SWH systems. Houri [48] has studied the current status and prospects of the thermosyphon-type domestic SWH system in Lebanon. The author found that the initial estimate for the Kypros SWH with two panels installed (2 $m^2$ each) with a 200 L hot water tank is about a 4 - 5 years payback period, while through RETScreen modeling a 2.5 $m^2$ flat plate glazed collector with 114 L storage capacity placed at a slope of 33.88 have a payback period within 7 years while producing $ 2610 in cash savings during its 20-years lifetime with greenhouse gas reduction potential of 1.42 ton of $CO_2$ per year, and the author also analyzed evacuated tube SWH and found payback period within 8 - 9 years and will save $ 2060 during its lifetime along with saving of 1.78 ton of $CO_2$. Purohit and Michaelowa [49] have estimated that there is a vast theoretical potential for $CO_2$ mitigation by the use of SWHs in India. The annual CERs potential of SWHs could theoretically reach 27 million tonnes. The potential number of SWHs has been estimated at 26.7 million. Under more realistic assumptions about the implementation of SWHs based on past experiences with government-run programs, annual CER volumes by 2012 could reach around 3.6 – 9 million, and by 2020, 15 – 22 million. Gastli and Charabi [50] have investigated the potential application of the SWH system in Oman by considering a case study of the Seeb district with the help of RETScreen Clean Energy Software. The authors found that a 50 % sharing of the capital cost between homeowners and the Government will benefit both parties and will produce profitable investments. Through the case study, the authors found that the IRR ranges between 12.2 and 16.5 %, and the SPP is between 7 to 10 years. Stevanovic and Pucar [51] have suggested the level of the subsidy through the RETScreen financial analysis which the Serbian government should offer the number of SWH deployments as compared to developed countries. The authors study reveals that installation is always profitable, having an EPP of 9.5 – 10.3 years without any government subsidy, 7.6 – 8.3 years with a 25 % subsidy, and 5.5 – 6 years with 50 % subsidy of the total initial costs for five of the six considered cities, and even better results for a small mountain city of Sjenica. Ramedani et al. [66] have investigated the potential of SWH application for heating commercial greenhouses through a case study in the Hashtgerd city of Alborz province in Iran. The authors found that the energy production analysis shows 22 % in January at worst and 71 % in November or March at best of energy needs, which can be supplied by introducing SWH systems. Hagos et al. [67] have investigated the possibility of using SWH for residential applications in Inland Norway. The authors evaluated that a typical tubular collector in Inland Norway could supply 62 % of the annual water heating energy demand for a single residential household, while glazed flat plates of the same size were able to supply 48 %. If the SWH system is deployed in all detached dwellings in Inland could have the potential to save 182 GWh of electrical energy, equivalent to a reduction of 15,690 tonnes of oil energy and 48.6 kt$CO_2$ emissions. Rehman and Sulaiman [52] have evaluated the optimum selection criteria for domestic SWH systems based on the techno-comparative aspects of the evacuated tube and glazed flat plat solar collectors. Ten different cities in Saudi Arabia are considered, and the financial assessment reveals that Nejran, Bisha, and Madina are the most favorable regions followed by Jeddah, Guriat, and Abha. Economic feasibility for both evacuated tubes and glazed flat plate collectors for these cities is justified because of obtaining almost the same results of the payback period and benefit to cost ratio. Riyadh, Dhahran, and Gaseem show noticeable financial advantages by using evacuated tube collectors overglazed flat plate collectors. Sulayyil is not a feasible option with either type of SWH system because of high initial investment and long payback periods. Yasin [68] has analyzed technical and financial assessment of glazed and evacuated tubes solar collectors for domestic water heating applications in Palestine through RETScreen software analysis. The author found that utilizing SWH technology in Palestine for water heating is feasible, efficient, and cost-effective whether glazed or evacuated tubes are used. The performance of SWH systems is mostly similar all-over Palestinian territories with slight variations. S. Mekhilef et al. [69] have presented a study about the utilization of solar thermal energy in industries in various processes and applications. The authors discussed the potential applications and benefits of using solar energy for industrial sectors. A. Gautam et al. [70] have presented a review study focusing on the economical feasibility and technical improvements of the SWH system according to the worldwide scenario. The authors found that economic viability is equally important as technical viability, and economic viability is greatly dependent on some factors like alternative fossil fuel cost, subsidy rate, solar energy intensity, etc around the world. R. Zhang et al. [71] have presented a review study focusing on the existing techno-economic analysis of the SWH systems. The author's study aimed to improve the techno-economic analysis method for the SWH system.

### 4.2. Case studies

In this section, three different case studies of SWH systems for residential, commercial, and industrial applications at different geographical coordinate locations in India have been discussed as,

#### 4.2.1 Residential case study

In this case study, the Leh district of Ladakh Union territory of India is considered for the residential model of the SWH system. Leh is the largest town and joint capital of the Ladakh Union territory. It has a cold climate and receives solar radiation of about 5.4 kWh/m$^2$/day. Having very cold climate conditions hot water is required throughout the year. Based on the demand pattern it is expected that on average a 100 L/day SWH system is required per household to meet their hot water demand. The pictorial view of the facility location is presented in Figure 4.4 and the geographical coordinates are depicted in Table 4.1.

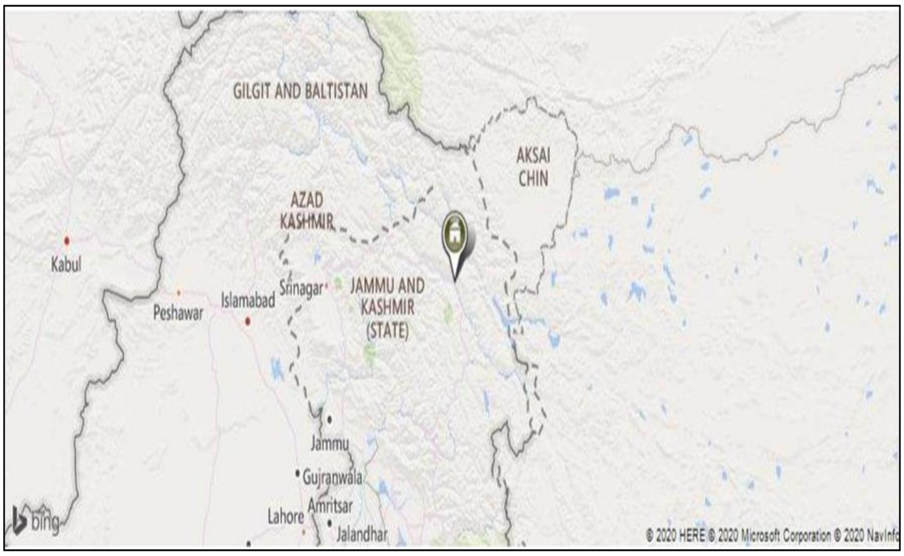


**Figure 4.4. Pictorial view of facility location**

**Table 4.1: Geographical coordinates of facility location**

| Facility location | Latitude (°N) | Longitude (°E) | Climate zone | Elevation (m) |
|---|---|---|---|---|
| Leh | 34.2 | 77.6 | Subarctic | 4764 |

### 4.2.1.1 Climate resource assessments

In this section of a residential case study, some climatic parameters are considered from the NASA database for modeling the SWH system, like air temperature, relative humidity, daily solar radiation, wind speed, earth temperature, heating degree days and cooling degree days, etc. These climatic parameters are presented in Table 4.2.

**Table 4.2: Climate parameters of the selected location**

| Month | Air temperature (°C) | Relative humidity (%) | Daily solar radiation - horizontal ($kWh/m^2/d$) | Wind speed (m/s) | Earth temperature (°C) | Heating degree-days 18°C (°C-d) | Cooling degree-days 10°C (°C-d) |
|---|---|---|---|---|---|---|---|
| January | -17.0 | 53.2% | 2.86 | 2.6 | -19.2 | 1085 | 0 |
| February | -15.7 | 57.6% | 3.54 | 2.9 | -17.1 | 944 | 0 |
| March | -10.7 | 53.3% | 4.45 | 3.1 | -10.1 | 890 | 0 |
| April | -4.8 | 45.9% | 5.43 | 3.1 | -2.0 | 684 | 0 |
| May | -0.4 | 42.7% | 6.19 | 2.9 | 3.3 | 570 | 0 |
| June | 4.2 | 38.8% | 6.91 | 2.7 | 8.4 | 414 | 0 |
| July | 8.2 | 39.6% | 6.72 | 2.5 | 12.1 | 304 | 0 |
| August | 7.8 | 42.5% | 6.14 | 2.3 | 10.9 | 316 | 0 |
| September | 2.9 | 37.7% | 5.66 | 2.3 | 5.0 | 453 | 0 |
| October | -4.1 | 33.6% | 4.79 | 2.2 | -2.9 | 685 | 0 |
| November | -9.5 | 35.8% | 3.61 | 2.3 | -10.2 | 825 | 0 |
| December | -14.0 | 44.7% | 2.76 | 2.5 | -16.0 | 992 | 0 |

(Source: NASA Database)

The monthly variation of daily solar radiation - horizontal with an air temperature of the selected facility location is presented in Figure 4.5. It is observed from the figure that the daily solar radiation-horizontal is varied from 2.76 $kWh/m^2/d$ to 6.91 $kWh/m^2/d$. Apart from a few months (i.e. two), the value of solar radiation-horizontal is greater than 3.5 $kWh/m^2/d$ which is sufficient for generating heat energy for heating water at the facility location. The air temperature is varied in the range of -17 °C to 8.2 °C, which could be favorable for avoiding the overheating of solar panels.

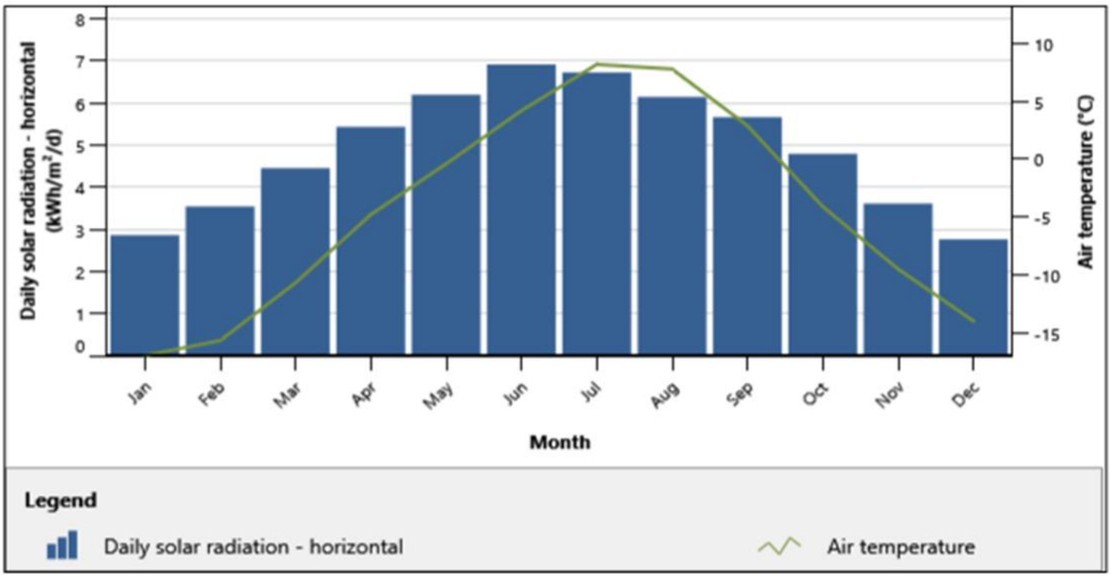


**Figure 4.5. Daily solar radiation-horizontal vs. air temperature**

The heating requirement in hours of each month for the whole year of the selected facility location is represented in Figure 4.6. It is observed from the figure that there is only a requirement for heating each month throughout the year. There is no cooling requirement for the whole year according to the climate parameters of Table 4.2 due to being a cold climatic region of the facility location.

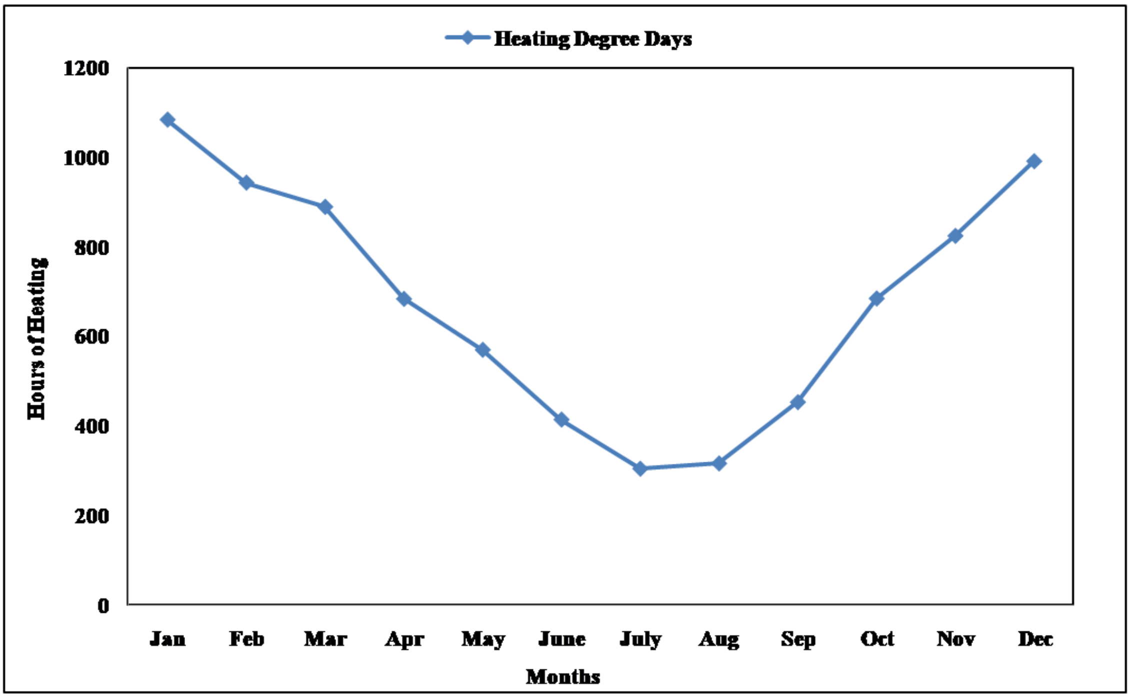


**Figure 4.6. The heating requirement at the facility location**

#### 4.2.1.2 Simulation model

In this section, a simulation model is analyzed for the different numbers of occupants, for example, taking 3 to 14 numbers of occupants per house. Here the variations in the number of occupants are taken for the application of a model for small, medium, and large houses.

**(i) Simulation input parameters**

The simulation input parameters of the basic scenario model (1) are presented in Table 4.3.

**Table 4.3: Energy model input parameters of the basic scenario model (1)**

| Input Parameter | Values |
|---|---|
| Number of occupants per house | 3 to14 |
| Occupancy rate (%) | 100 |
| Hot water temperature(°C) | 60 |
| Solar tracking mode | Fixed |
| Slope | 35° |
| Azimuth | 0 |
| Operating days per week | 7 |
| Solar water heater type | Evacuated |
| Miscellaneous losses (%) | 3 |
| Conventional fuel type | Electricity |
| Seasonal efficiency (%) | 90 |
| Electricity rate annual (USD/kWh) | 0.11 |
| Fuel cost escalation rate (%) | 5 |
| Discount rate (%) | 8 |
| Reinvestment rate (%) | 9 |
| Inflation rate (%) | 4 |
| Project life (years) | 25 |
| Debt ratio (% of the initial cost) | 0 |
| Initial grant (% of the initial cost) | 0 |
| Annual O&M cost (USD) | 0 |
| GHG emission factor for coal ($tCO_2$/MWh) | 1.26 |

The technical specification of the selected model of the SWH system for simulation is presented in Table 4.4.

**Table 4.4: Technical specifications of residential SWH system**

| Parameters | Evacuated tube collector |
|---|---|
| Manufacturer | Thermomax |
| Model | MS 20 - TMO 500 |
| Gross area per solar collector ($m^2$) | 2.779 |
| Aperture area per solar collector ($m^2$) | 2.135 |
| Fr(tau alpha) coefficient | 0.578 |
| Fr UL coefficient ($W/m^2$)/°C | 1.05 |
| Temperature coefficient for Fr UL | 0 |

### (ii) Simulation output parameters

To evaluate the optimum tilt angle for maximum heating delivered, the variations of daily solar radiation-tilted and heating delivered at different tilt angles are presented in Table 4.5.

**Table 4.5: Variations of daily solar radiation-tilted and heating delivered at the different tilt angles**

| Tilt Angle | 25° | | 30° | | 35° | | 40° | | 45° | | 50° | |
|---|---|---|---|---|---|---|---|---|---|---|---|---|
| Month | Daily solar radiation-tilted ($kWh/m^2/d$) | Heating delivered (kWh) | Daily solar radiation-tilted ($kWh/m^2/d$) | Heating delivered (kWh) | Daily solar radiation-tilted ($kWh/m^2/d$) | Heating delivered (kWh) | Daily solar radiation-tilted ($kWh/m^2/d$) | Heating delivered (kWh) | Daily solar radiation-tilted ($kWh/m^2/d$) | Heating delivered (kWh) | Daily solar radiation-tilted ($kWh/m^2/d$) | Heating delivered (kWh) |
| January | 4.11 | 255.559 | 4.31 | 266.322 | 4.48 | 275.672 | 4.64 | 283.628 | 4.76 | 290.209 | 4.87 | 295.436 |
| February | 4.55 | 253.256 | 4.70 | 260.093 | 4.83 | 265.818 | 4.93 | 270.440 | 5.01 | 273.972 | 5.07 | 276.423 |
| March | 5.13 | 313.135 | 5.21 | 316.883 | 5.27 | 319.600 | 5.31 | 321.291 | 5.32 | 321.958 | 5.31 | 321.604 |
| April | 5.73 | 333.713 | 5.72 | 333.542 | 5.70 | 332.458 | 5.65 | 330.459 | 5.58 | 327.541 | 5.50 | 323.699 |
| May | 5.98 | 359.054 | 5.85 | 353.527 | 5.69 | 346.571 | 5.50 | 338.143 | 5.28 | 328.199 | 5.04 | 316.690 |
| June | 6.44 | 369.242 | 6.26 | 362.040 | 6.04 | 353.277 | 5.78 | 342.880 | 5.50 | 330.774 | 5.19 | 316.880 |
| July | 6.36 | 381.327 | 6.19 | 374.590 | 5.99 | 366.281 | 5.76 | 356.333 | 5.50 | 344.676 | 5.21 | 331.235 |
| August | 6.17 | 373.298 | 6.07 | 369.349 | 5.94 | 363.928 | 5.78 | 356.991 | 5.59 | 348.490 | 5.36 | 338.369 |
| September | 6.26 | 361.202 | 6.27 | 361.674 | 6.25 | 360.707 | 6.19 | 358.293 | 6.09 | 354.408 | 5.96 | 349.019 |
| October | 6.15 | 363.482 | 6.34 | 371.090 | 6.50 | 377.224 | 6.62 | 381.939 | 6.71 | 384.090 | 6.76 | 384.090 |
| November | 5.24 | 308.871 | 5.50 | 320.293 | 5.72 | 330.076 | 5.92 | 338.281 | 6.08 | 344.967 | 6.22 | 350.184 |
| December | 4.16 | 260.396 | 4.38 | 272.546 | 4.58 | 283.154 | 4.76 | 292.249 | 4.91 | 299.860 | 5.04 | 306.017 |
| Annually | 5.53 | 3932.539 | 5.57 | 3961.950 | 5.58 | 3974.765 | 5.57 | 3970.928 | 5.53 | 3949.145 | 5.46 | 3909.645 |

The various results obtained from the simulation model by the variation of the number of occupants like daily hot water usage, the numbers of collectors, collector area, capacity, energy saved, solar fraction, GHG reduction, SPP, EPP, IRR, MIRR are summarised and presented in Table 4.6. These parameters have been used for the analysis of the feasibility of the residential model.

**Table 4.6: Variations of results**

| Case No. | Number of occupants | Daily hot water usage estimate (L/day) | Number of collectors | Solar collector area ($m^2$) | Capacity (kW) | Storage capacity (L) | Initial cost (USD) | Energy saved (MWh) | Solar fraction (%) | Gross annual GHG reduction ($tCO_2$) | Simple payback period (Yr.) | Equity payback period (Yr.) | Pre-tax IRR-equity (%) | Pre-tax MIRR-equity (%) |
|---|---|---|---|---|---|---|---|---|---|---|---|---|---|---|
| 1 | 3 | 180 | 02 | 5.60 | 3.0 | 100 | 4618 | 4.0 | 88.4 | 5.6 | 9.4 | 7.6 | 14.7 | 11.2 |
| 2 | 4 | 240 | 02 | 5.60 | 3.0 | 100 | 4618 | 4.4 | 72.6 | 6.1 | 8.6 | 7.1 | 15.9 | 11.6 |
| 3 | 5 | 300 | 03 | 8.30 | 4.5 | 150 | 4618 | 6.2 | 82.5 | 8.7 | 6.1 | 5.2 | 21.7 | 13.2 |
| 4 | 6 | 360 | 03 | 8.30 | 4.5 | 150 | 4618 | 6.6 | 72.6 | 9.2 | 5.8 | 5.0 | 22.7 | 13.5 |
| 5 | 7 | 420 | 04 | 11.1 | 6.0 | 200 | 4618 | 8.4 | 79.8 | 11.8 | 4.5 | 4.0 | 28.1 | 14.6 |
| 6 | 8 | 480 | 04 | 11.1 | 6.0 | 200 | 4618 | 8.8 | 72.6 | 12.3 | 4.3 | 3.8 | 29.1 | 14.8 |
| 7 | 9 | 540 | 04 | 11.1 | 6.0 | 200 | 4618 | 9.0 | 66.5 | 12.6 | 4.2 | 3.7 | 29.8 | 14.9 |
| 8 | 10 | 600 | 05 | 13.9 | 7.5 | 250 | 4618 | 10.9 | 72.6 | 15.3 | 3.5 | 3.1 | 35.3 | 15.8 |
| 9 | 11 | 660 | 05 | 13.9 | 7.5 | 250 | 4618 | 11.2 | 67.6 | 15.7 | 3.4 | 3.0 | 36.0 | 16.0 |
| 10 | 12 | 720 | 06 | 16.7 | 9.0 | 300 | 4618 | 13.1 | 72.6 | 18.4 | 2.9 | 2.6 | 41.4 | 16.7 |
| 11 | 13 | 780 | 06 | 16.7 | 9.0 | 300 | 4618 | 13.4 | 68.4 | 18.8 | 2.8 | 2.6 | 42.2 | 16.8 |
| 12 | 14 | 840 | 07 | 19.5 | 10.5 | 350 | 4618 | 15.3 | 72.6 | 21.4 | 2.5 | 2.3 | 47.5 | 17.4 |

### 4.2.2 Commercial case study

In this case study, the hostel campus of Rajiv Gandhi Institute of Petroleum Technology (R.G.I.P.T) in Jais, Amethi district of Uttar Pradesh, India has been chosen for the commercial model of the SWH system. Jais is located 31.6 km away from the main Raebareli city. The climate data of Raebareli is used for this simulation model through the RETScreen software. The hostel campus contains about 500 rooms for the accommodation of students and to fulfill the need of hot water requirement a 2 kW geyser system is in-built in each room. Due to the geyser, lots of electrical energy is consumed by it, which could be replaced by the simulated model of the SWH system in this case. The pictorial view of the facility location is shown in Figure 4.7 and the geographical coordinates are presented in Table 4.7.

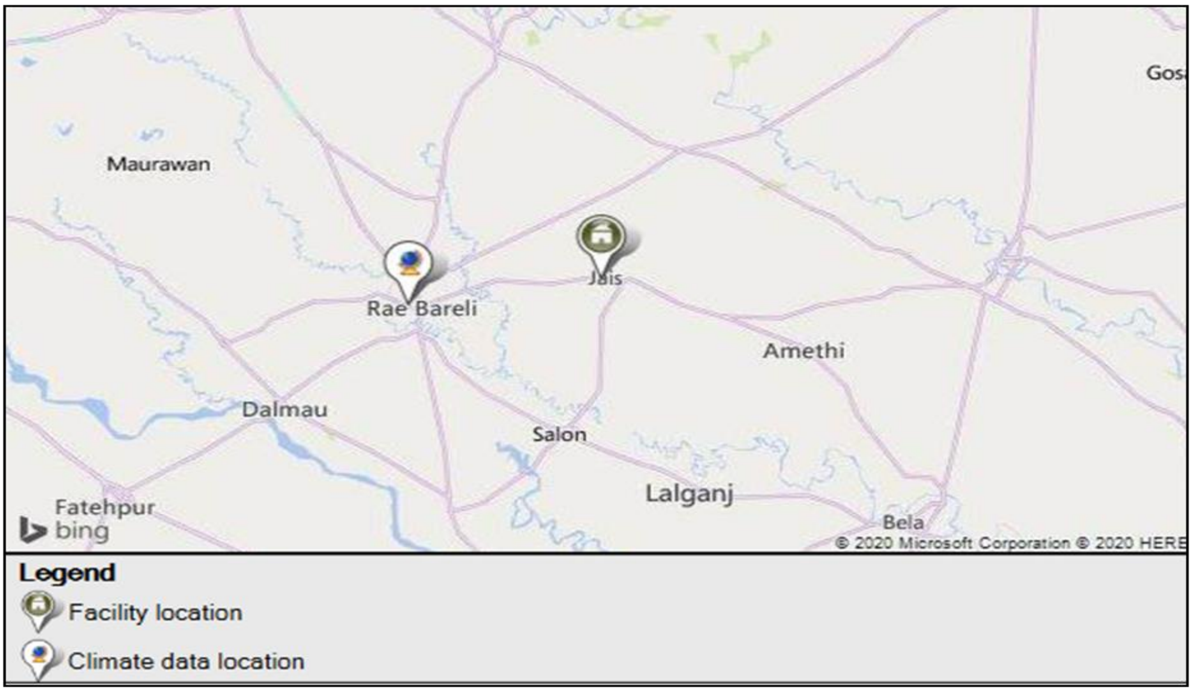


**Figure 4.7. Pictorial view of facility location**

**Table 4.7: Geographical coordinates of facility location**

| Particulars | Location | Latitude (°N) | Longitude(°E) | Climate zone | Elevation (m) |
|---|---|---|---|---|---|
| Facility | R.G.I.P.T | 26.3 | 81.5 | Very hot humid | 114 |

#### 4.2.2.1 Climate resource assessments

In this section of a commercial case study, some climatic parameters are chosen from the NASA database for modeling the commercial SWH system, like air temperature, relative humidity, daily solar radiation, wind speed, earth temperature, heating degree days, cooling degree days, etc. These climatic parameters are presented in Table 4.8.

**Table 4.8: Climate parameters of the selected location**

| Month | Air temperature (°C) | Relative humidity (%) | Daily solar radiation - horizontal ($kWh/m^2/d$) | Wind speed (m/s) | Earth temperature (°C) | Heating degree-days 18°C (°C-d) | Cooling degree-days 10°C (°C-d) |
|---|---|---|---|---|---|---|---|
| January | 15.7 | 41.2 | 3.81 | 2.7 | 14.9 | 71 | 177 |
| February | 19.4 | 33.9 | 4.88 | 3.0 | 19.0 | 0 | 263 |
| March | 25.8 | 22.9 | 6.03 | 3.4 | 26.2 | 0 | 490 |
| April | 32.1 | 16.2 | 6.61 | 3.5 | 33.3 | 0 | 663 |
| May | 36.1 | 20.1 | 6.69 | 3.6 | 38.2 | 0 | 809 |
| June | 36.0 | 37.6 | 5.84 | 3.7 | 38.1 | 0 | 780 |
| July | 31.5 | 67.5 | 4.74 | 3.5 | 32.3 | 0 | 667 |
| August | 29.5 | 78.6 | 4.47 | 3.2 | 29.7 | 0 | 605 |
| September | 27.7 | 80.3 | 4.57 | 2.9 | 27.7 | 0 | 531 |
| October | 25.0 | 62.5 | 4.93 | 2.1 | 24.4 | 0 | 465 |
| November | 20.8 | 47.4 | 4.35 | 2.1 | 19.6 | 0 | 324 |
| December | 16.8 | 43.6 | 3.72 | 2.3 | 15.4 | 37 | 211 |
| Annual | 26.4 | 46.1 | 5.05 | 3.0 | 26.6 | 109 | 5984 |

(Source: NASA Database)

The monthly variation of daily solar radiation-horizontal with an air temperature of the selected facility location is presented in Figure 4.8. It is observed from the figure that the daily solar radiation-horizontal is varied from 3.72 $kWh/m^2/d$ to 6.69 $kWh/m^2/d$. It is evaluated that the value of solar radiation-horizontal is greater than 3.5 $kWh/m^2/d$ for each month which is sufficient for generating heat energy for heating water at the facility location. The air temperature is varied in the range of 15.7 to 36.1 °C.

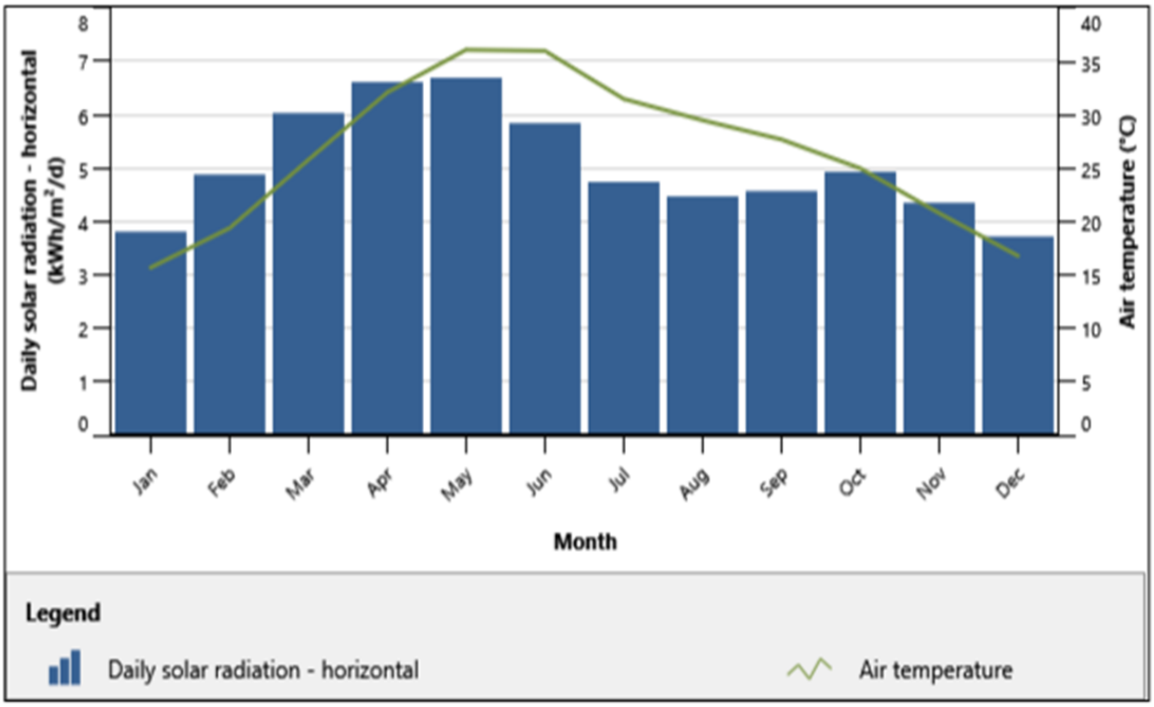


**Figure 4.8. Daily solar radiation-horizontal vs. air temperature**

#### 4.2.2.2 Simulation model

In this section, the simulation model of the commercial sector is analyzed by the variation of the number of rooms in the hostel facility. The variation in the number of rooms is taken from 50 to 500 rooms in the model. The variation of rooms shows how much this simulated model is feasible for different capacity requirements for hostels.

**(i) Simulation input parameters**

The simulation input parameters for the basic scenario model (1) are presented in Table 4.9.

**Table 4.9: Energy model input parameters for the basic scenario model (1)**

| Input Parameters | Values |
|---|---|
| Number of rooms | 50 to 500 |
| Occupancy rate (%) | 90 |
| Hot water temperature (°C) | 60 |
| Solar tracking mode | Fixed |
| Slope | 25° |
| Azimuth | 0 |
| Operating days per week | 7 |

| | |
|---|---|
| Solar water heater type | Evacuated |
| Miscellaneous losses (%) | 3 |
| Conventional fuel type | Electricity |
| Seasonal efficiency (%) | 90 |
| Electricity rate  annual (USD/kWh) | 0.17 |
| Fuel cost escalation rate (%) | 5 |
| Discount rate (%) | 8 |
| Reinvestment rate (%) | 9 |
| Inflation rate (%) | 4 |
| Project life (years) | 25 |
| Debt ratio (% of the initial cost) | 0 |
| Initial grant (% of the initial cost) | 0 |
| Annual O&M cost (USD) | 0 |
| GHG emission factor for coal ($tCO_2$/MWh) | 1.26 |

The technical specification of the selected model of the SWH system for simulation purposes is presented in Table 4.10.

**Table 4.10: Technical specifications of commercial SWH system**

| Parameters | Evacuated tube collector |
|---|---|
| Manufacturer | Thermomax |
| Model | MS 20 - TMO 500 |
| Gross area per solar collector ($m^2$) | 2.779 |
| Aperture area per solar collector ($m^2$) | 2.135 |
| Fr (tau alpha) coefficient | 0.578 |
| Fr UL coefficient ($W/m^2$)/°C | 1.05 |
| Temperature coefficient for Fr UL | 0 |

**(ii) Simulation output parameters**

To evaluate the optimum tilt angle for maximum heating delivered, the variations of daily solar radiation-tilted and heating delivered at different tilt angles are presented in Table 4.11.

**Table 4.11: Variations of daily solar radiation-tilted and heating delivered at the different tilt angles**

| Tilt angle | 25° | | 30° | | 35° | | 40° | | 45° | | 50° | |
|---|---|---|---|---|---|---|---|---|---|---|---|---|
| Month | Daily solar radiation-tilted ($kWh/m^2/d$) | Heating Delivered (kWh) | Daily solar radiation-tilted ($kWh/m^2/d$) | Heating Delivered (kWh) | Daily solar radiation-tilted ($kWh/m^2/d$) | Heating Delivered (kWh) | Daily solar radiation-tilted ($kWh/m^2/d$) | Heating Delivered (kWh) | Daily solar radiation-tilted ($kWh/m^2/d$) | Heating Delivered (kWh) | Daily solar radiation-tilted ($kWh/m^2/d$) | Heating Delivered (kWh) |
| January | 4.98 | 24919.45 | 5.13 | 25591.20 | 5.24 | 26114.85 | 5.33 | 26490.32 | 5.38 | 26717.59 | 5.40 | 26840.819 |
| February | 5.92 | 26454.26 | 6.03 | 26861.66 | 6.10 | 27128.23 | 6.13 | 27254.26 | 6.13 | 27239.87 | 6.09 | 27128.431 |
| March | 6.64 | 32149.70 | 6.65 | 32174.59 | 6.61 | 32044.15 | 6.54 | 31758.07 | 6.43 | 31315.77 | 6.28 | 30764.664 |
| April | 6.59 | 30512.09 | 6.47 | 30074.75 | 6.32 | 29494.96 | 6.13 | 28771.51 | 5.90 | 27903.10 | 5.65 | 26931.35 |
| May | 6.22 | 29579.83 | 6.02 | 28828.55 | 5.79 | 27936.08 | 5.53 | 26900.98 | 5.24 | 25722.13 | 4.94 | 24489.387 |
| June | 5.30 | 24777.59 | 5.12 | 24043.19 | 4.91 | 23192.51 | 4.67 | 22225.73 | 4.42 | 21170.67 | 4.16 | 20089.768 |
| July | 4.40 | 21620.90 | 4.27 | 21041.18 | 4.12 | 20364.85 | 3.95 | 19593.32 | 3.76 | 18729.65 | 3.57 | 17854.729 |
| August | 4.33 | 21523.51 | 4.23 | 21100.97 | 4.12 | 20582.06 | 3.99 | 19967.99 | 3.84 | 19260.32 | 3.67 | 18493.004 |
| September | 4.74 | 22663.01 | 4.69 | 22487.78 | 4.63 | 22206.90 | 4.54 | 21820.74 | 4.43 | 21329.81 | 4.29 | 20769.804 |
| October | 5.74 | 27732.70 | 5.81 | 27998.07 | 5.84 | 28124.10 | 5.84 | 28111.00 | 5.80 | 27958.75 | 5.73 | 27710.549 |
| November | 5.65 | 26530.41 | 5.81 | 27172.62 | 5.93 | 27662.97 | 6.02 | 28002.47 | 6.07 | 28191.92 | 6.08 | 28275.632 |
| December | 5.03 | 24922.20 | 5.21 | 25698.82 | 5.35 | 26323.10 | 5.46 | 26795.32 | 5.53 | 27115.84 | 5.57 | 27329.010 |
| Annually | 5.46 | 313385.71 | 5.45 | 313073.42 | 5.41 | 311174.81 | 5.34 | 307691.75 | 5.24 | 302655.48 | 5.11 | 296677.151 |

The various results obtained from the simulation model by the variations like the number of rooms, daily hot water usage, the number of collectors, collector area, capacity, energy saved, solar fraction, GHG reduction, SPP, EPP, IRR, and MIRR are summarised and presented in Table 4.12. These parameters are used for the analysis of the feasibility of a commercial model.

**Table 4.12: Variations of the results**

| Case No. | Number of rooms | Daily hot water usage estimate (L/day) | Number of collectors | Solar collector area ($m^2$) | Capacity (kW) | Storage capacity (L) | Initial cost (USD) | Energy saved (MWh) | Solar fraction (%) | Gross annual GHG reduction ($tCO_2$) | Simple payback period (Yr.) | Equity payback period (Yr.) | Pre-tax IRR-equity (%) | Pre-tax MIRR-equity (%) |
|---|---|---|---|---|---|---|---|---|---|---|---|---|---|---|
| 1 | 50 | 3411 | 14 | 38.9 | 20.9 | 3000 | 312593 | 31.6 | 64.7 | 44.2 | 19.6 | 15.3 | 6.8 | 8.2 |
| 2 | 100 | 6822 | 28 | 77.8 | 41.8 | 6000 | 312593 | 63.2 | 64.7 | 88.4 | 14.3 | 11.9 | 11.1 | 10.2 |
| 3 | 150 | 10233 | 42 | 117 | 62.8 | 9000 | 312593 | 94.8 | 64.7 | 132.6 | 11.2 | 9.8 | 15.2 | 12 |
| 4 | 200 | 13644 | 56 | 156 | 83.7 | 12000 | 312593 | 126 | 64.7 | 176.8 | 9.2 | 8.4 | 19.4 | 13.7 |
| 5 | 250 | 17055 | 70 | 195 | 105 | 15000 | 312593 | 158 | 64.7 | 221.1 | 7.8 | 7.3 | 23.8 | 15.5 |
| 6 | 300 | 20466 | 83 | 231 | 124 | 18000 | 312593 | 188 | 64.1 | 262.8 | 6.9 | 6.5 | 28.3 | 17.3 |
| 7 | 350 | 23877 | 97 | 270 | 145 | 21000 | 312593 | 219 | 64.2 | 307.0 | 6.1 | 5.8 | 33.7 | 19.4 |
| 8 | 400 | 27288 | 111 | 308 | 166 | 24000 | 312593 | 251 | 64.3 | 351.2 | 5.4 | 5.3 | 39.7 | 21.1 |
| 9 | 450 | 30699 | 125 | 347 | 187 | 27000 | 312593 | 283 | 64.3 | 395.5 | 4.9 | 4.4 | 46.6 | 21.8 |
| 10 | 500 | 34110 | 139 | 386 | 208 | 30000 | 312593 | 314 | 64.4 | 439.7 | 4.5 | 3.1 | 54.3 | 22.4 |

### 4.2.3 Industrial case study

In this case study, the Ludhiana district of Punjab state of India is chosen for the industrial model of the SWH system. It is one of the richest cities for industries in India. The main industries in this city are the production of bicycle parts and hosiery manufacturing units. The hosiery industry requires a large amount of hot water throughout the year which is generally fulfilled by electrical sources; it consumes lots of electrical energy. This electrical source could be replaced by the simulated SWH system to make more profits in the business models. Ludhiana falls under the composite climate and receives good solar radiation of 5.5 kWh/m$^2$/day. The pictorial view of the facility location is shown in Figure 4.9 and the geographical coordinates are presented in Table 4.13.


**Figure 4.9. Pictorial view of facility location**

**Table 4.13: Geographical coordinates of the facility location**

| Facility location | Latitude (°N) | Longitude (°E) | Climate zone | Elevation (m) |
|---|---|---|---|---|
| Ludhiana | 30.9 | 75.8 | Very hot-dry | 247 |

#### 4.2.3.1 Climate resource assessments

In this section of the industrial case study, some climatic parameters are chosen from the NASA database for modeling the industrial SWH system, like air temperature, relative humidity, daily solar radiation, wind speed, earth temperature, heating degree days, cooling degree days, etc. These climatic parameters are presented in Table 4.14.

**Table 4.14: Climate parameters of the selected location**

| Month | Air temperature (°C) | Relative humidity (%) | Daily solar radiation - horizontal (kWh/m$^2$/d) | Wind speed (m/s) | Earth temperature (°C) | Heating degree-days 18°C (°C-d) | Cooling degree-days 10°C (°C-d) |
|---|---|---|---|---|---|---|---|
| January | 12.9 | 40.0 | 3.50 | 2.6 | 11.9 | 158 | 90 |
| February | 16.0 | 38.4 | 4.42 | 2.9 | 15.5 | 56 | 168 |
| March | 22.3 | 30.8 | 5.61 | 3.0 | 22.3 | 0 | 381 |
| April | 28.9 | 22.5 | 6.60 | 3.1 | 29.7 | 0 | 567 |
| May | 34.6 | 18.1 | 6.48 | 3.1 | 36.4 | 0 | 763 |
| June | 36.3 | 28.3 | 6.36 | 2.9 | 38.3 | 0 | 789 |
| July | 34.0 | 49.6 | 5.95 | 2.6 | 35.4 | 0 | 744 |
| August | 31.6 | 60.0 | 5.73 | 2.3 | 32.5 | 0 | 670 |
| September | 29.5 | 53.7 | 5.67 | 2.1 | 30.0 | 0 | 585 |
| October | 25.2 | 36.6 | 4.92 | 2.3 | 24.7 | 0 | 471 |
| November | 19.8 | 30.9 | 4.18 | 2.4 | 18.6 | 0 | 294 |
| December | 14.9 | 34.4 | 3.38 | 2.5 | 13.5 | 96 | 152 |
| Annual | 25.5 | 37.0 | 5.23 | 2.6 | 25.8 | 310 | 5674 |

(Source: NASA Database)

The monthly variation of daily solar radiation-horizontal with an air temperature of the selected facility location is presented in Figure 4.10. It is observed from the figure that the daily solar radiation-horizontal is varied from 3.38 kWh/m$^2$/d to 6.60 kWh/m$^2$/d. It can be evaluated that apart from one month (i.e. December) the value of solar radiation-horizontal is greater than 3.5 kWh/m$^2$/d, which is sufficient for generating heat energy for heating water at the facility location. The air temperature is varied in the range of 12.9 to 36.3 °C.

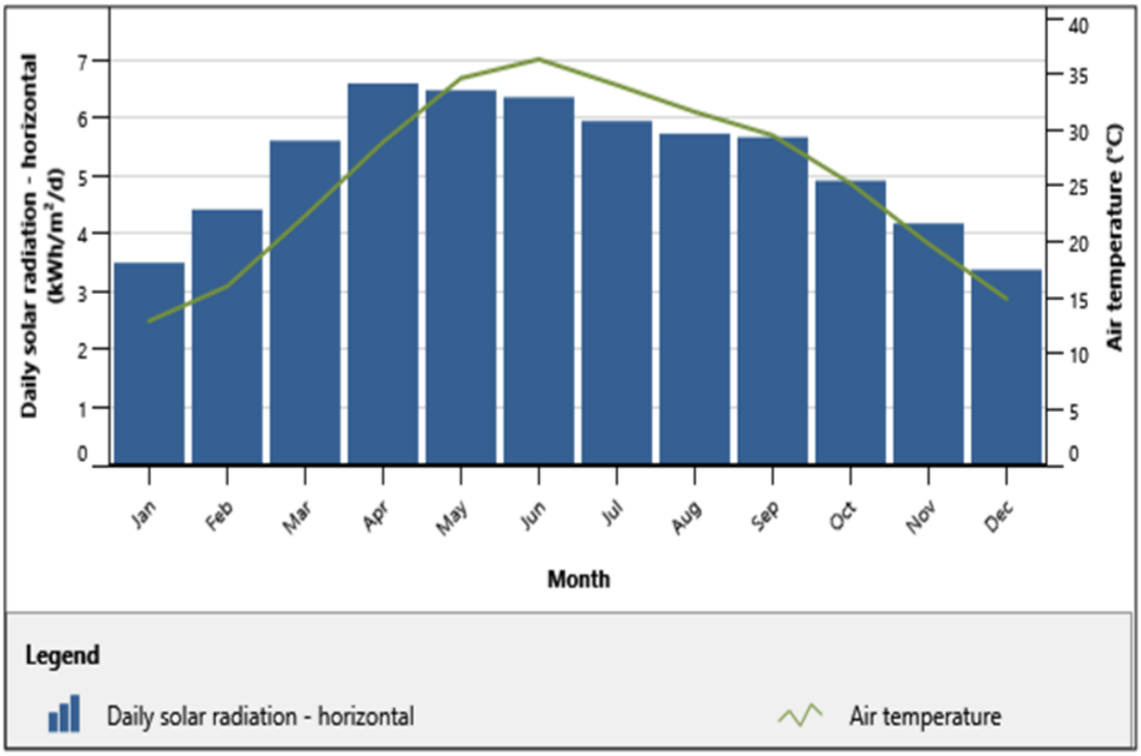


**Figure 4.10. Daily solar radiation-horizontal vs. air temperature**

### 4.2.3.2 Simulation model

In this section, the simulation model of the industrial sector is analyzed by variation of estimated daily hot water requirements at the facility location. The range of this variation is from 3000 L/day to 15000 L/day. The different values of variations are taken so that the simulated model could be applicable to small, medium, and large size industries.

#### (i) Simulation input parameters

The simulation input parameters for the basic scenario model (1) are presented in Table 4.15

**Table 4.15: Energy model input parameters for the basic scenario model (1)**

| Input parameters | Values |
|---|---|
| Daily hot water usage-estimated (L/day) | 3000 to 15000 |
| Occupancy rate (%) | 100 |
| Hot water temperature (°C) | 80 |
| Solar tracking mode | Fixed |
| Slope | 30° |
| Azimuth | 0 |
| Operating days per week | 7 |
| Solar water heater type | Evacuated |
| Miscellaneous losses (%) | 4 |
| Conventional fuel type | Electricity |
| Seasonal efficiency (%) | 90 |
| Electricity rate annual (USD/kWh) | 0.17 |
| Fuel cost escalation rate (%) | 5 |
| Discount rate (%) | 8 |
| Reinvestment rate (%) | 9 |
| Inflation rate (%) | 4 |
| Project life (years) | 25 |
| Debt ratio (% of the initial cost) | 0 |
| Initial grant (% of the initial cost) | 0 |
| Annual O&M cost (USD) | 0 |
| GHG emission factor for coal ($tCO_2$/MWh) | 1.26 |

The technical specification of the selected model of the SWH system for simulation purposes is presented in Table 4.16.

**Table 4.16: Technical specifications of industrial SWH system**

| Parameters | Evacuated tube collector |
|---|---|
| Manufacturer | Thermomax |
| Model | MS 20 - TMO 500 |
| Gross area per solar collector ($m^2$) | 2.779 |
| Aperture area per solar collector ($m^2$) | 2.135 |
| Fr(tau alpha) coefficient | 0.578 |
| Fr UL coefficient (W/$m^2$)/°C | 1.05 |
| Temperature coefficient for Fr UL | 0 |

### (ii) Simulation output parameters

To evaluate the optimum tilt angle for maximum heating delivered, the variations of daily solar radiation-tilted and heating delivered at different tilt angles are presented in Table 4.17.

**Table 4.17: Variations of daily solar radiation-tilted and heating delivered at the different tilt angle**

| Tilt Angle | 25° | | 30° | | 35° | | 40° | | 45° | | 50° | |
|---|---|---|---|---|---|---|---|---|---|---|---|---|
| Month | Daily solar radiation-tilted ($kWh/m^2/d$) | Heating Delivered (kWh) | Daily solar radiation-tilted ($kWh/m^2/d$) | Heating Delivered (kWh) | Daily solar radiation-tilted ($kWh/m^2/d$) | Heating Delivered (kWh) | Daily solar radiation-tilted ($kWh/m^2/d$) | Heating Delivered (kWh) | Daily solar radiation-tilted ($kWh/m^2/d$) | Heating Delivered (kWh) | Daily solar radiation-tilted ($kWh/m^2/d$) | Heating Delivered (kWh) |
| January | 4.86 | 632.238 | 5.05 | 657.023 | 5.21 | 677.607 | 5.33 | 693.833 | 5.42 | 705.574 | 5.47 | 712.740 |
| February | 5.50 | 656.215 | 5.62 | 670.774 | 5.71 | 681.264 | 5.76 | 687.605 | 5.78 | 689.750 | 5.76 | 687.681 |
| March | 6.35 | 839.600 | 6.39 | 844.708 | 6.39 | 844.792 | 6.36 | 839.849 | 6.28 | 829.919 | 6.17 | 815.076 |
| April | 6.75 | 863.507 | 6.67 | 852.390 | 6.54 | 836.380 | 6.38 | 815.597 | 6.18 | 790.201 | 5.95 | 760.384 |
| May | 6.16 | 813.422 | 5.99 | 792.116 | 5.80 | 766.585 | 5.58 | 737.023 | 5.32 | 703.654 | 5.05 | 666.732 |
| June | 5.87 | 750.336 | 5.68 | 726.732 | 5.47 | 699.385 | 5.23 | 668.503 | 4.96 | 634.321 | 4.68 | 598.291 |
| July | 5.57 | 736.382 | 5.41 | 715.494 | 5.23 | 690.963 | 5.02 | 662.974 | 4.78 | 631.742 | 4.52 | 597.736 |
| August | 5.66 | 748.166 | 5.56 | 734.258 | 5.42 | 716.454 | 5.26 | 694.889 | 5.07 | 669.726 | 4.85 | 641.159 |
| September | 6.13 | 783.974 | 6.12 | 782.374 | 6.07 | 776.265 | 5.99 | 765.694 | 5.87 | 750.742 | 5.72 | 731.519 |
| October | 6.01 | 794.467 | 6.13 | 809.548 | 6.20 | 819.685 | 6.24 | 824.801 | 6.24 | 824.856 | 6.20 | 819.851 |
| November | 5.80 | 740.801 | 6.03 | 769.113 | 6.21 | 792.428 | 6.35 | 810.571 | 6.45 | 823.401 | 6.51 | 830.821 |
| December | 4.89 | 637.329 | 5.11 | 665.984 | 5.30 | 690.317 | 5.45 | 710.142 | 5.56 | 725.305 | 5.64 | 735.690 |
| Annually | 5.80 | 8996.437 | 5.81 | 9020.514 | 5.79 | 8992.124 | 5.74 | 8911.479 | 5.66 | 8779.189 | 5.54 | 8597.681 |

The various results obtained from the simulation model by the variations of estimated daily hot water usage like the number of collectors, collector area, capacity, energy saved, solar fraction, GHG reduction, SPP, EPP, IRR, MIRR are summarised and presented in Table 4.18. These parameters are used for the analysis of the feasibility of the industrial model.

**Table 4.18: Variations of results**

| Case No. | Daily hot water usage estimate (L/day) | Number of collectors | Solar collector area ($m^2$) | Capacity (kW) | Initial cost (USD) | Energy saved (MWh) | Solar fraction (%) | Gross annual GHG reduction ($tCO_2$) | Simple payback period (Yr.) | Equity payback period (Yr.) | Pre-tax IRR-equity (%) | Pre-tax MIRR-equity (%) |
|---|---|---|---|---|---|---|---|---|---|---|---|---|
| 1 | 3000 | 3 | 8.3 | 4.5 | 15800 | 09.0 | 13 | 12.6 | 9.3 | 7.5 | 15.2 | 10.8 |
| 2 | 4000 | 4 | 11.1 | 6.0 | 15800 | 12.0 | 13 | 16.8 | 7.0 | 5.9 | 19.5 | 12.1 |
| 3 | 5000 | 5 | 13.9 | 7.5 | 15800 | 15.0 | 13 | 21.0 | 5.6 | 4.8 | 23.6 | 13.1 |
| 4 | 6000 | 6 | 16.7 | 9.0 | 15800 | 18.0 | 13 | 25.2 | 4.6 | 4.1 | 27.5 | 13.9 |
| 5 | 7000 | 7 | 19.5 | 10.5 | 15800 | 21.0 | 13 | 29.5 | 4.0 | 3.5 | 31.3 | 14.7 |
| 6 | 8000 | 8 | 22.2 | 12.0 | 15800 | 24.1 | 13 | 33.7 | 3.5 | 3.1 | 35.1 | 15.3 |
| 7 | 9000 | 9 | 25.0 | 13.5 | 15800 | 27.1 | 13 | 37.9 | 3.1 | 2.8 | 38.9 | 15.8 |
| 8 | 10000 | 10 | 27.8 | 14.9 | 15800 | 30.1 | 13 | 42.1 | 2.8 | 2.5 | 42.7 | 16.3 |
| 9 | 11000 | 11 | 30.6 | 16.4 | 15800 | 33.1 | 13 | 46.3 | 2.5 | 2.3 | 46.5 | 16.7 |
| 10 | 12000 | 12 | 33.3 | 17.9 | 15800 | 36.1 | 13 | 50.5 | 2.3 | 2.1 | 50.3 | 17.2 |
| 11 | 13000 | 13 | 36.1 | 19.4 | 15800 | 39.1 | 13 | 54.7 | 2.1 | 2.0 | 54.1 | 17.5 |
| 12 | 14000 | 14 | 38.9 | 20.9 | 15800 | 42.1 | 13 | 58.9 | 2.0 | 1.8 | 57.8 | 17.9 |
| 13 | 15000 | 15 | 41.7 | 22.4 | 15800 | 45.1 | 13 | 63.1 | 1.9 | 1.7 | 61.6 | 18.2 |

### 4.3. Result and discussion

#### 4.3.1 Optimum tilt angle for the collector

The heat generated by the solar panel varies according to the tilt angle of the panel. So there is a requirement to find the optimum tilt angle at which the generated heat is maximum. In the case of installing the SWH system, it is found that the tilt angle is not varied according to sessions; otherwise, the capital cost of the unit will be increased. It is recommended that at one angle at the time of installation, the panels will be fixed for all sessions. In the present study, the monthly variation of daily solar radiation- tilted and heat delivered by the panels at various tilt angles are shown in Table 4.5, Table 4.11, and Table 4.17 for residential, commercial, and industrial sectors respectively. To find the optimum tilt angle, the annual variation of solar radiation- tilted at various tilt angles i.e. 25°, 30°, 35°, 40°, 45°, and 50° for the residential, commercial, and industrial models have been drawn in figure 4.11. The heat delivered by the collector at various tilt angles is plotted in Figure 4.12 for the residential, commercial, and industrial models respectively.

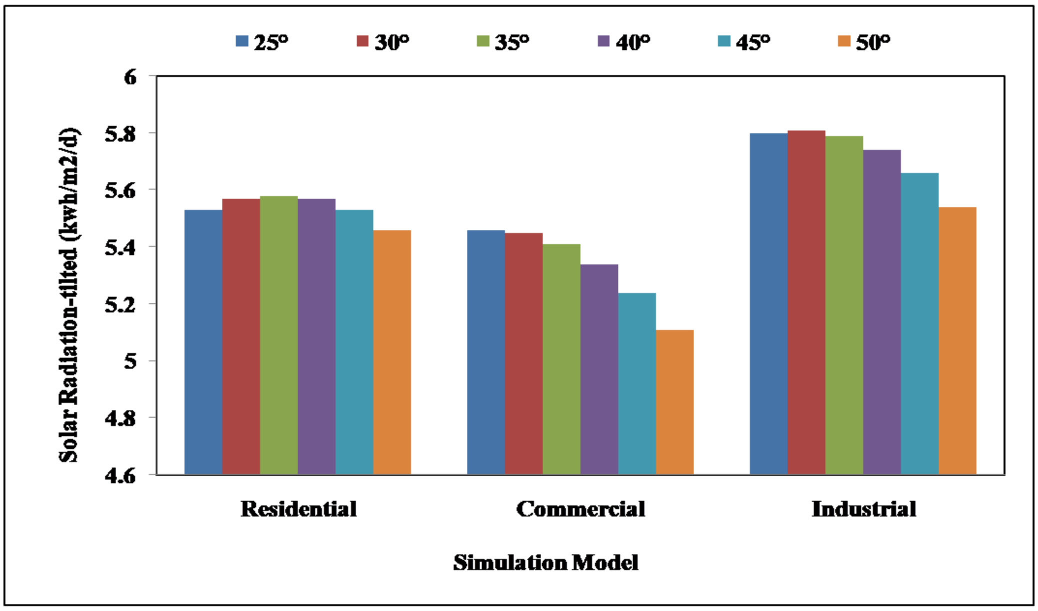


**Figure 4.11. Annual values of solar radiation tilted at different tilt angles**

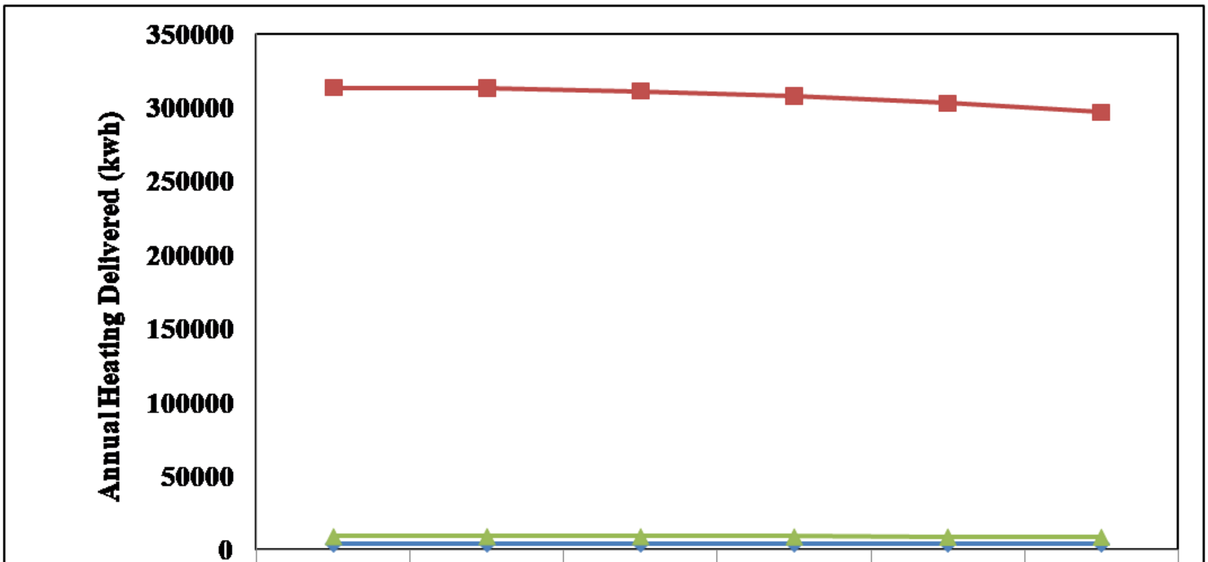


| | 25° | 30° | 35° | 40° | 45° | 50° |
|---|---|---|---|---|---|---|
| Residential | 3932.539 | 3961.95 | 3974.766 | 3970.928 | 3949.145 | 3909.645 |
| Commercial | 313385.71 | 313073.42 | 311174.81 | 307691.75 | 302655.48 | 296677.151 |
| Industrial | 8996.437 | 9020.514 | 8992.124 | 8911.479 | 8779.189 | 8597.681 |

**Figure 4.12. Annual heating is delivered at different tilt angles at all facility locations**

It is found from Figures 4.11 and 4.12, that the optimum tilt angle for residential, commercial, and industrial models is 35°, 25°, and 30° respectively. The values of solar radiation-tilted and heating delivered at these values are maximum among other values of tilt. The values of solar radiation- tilted for residential, commercial, and industrial models are 5.58, 5.46, and 5.81 kWh/m$^2$/d respectively and values of heating delivered are 3974.766, 313385.71, and 9020.514 kWh respectively. In the present study, these optimum angles of tilt are used for modeling of SWH system.

### 4.3.2 Performance evaluation and energy savings

The performance of the SWH system is calculated by an SF. It is recommended, that the value of an SF of SWH systems having storage capacity should be above 50 %, and without storage capacity, it should be usually less than 15 %. Here, for the case of a residential model, the simulation model presents the range of SF that had been listed in Table 4.6. This table indicates the variation of SF from 66.5 % to 88.4 % for occupants of 9 and 3 respectively. In the case of a commercial model, it can be found in Table 4.12 which states that the SF varies from 64.1 % to 64.7 %. The variation of the SF of these two models is well above the desired value of 50 % so the simulated model of residential and commercial is feasible according to the performance evaluation parameter. While, in the case of the industrial model, there is no requirement for storage capacity so the SF must be below 15 % which is evident from Table 4.18 for all cases of estimated hot water requirement it is 13 %. This shows that this industrial model is also feasible according to performance evaluation. The comparative variations of SF values of all three models of all cases have been presented in Figure 4.13.

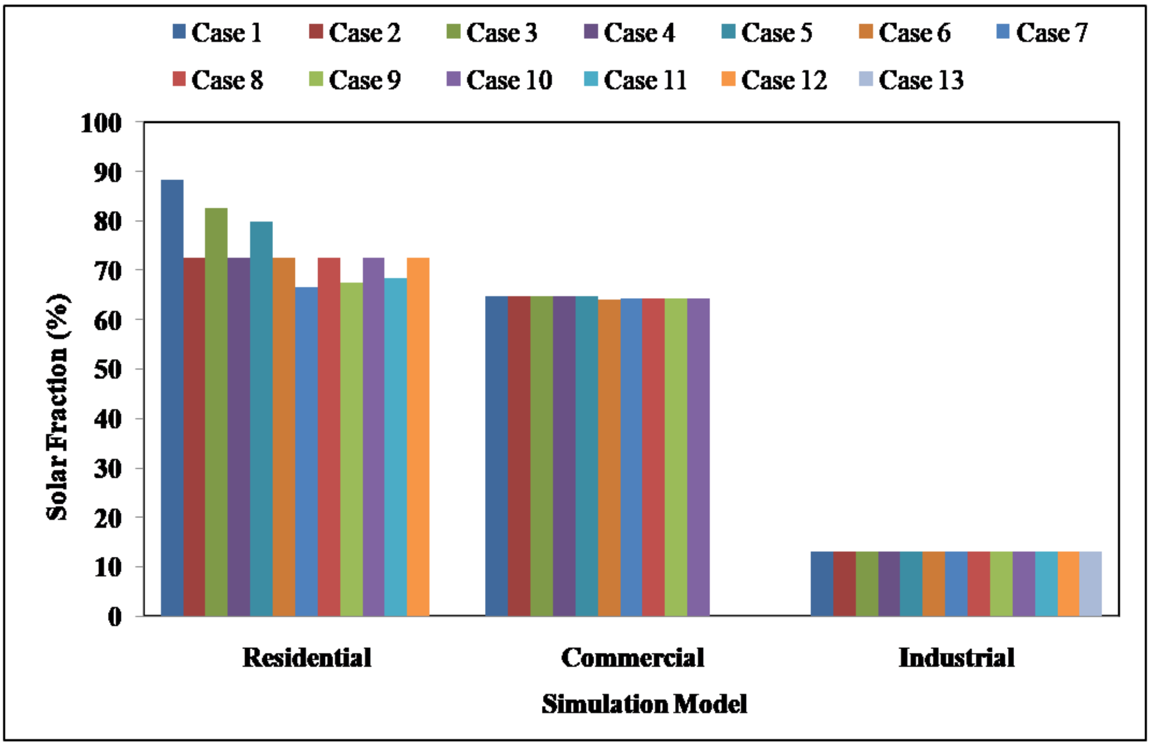


**Figure 4.13. Solar fraction of all three models**

The annual heating energy saved represents the amount of the proposed case heating energy use on the heating system that is reduced as a result of implementing the proposed case end-use. It is directly related to the SF, for the higher value of the SF, there will be higher energy-saving potential. The variations of the energy-saving potential of all three models are presented in Figure 4.14. In the case of the residential model, the minimum and maximum value of energy savings are 4.0 MWh and 15.3 MWh for the number of occupants 3 and 14 respectively. From the figure, it can be also observed that the amount of energy savings regularly increases as the number of occupants increases. It is also calculated from the figure that the cumulative value of energy-saving for this model is 111.3 MWh for all occupants ranging from 3 to 14. In the case of the commercial model, the minimum and maximum value of energy savings are 31.6 MWh and 314 MWh for the number of rooms of 50 and 500 respectively. It can be evaluated from Figure 4.14 that the energy-saving potential increases linearly as the number of rooms increases. The cumulative value of energy-saving for this model is 1728.6 MWh for all numbers of rooms ranging from 50 to 500. While, in the case of the industrial model, the minimum and maximum values of energy savings are 9 MWh and 45.1 MWh corresponding to the estimated daily hot water usage of 3000 L/day and 15000 L/day respectively. It is also evaluated from the figure that energy savings increase linearly as estimated daily hot water usage increases.

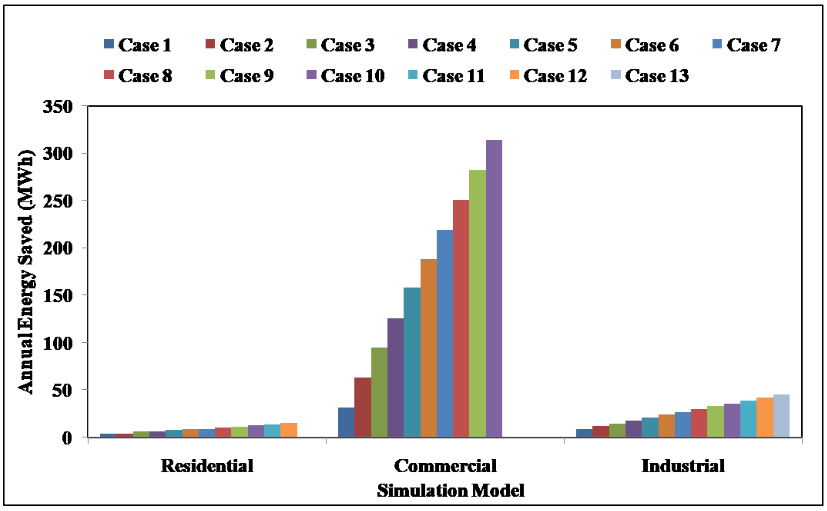


**Figure 4.14. Annual energy saving potentials of all three models**

### 4.3.3 Greenhouse gas emission reduction potential

The SWH system is a clean energy technology hence it does not emit any greenhouse gases into the environment. By, using the SWH system in place of the conventional fuel-based system i.e. electric geysers, it saves a plenty amount of greenhouse gas emissions. Here the calculation of GHG reduction is based on the emissions for both, the base case and the proposed case systems on an annual basis. Units are provided in equivalent tonnes of $CO_2$ emissions per year (i.e. $tCO_2$/yr.). In the case of the residential model, the minimum and maximum values of annual GHG reduction potentials are 5.6 $tCO_2$ and 21.4 $tCO_2$ per year corresponding to the number of occupants of 3 and 14. From Figure 4.15, it can be evaluated that the variation of annual GHG reduction is increasing linearly along with the increase in the number of occupants. The cumulative value of gross annual GHG reduction potential is 155.9 $tCO_2$/yr. In the case of the commercial model, the minimum and maximum values of annual GHG reduction potentials are 44.2 $tCO_2$ and 439.7 $tCO_2$ per year corresponding to the number of rooms of 50 and 500. It had been observed from Figure 4.15 that these values of GHG reduction increase linearly with an increase in the number of rooms. The cumulative value of gross annual GHG reduction potential is 2419.3 $tCO_2$/yr. While in the case of the industrial model, the minimum and maximum values of gross annual GHG reduction potentials are 12.6 $tCO_2$ and 63.1 $tCO_2$ per year corresponding to the estimated daily hot water usage of 3000 L/day and 15000 L/day. It has been also evaluated from Figure 4.15 that the amount of gross annual GHG reduction potential increases linearly as the value of estimated daily hot water usage increases. The cumulative value of gross annual GHG reduction potential is 492.3 $tCO_2$/yr.

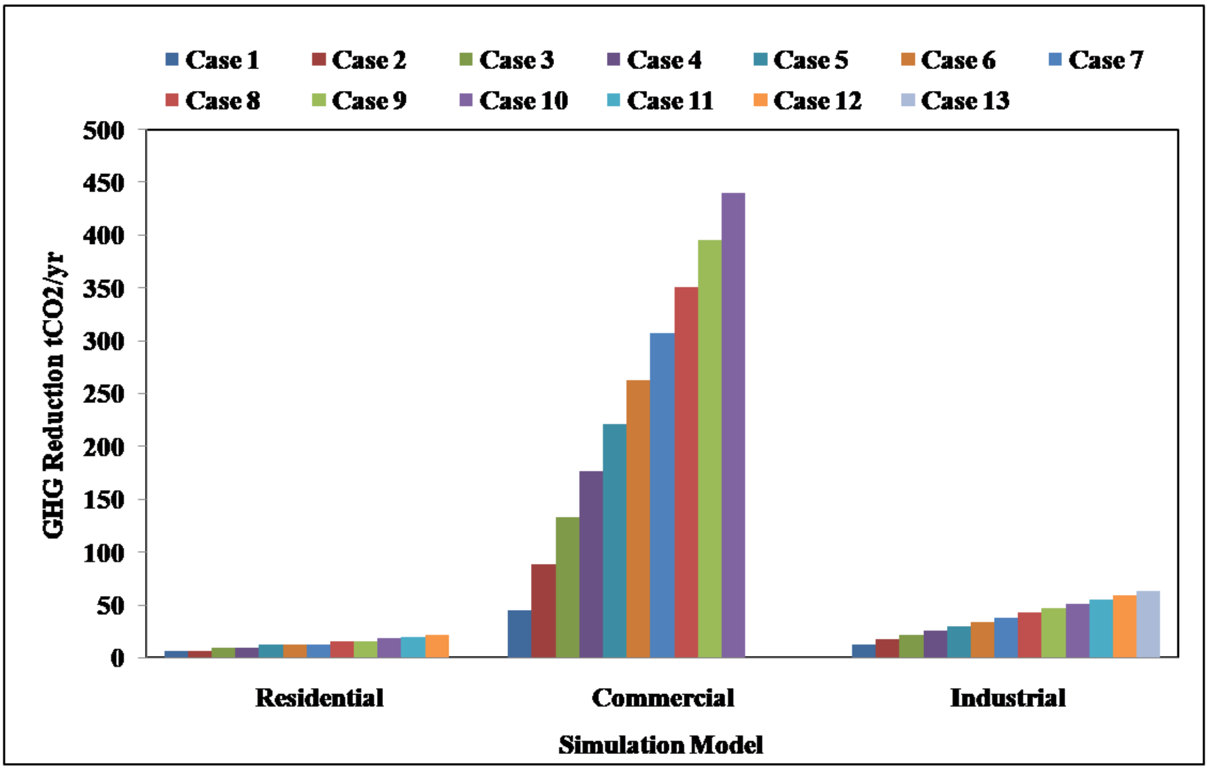


**Figure 4.15. The gross annual GHG reduction potential of all three models**

### 4.3.4 Financial viability analysis

In this section, the financial viability of SWH systems for all three models i.e. residential, commercial, and industrial have been analyzed through financial terms of SPP, EPP, IRR, and MIRR as,

#### 4.3.4.1 Simple payback period and equity payback period

The SPP is the most desirable parameter of financial viability for deciding to get approval for SWH system projects. Its positive value denotes the number of years to recoup its initial cost like 1 year, 1.5 years, 2 years, etc. While, the negative value is an indication that the annual costs incurred are higher than the annual savings generated, which is not desirable in the case of renewable energy projects. The comparative variations of SPP have been plotted in Figure 4.16 for all three modes of the SWH system included in this study. In the case of the residential model, looking at Table 4.6, the variation of SPP is from 9.4 years to 2.5 years for the number of occupants of 3 and 14. It has been evaluated from Figure 4.16 that the values of SPP are decreasing as the values of the number of occupants increase regularly. It means that the simulated model is more beneficial if the number of occupants is high. The average value of SPP of all considered numbers of occupants in the residential model is 4.83 years, which denotes the financial viability as per the SPP. In the case of the commercial model from Table 4.12, the maximum and minimum value of SPP is 19.6 years and 4.5 years corresponding to the number of rooms 50 and 500. It has been observed from Figure 4.16 that the value of SPP is regularly decreasing as the number of rooms increases in the simulation model. The average value of SPP for this commercial model including all number of rooms in the simulated model is 8.99 years. In the case of the industrial model from Table 4.18, the maximum and minimum values of SPP are 9.3 years and 1.9 years corresponding to the estimated daily hot water usage of 3000 L/day and 15000 L/day respectively. The values of SPP for this model decrease as the value of the estimated daily hot water usage increases as shown in Figure 4.16. The average value of SPP for this model is 3.90 years including all variations of estimated daily hot water usage of the model.

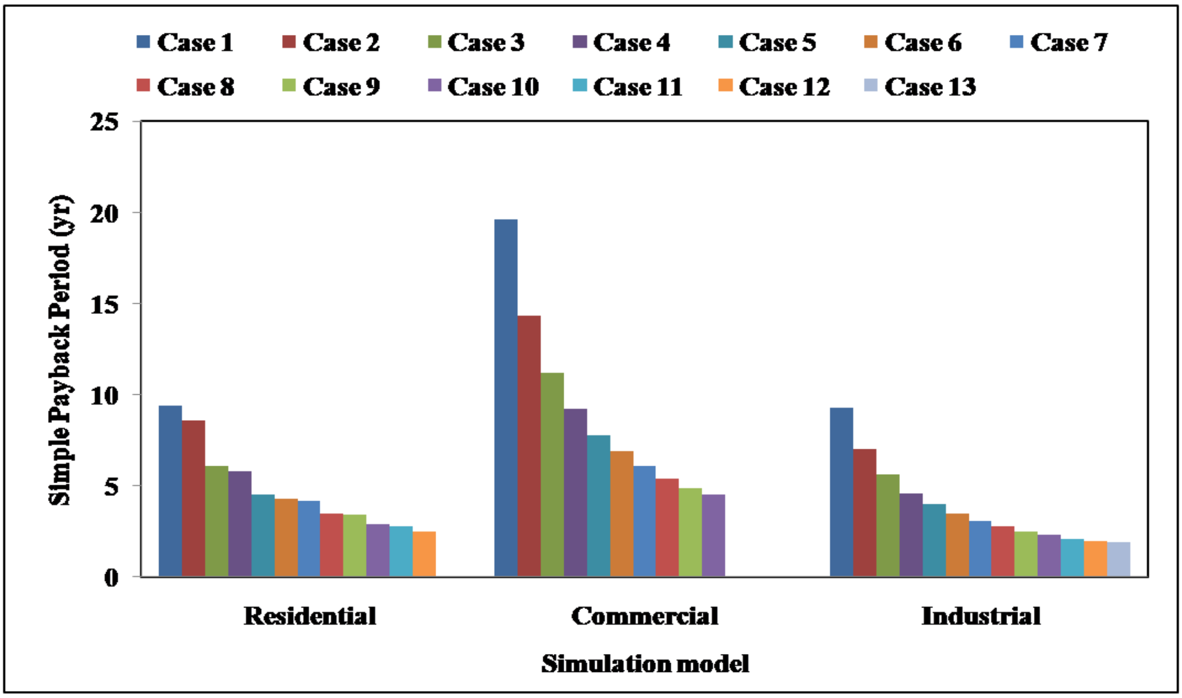


**Figure 4.16. The simple payback period for all three models**

The cumulative cash flow graphs showing the payback period for the residential model (number of occupants of 14), commercial model (number of rooms of 500), and industrial model (estimated daily hot water of 15000 L/day) have been shown in Figure 4.17, 4.18, and 4.19 respectively.

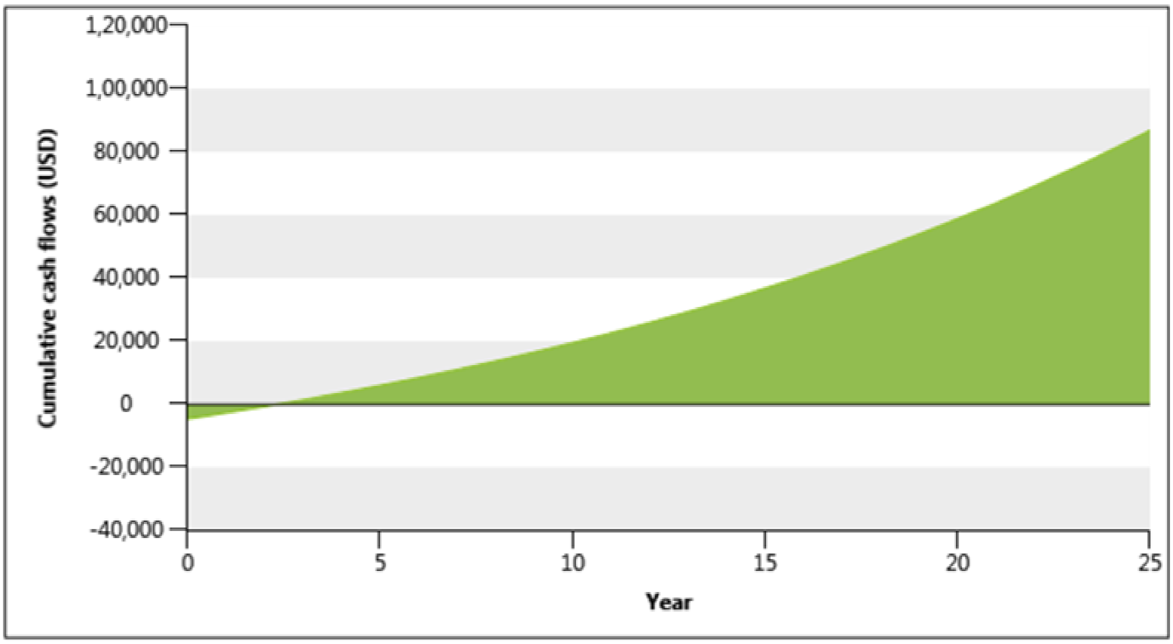


**Figure 4.17. Cumulative cash flow for the residential sector (number of occupants 14)**

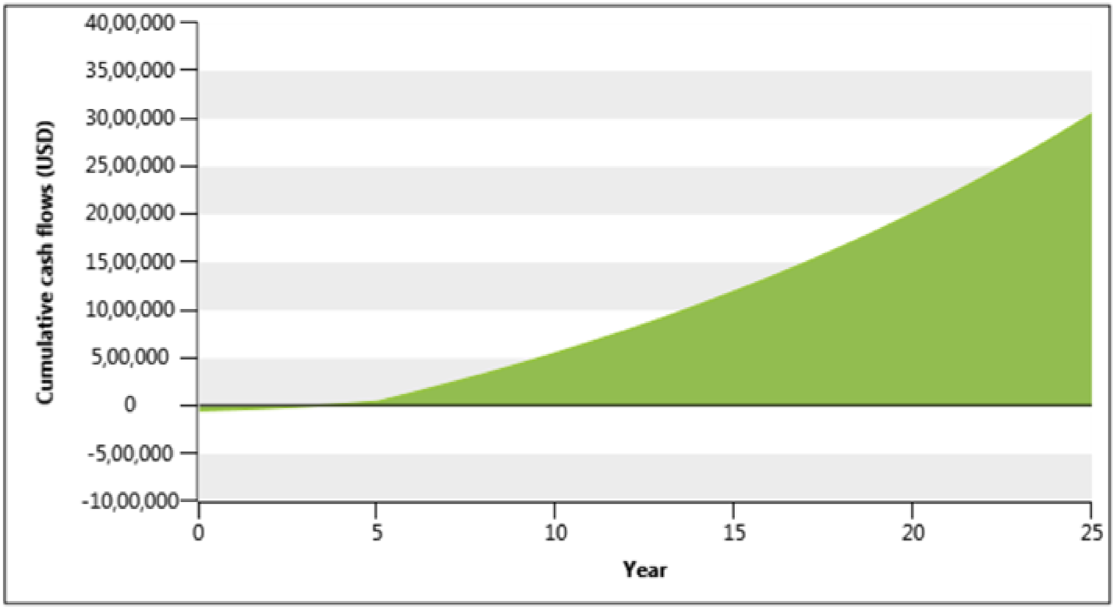


**Figure 4.18. Cumulative cash flow for the commercial sector (number of rooms 500)**

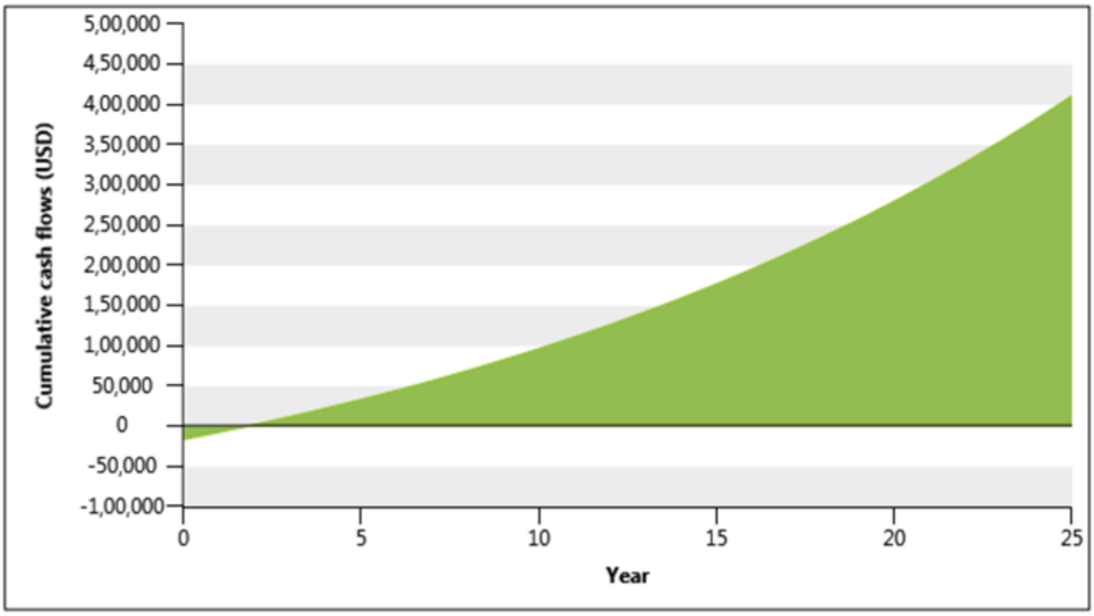


**Figure 4.19. Cumulative cash flow for the industrial sector (daily hot water 15000 L/day)**

The EPP considers project cash flows from its inception as well as the leverage (i.e. level of debt) of the project, which makes it a better time indicator of the project merits than the simple payback. The energy model uses the year number and the cumulative after-tax cash flows to calculate this value. In the case of the residential model, from Table 4.6, the maximum and minimum values of EPP are 7.6 years and 2.3 years corresponding to the number of occupants of 3 and 14 respectively. The EPP is decreasing if the number of occupants increases as shown in Figure 4.20. The average value of EPP for this model is 4.16 years considering the variations of all occupants from 3 to 14 in the model. In the case of the commercial model from Table 4.12, the maximum and minimum values of EPP are 15.3 years and 3.1 years corresponding to the number of rooms of 50 and 500 respectively. It is observed from Figure 4.20 that EPP is decreasing with the increase in the number of rooms from 50 to 500. The average value of EPP for this model is 7.78 years when including the number of rooms from 50 to 500. While, in the case of the industrial model from Table 4.18, the maximum and minimum values of EPP are 7.5 years and 1.7 years corresponding to the estimated daily hot water usage of 3000 L/day and 15000 L/day respectively. It is also observed from Figure 4.20 that the value of EPP is decreasing as estimated daily hot water usage increases. The average value of EPP after considering all values of estimated daily hot water usage from 3000 L/day to 15000 L/day, is 3.39 years.

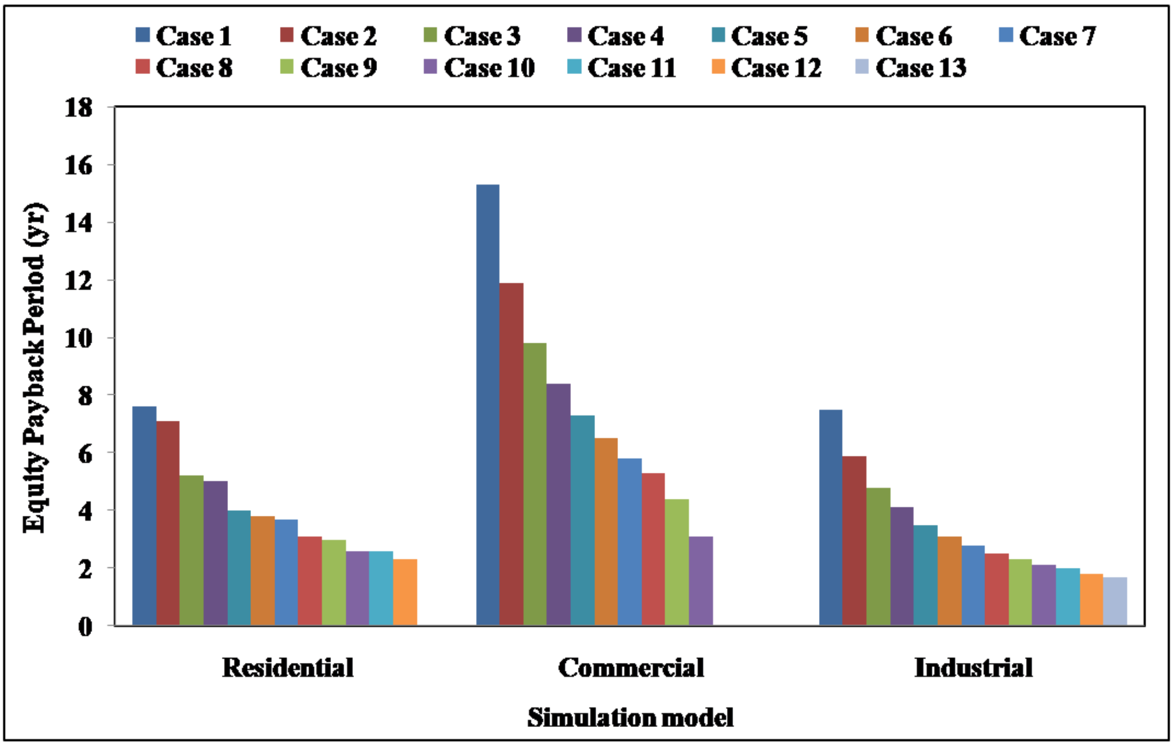


**Figure 4.20. Equity payback period of all three models**

### 4.3.4.2 Internal rate of return and modified internal rate of return

The IRR on percentage equity is evaluated using the pre-tax yearly cash flows and project life. If the IRR is equal to or greater than the required rate of return then the project will likely be considered acceptable financially. If it is less than the required rate of return, the project is rejected. The comparative analysis of the IRR of all included models is shown in Figure 4.21. In the case of a residential model from Table 4.6, the minimum and maximum values of IRR are 14.7 % and 47.5 %. It has been evaluated from Figure 4.21 that the values of IRR are increasing linearly with an increase in the number of rooms in the model. The average value of IRR after including all numbers of occupants ranging from 3 to 14 is 30.36 %. In the case of a commercial model, from Table 4.12, the minimum and maximum values of IRR are 6.8 % and 54.3 %. From Figure 4.21, the values of IRR increase linearly as the number of rooms increases. The average value of IRR including all numbers of rooms ranging from 50 to 500 is 27.89 %. While in the case of the industrial model, the minimum and maximum values of IRR are 15.2 % and 61.6 % corresponding to the estimated daily hot water usage of 3000 L/day and 15000 L/day. It has been observed from Figure 4.21 that the values of IRR are increasing linearly as the value of estimated daily hot water usage increases.

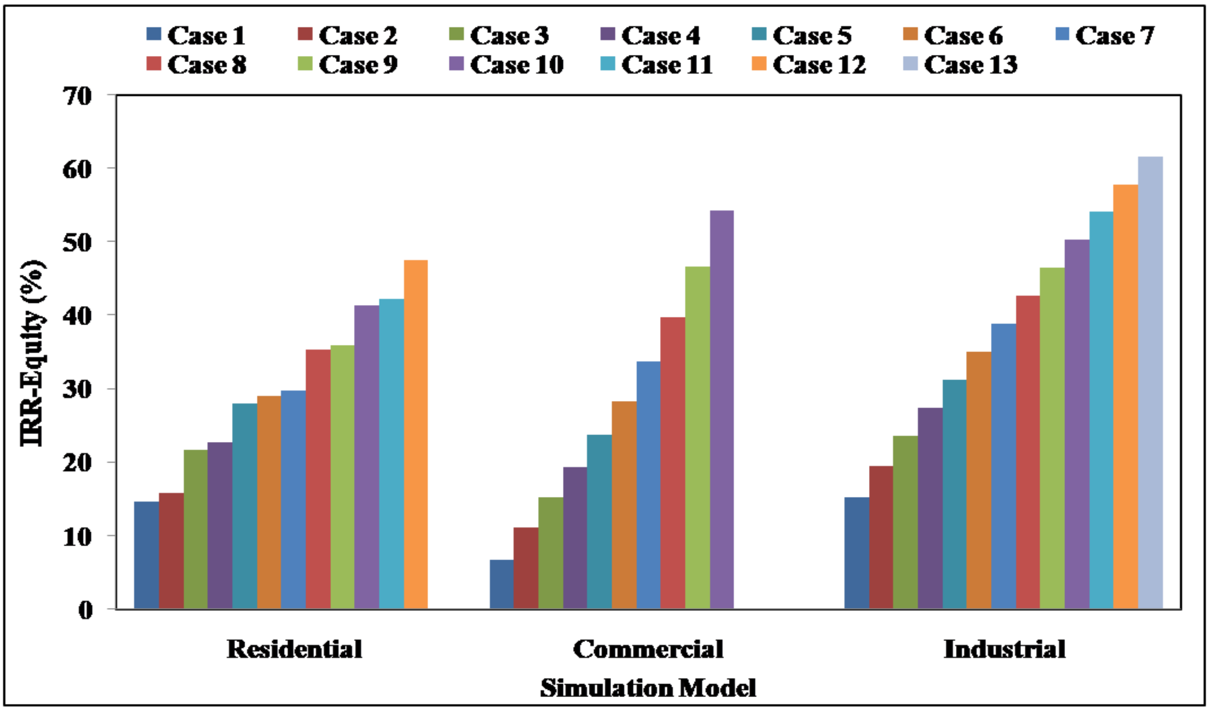


**Figure 4.21. Internal rate of return of all three models**

The modified internal rate of return is a financial viability parameter similar to the IRR. It is evaluated as the pre-tax modified internal rate of return on percentage equity, which represents the cost and profitability provided by the project equity over its life before income tax. It is calculated using the pre-tax yearly cash flows, the project life, the discount rate, and the reinvestment rate. If the MIRR is equal to or greater than the required rate of return then the project will likely be considered financially acceptable. If it is less than the required rate of return, the project will be rejected. The comparative analysis of MIRR for all included models is shown in Figure 4.22. In the case of a residential model from Table 4.6, the minimum and maximum values of MIRR are 11.2 % and 17.4 %. From Figure 4.22, the values of MIRR increase linearly as the values of the number of occupants increase. The average value of MIRR for this model is 14.70 %. In the case of a commercial model from Table 4.12, the minimum and maximum values of MIRR are 8.2 % and 22.4 % corresponding to the number of rooms of 50 and 500 respectively. It has been observed from Figure 4.22 that the MIRR increases linearly as the values of the number of rooms increase from 50 to 500. The average value of MIRR is 16.16 % for this model. While, in the case of the industrial model from Table 4.18, the minimum and maximum values of MIRR are 10.8 % and 18.2 % corresponding to values of estimated daily hot water usage of 3000 L/day and 15000 L/day respectively. It has been observed from Figure 4.22 that the MIRR is increasing linearly as the value of estimated daily hot water usage increases. The average value of MIRR for this model is 15.34 %.

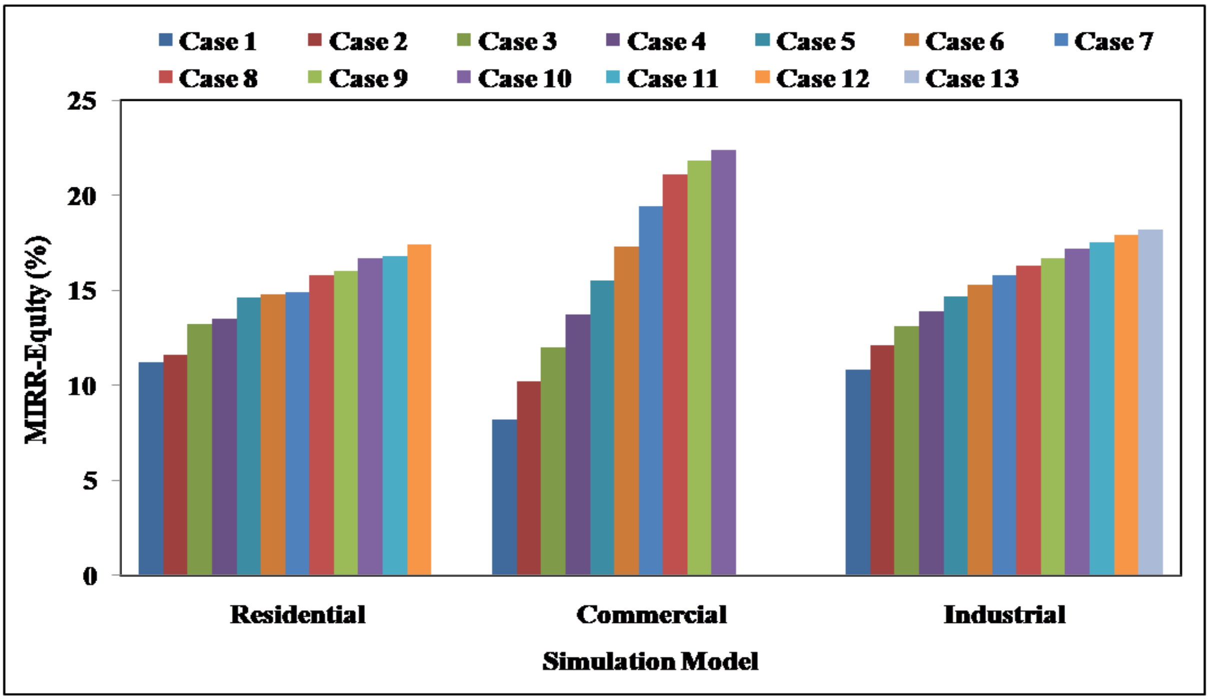


**Figure 4.22. Modified internal rate of return of all three models**

# Chapter 5: Numerical simulation for the storage tank of the SWH system

It is observed that the SWH systems are getting attention now these days, but not at the desired pace it should be. The main reason behind it is low thermal efficiency. It is evident from many studies that PCMs have the excessive potential of storing latent heat to improve the thermal performance of the storage tank of the SWH system.

So there is a requirement for the simulated model that could be proficient in presenting the benefits of using various types of PCMs of different thermophysical properties and melting temperatures in the form of their effectiveness for the storage tank of the SWH system. The presented chapter describes the required simulation model and by application of this model, the various types of PCMs of different thermophysical properties and melting temperatures can be tested theoretically for the required design criteria of the storage tank of the SWH system.

This chapter evaluates the effectiveness of various enumerated PCMs along with the effect of enhancing the thermal performance of the storage tank of the SWH system by the application of the simulation model. After that, it presents the melt fraction analysis of all enumerated PCMs for different container materials to recognize the suitable container material by making a coding program on the FORTRAN programming language for various container materials. The detailed analysis has been presented in the following subsequent sections as,

## 5.1. Introduction

There is a variation of incident solar radiation at each geographical location throughout each day of the year i.e., from morning to evening, due to this variation, the amount of heat stored in the water is not enough according to the prerequisite. This uneven variation of solar radiation leads to accumulating energy in another form, i.e. latent heat, as an energy reservoir to compensate for the time of demand. At the present age of time, SWH technology is moderately and adequately matured through many research studies and there is continuous effort is going on to enhance the thermal efficiency of the storage tank of the SWH system. In this sequence, the Thermal Energy Storage (TES) medium in the form of PCMs for the storage tank is evaluated by many studies and it is found that the PCMs have great potential for storing heat in the form of latent heat. Thus, thermal stratification of encapsulated PCMs is an emerging effective phenomenon for improving the thermal efficiency of the storage tank of SWH systems. The PCMs are capable of storing heat energy during the daytime duration when these materials are incorporated inside the storage tank. And when heat is required during off-sunshine hours, these materials provide the heating action of water. The PCMs absorb heat in the form of latent heat and these materials are capable of exchanging heat energy with water in several thermal cycles. These materials are generally kept inside metallic containers in submerged conditions of the water. When the temperature of the water around these containers rises from the melting temperature of PCM, then PCM becomes melted inside of these containers and latent heat is stored in the PCM. And when the temperature of the water goes down well below from solidification temperature of PCMs then heating of water by the PCMs takes place. The storing heat of PCMs along with the temperature rise has been shown in Figure 5.1. It is also observed that when PCMs are kept inside container materials in an encapsulated condition then the overall size requirement of the storage tank could be decreased up to an appreciable amount. So, by using PCMs inside the storage tank, the existing design of the storage tank can be reduced compactly. Here one thing should be noted the selection of PCMs should be also important for successfully improving the performance of the storage tank of the SWH system. The selected materials should be capable of storing an appreciable amount of heat energy within themselves.

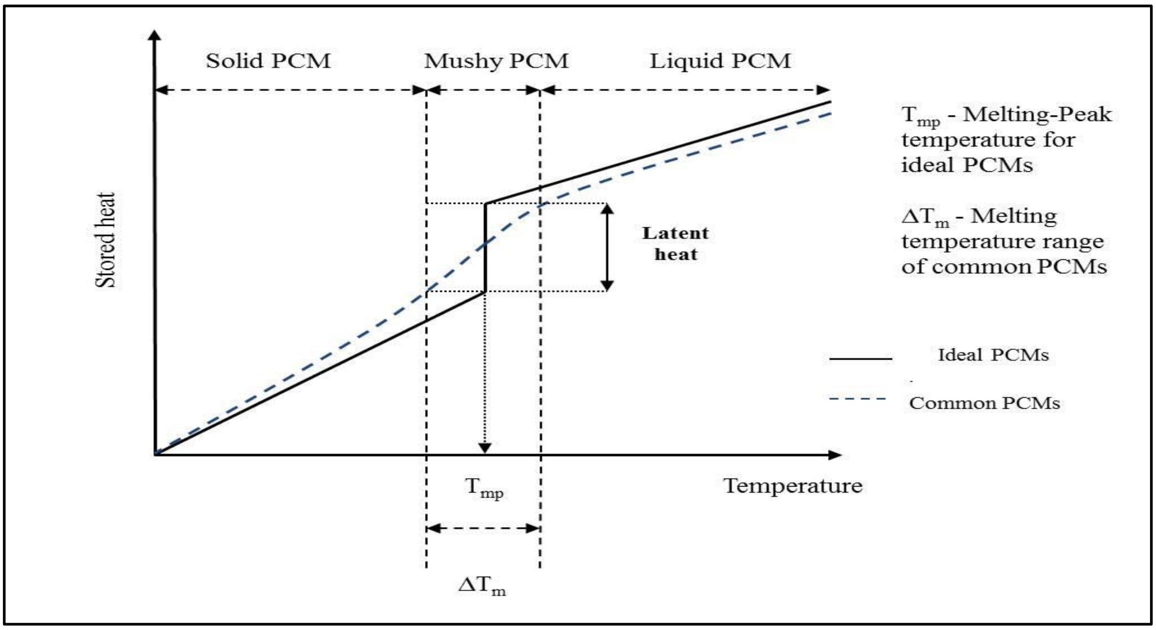


**Figure 5.1. Stored heat of PCMs**

### 5.1.1 Desired properties of PCM for encapsulation in the storage tank of the SWH system

In this section, some of the most important desired properties of PCMs for encapsulation purposes in the storage tank of SWHs are presented as,

- Thermal Properties

During the encapsulation of PCMs, they should be in the desired temperature range of phase transition. It is also favorable that PCMs should have high latent heat of transition along with high thermal conductivity.

- Physical Properties

According to the need for physical properties, the PCMs should have high density, low vapor pressure, negligible volume change, and desired phase equilibrium.

- Kinetic properties

According to the need for kinetic properties, PCMs should have an adequate rate of crystallization along with no supercooling.

- Chemical properties

In case of desirable chemical properties, PCMs should not be decomposed and they have to be in chemical stability for a long duration of time. It is also desirable that PCMs have good compatibility with encapsulated container materials along with non-toxic, non-explosive, and non-flammable in nature.

- Technical criteria

According to the requirement of technical criteria, it is desirable that the PCMs should be reliable, effective, compatible, and viable in nature for storage inside tanks of SWHs.

- Economics

According to the economic point of view of PCMs, they should be available at a cheaper cost for use in the storage tank of SWHs.

### 5.1.2 Suitable compounds used as PCMs for storage tank of SWH system

Many substances proved themselves as suitable PCMs for storing heat energy. Among them few are listed here in Tables 5.1 – 5.5, these substances are the most suitable materials for encapsulation purposes as PCMs in the storage tank of the SWH system.

These materials are recommended due to their favorable properties of melting temperature and latent heat of fusion.

**Table 5.1: Inorganic compounds as PCMs**

| Compound | Melting temperature, $T_m$ (°C) | Heat of fusion (kJ/Kg) | References |
|---|---|---|---|
| $LiNO_3.3H_2O$ | 30.0 | 296.0 | B. Zalba et al. [72] |
| $Na_2SO_4.10H_2O$ | 31-32 | -- | B. Zalba et al. [72] |
| | 32.0 | 251.1 | B. Zalba et al. [72] |
| | 32.4 | 254.0 | A. Abhat.[73]<br>R. Naumann et al.[74]<br>D.W. Hawes et al.[75] |
| $Na_2CO_3.10H_2O$ | 33.0 | 247.0 | R. Naumann et al.[74] |
| | 32.0-36.0 | 246.5 | B. Zalba et al. [72] |
| $CaBr_2.6H_2O$ | 34.0 | 115.5 | I. Dincer et al.[76]<br>R. Naumann et al.[74]<br>G.A. Lane.[77] |
| $Na_2HPO_4.12H_2O$ | 35.0 | 281.0 | D.W. Hawes et al.[75] |
| | 35.2 | -- | R. Naumann et al.[74] |
| | 35.5 | 265.0 | B. Zalba et al. [72] |
| | 36.0 | 280.0 | B. Zalba et al. [72] |
| $Zn(NO_3)_2.6H_2O$ | 36.0 | 146.9 | I. Dincer et al.[76]<br>R. Naumann et al.[74]<br>G.A. Lane.[77] |
| | 36.4 | 147.0 | A. Abhat.[73]<br>D.W. Hawes et al.[75] |
| $KF.2H_2O$ | 41.4 | -- | R. Naumann et al.[74] |
| $K(CH_3COO).1\frac{1}{2}H_2O$ | 42.0 | -- | B. Zalba et al. [72] |
| $K_3PO_4.7H_2O$ | 45.0 | -- | B. Zalba et al. [72] |

| | | | |
|---|---|---|---|
| $Zn(NO_3)_2.4H_2O$ | 45.5 | -- | B. Zalba et al. [72] |
| $Ca(NO_3)_2.4H_2O$ | 42.7 | -- | R. Naumann et al.[74] |
| | 47.0 | -- | B. Zalba et al. [72] |
| $Na_2\ HPO_4.7H_2O$ | 48.0 | -- | R. Naumann et al.[74] |
| $Na_2S_2O_3.5H_2O$ | 48.0 | 201.0 | A. Abhat.[73]<br>R. Naumann et al.[74] |
| | 48.0-49.0 | 209.3 | B. Zalba et al. [72] |
| $Zn(NO_3)_2.2H_2O$ | 54.0 | -- | B. Zalba et al. [72] |
| $NaOH.H_2O$ | 58.0 | -- | R. Naumann et al.[74] |
| $Na(CH_3COO).3H_2O$ | 58.0 | 264.0 | B. Zalba et al. [72] |
| | 58.4 | 226.0 | R. Naumann et al.[74]<br>B. Zalba et al. [72] |
| $Cd(NO_3)_2.4H_2O$ | 59.5 | -- | R. Naumann et al.[74] |
| $Fe(NO_3)_2.6H_2O$ | 60.0 | -- | B. Zalba et al. [72] |
| NaOH | 64.3 | 227.6 | B. Zalba et al. [72] |
| $Na_2B_4O_7.10H_2O$ | 68.1 | -- | R. Naumann et al.[74] |
| $Na_3PO_4.12H_2O$ | 69.0 | -- | R. Naumann et al.[74] |
| $Na_2P_2O_7.10H_2O$ | 70.0 | 184.0 | B. Zalba et al. [72] |
| $Ba(OH)_2.8H_2O$ | 78.0 | 265.7 | A. Abhat.[73]<br>I. Dincer et al.[76]<br>R. Naumann et al.[74]<br>G.A. Lane.[77]<br>B. Zalba et al. [72] |
| | --- | 267.0 | |
| | --- | 280.0 | |
| $AlK(SO_4)_2.12H_2O$ | 80.0 | -- | B. Zalba et al. [72] |
| $Kal(SO_4)_2.12H_2O$ | 85.8 | -- | R. Naumann et al.[74] |
| $Al_2(SO_4)_3.18H_2O$ | 88.0 | -- | R. Naumann et al.[74] |
| $Al(NO_3)_3.8H_2O$ | 89.0 | -- | B. Zalba et al. [72] |
| $Mg(NO_3)_2.6H_2O$ | 89.0 | 162.8 | I. Dincer et al.[76]<br>G.A. Lane.[77] |
| | 90.0 | 149.5 | R. Naumann et al.[74]<br>B. Zalba et al. [72] |
| $(NH_4)Al(SO_4).6H_2O$ | 95.0 | 269.0 | B. Zalba et al. [72] |
| $Na_2S.5\frac{1}{2}H_2O$ | 97.5 | -- | B. Zalba et al. [72] |

**Table 5.2: Inorganic eutectics as PCMs**

| Compound | Melting temperature, $T_m$ (ºC) | Heat of fusion (kJ/Kg) | References |
|---|---|---|---|
| 47% $Ca(NO_3)_2.4H_2O$+33% $Mg(NO_3)_2.6H_2O$ | 30 | 136 | A. Abhat.[73] |
| 60% $Na(CH_3COO).3H_2O$+40% $CO(NH_2)_2$ | 30 | 200.5 | B. Zalba et al. [72] |
| | 31.5 | 226 | |
| 61.5% $Mg(NO_3)_2.6H_2O$ + 38.5% $NH_4NO_3$ | 52.0 | 125.5 | G.A. Lane.[77] |
| | -- | -- | |
| | -- | -- | |
| 58.7% $Mg(NO_3).6H_2O$ + 41.3% $MgCl_2.6H_2O$ | 58.0 | 132.0 | B. Zalba et al. [72] |
| | --- | -- | |
| | --- | -- | |
| | 59.0 | 132.2 | G.A. Lane.[77] |
| 53% $Mg(NO_3)_2.6H_2O$ + 47% $Al(NO_3)_2.9H_2O$ | 61.0 | 148.0 | A. Abhat.[73] |
| 14% $LiNO_3$+86% $Mg(NO_3)_2.6H_2O$ | 72 | 180.0 | B. Zalba et al. [72] |
| 66.6% urea + 33.4% $NH_4Br$ | 76 | 161.0 | G.A. Lane.[77] |
| | --- | -- | |
| | --- | -- | |
| | --- | -- | |

**Table 5.3: Organic compounds as PCMs**

| Compound | Melting temperature, $T_m$ (°C) | Heat of fusion (kJ/Kg) | References |
|---|---|---|---|
| Paraffin $C_{18}$ | 27.5 | 243.5 | K. Sasaguchi et al. [78] |
| | --- | -- | |
| | 28.0 | 244.0 | A. Abhat.[73] |
| 1-Tetradecanol | 38.0 | 205.0 | D.W. Hawes et al.[75] |
| Paraffin $C_{16}$-$C_{28}$ | 42.0-44.0 | 189.0 | A. Abhat.[73] |
| Paraffin $C_{20}$-$C_{33}$ | 48.0-50.0 | 189.0 | A. Abhat.[73] |
| Paraffin $C_{22}$-$C_{45}$ | 58.0-60.0 | 189.0 | A. Abhat.[73] |
| Paraffin wax | 64.0 | 173.6 | I. Dincer et al.[76] |
| | --- | 266 | |
| | --- | --- | |
| Polyglycol E6000 | 66.0 | 190.0 | I. Dincer et al.[76] G.A. Lane.[77] |
| Paraffin $C_{21}$-$C_{50}$ | 66.0-68.0 | 189.0 | A. Abhat.[73] |
| Biphenyl | 71.0 | 119.2 | I. Dincer et al.[76] G.A. Lane.[77] |
| Propionamide | 79.0 | 168.2 | G.A. Lane. [77] |
| Naphthalene | 80.0 | 147.7 | I. Dincer et al.[76] G.A. Lane. [77] |
| | --- | --- | |

### Table 5.4: Fatty acids as PCMs

| Compound | Melting temperature, $T_m$ (°C) | Heat of fusion (kJ/Kg) | References |
|---|---|---|---|
| Vinyl stearate | 27.0-29.0 | 122.0 | D. Feldman et al.[79] |
| Capric acid | 31.5 | 153.0 | A. Abhat [73] |
| | --- | --- | |
| | 32 | 152.7 | I. Dincer et al.[76] G.A. Lane.[77] |
| Methyl-12 hydroxy-stearate | 42.0-43.0 | 120.0-126.0 | D. Feldman et al.[79] |
| Lauric acid | 42.0-44.0 | 178.0 | A. Abhat.[73] |
| | 44.0 | 177.4 | G.A. Lane.[77] |
| Myristic acid | 49.0-51.0 | 204.5 | B. Zalba et al.[72] |
| | 54.0 | 187.0 | A. Abhat.[73] |
| | 58.0 | 186.6 | G.A. Lane.[77] |
| Palmitic acid | 61.0 | 203.4 | A.Sari.et.al.[80] |
| | 63.0 | 187.0 | A. Abhat.[73] |
| | 64.0 | 185.4 | I. Dincer et al.[76] G.A. Lane.[77] |
| Stearic acid | 60.0-61.0 | 186.5 | A. Sari et al.[81] |
| | 69.0 | 202.5 | I. Dincer et al.[76] G.A. Lane.[77] |
| | 70.0 | 203.0 | A. Abhat.[73] |

### Table 5.5: Commercial PCMs

| Compound | Melting temperature, $T_m$ (°C) | Heat of fusion (kJ/Kg) | Source |
|---|---|---|---|
| ClimSel C 32 | 32 | 212 | Climator |
| RT40 | 43 | 181 | Rubitherm GmbH |
| STL47 | 47 | 221 | Mitsubishi Chemical |
| ClimSel C 48 | 48 | 227 | Climator |
| STL52 | 52 | 201 | Mitsubishi Chemical |
| RT50 | 54 | 195 | Rubitherm GmbH |

| | | | |
|---|---|---|---|
| STL55 | 55 | 242 | Mitsubishi Chemical |
| TH58 | 58 | 226 | TEAP |
| ClimSel C 58 | 58 | 259 | Climator |
| RT65 | 64 | 207 | Rubitherm GmbH |
| ClimSel C 70 | 70 | 194 | Climator |
| PCM72 | 72 | -- | B. Zalba et al. [72] |
| RT80 | 79 | 209 | Rubitherm GmbH |
| TH89 | 89 | 149 | TEAP |
| RT90 | 90 | 197 | Rubitherm GmbH |

### 5.1.3 Application of PCMs for storage tank of SWH system

There are many studies available around the globe representing of application of PCMs for the storage tank of SWH systems such as Dzikevics and Zandeckis [82] have presented a mathematical model for analyzing the performance of charging and discharging of encapsulated PCMs in the heat storage tank of the SWH system. The authors found that the multiple-layered PCM systems are capable of storing 23 % more energy as compared to the single-layered PCM system. Ebadi et al. [83] have explained a numerical model to study the behavior of encapsulated PCM inside of tube-shaped thermal energy storage system. The authors found that by adding PCM into the cylindrical storage system, thermal efficiency is improved significantly. Hahne and Chen [84] have calculated numerically, the characteristics of heat transfer and flow in tubular hot water storage in case of the charging process of PCM in adiabatic boundary conditions. The author's study reveals that thermal stratification in a hot water tank is mainly influenced by its heat transfer and flow parameters. Ismail and Henriquez [85] have explained a numerical model to study the performance of PCM kept in the form of spherical capsules fitted into a tubular tank in the form of a packed bed as a latent heat storage system. The authors calculated charging and discharging times for encapsulated PCM and they showed the advantage of using PCM in the storage tank. Xia et al. [86] have presented the numerical heat transfer study for the packed bed latent thermal energy storage system including PCM sphere balls to calculate the efficiency of packed based bed model. The author's results conclude that random packaging of PCM balls is more favorable in comparison to special packaging of balls for recovery of stored heat from the thermal system in the storage tank. Raul et al. [87] have presented the numerical model for encapsulated PCMs to act as latent heat thermal energy material. The authors found that the PCM diameter of the capsule is a significant parameter for scheming an effective thermal system. Bellan et al. [88] have presented a numerical study for the identification of the thermal compatibility characteristics of sodium nitrate as encapsulated PCM along with heat transfer fluid flow. The authors found that Stefan number has a great influence on the characteristics of heat storage of PCM. Liu and Ma [89] have presented a numerical model to predict the complete melting time of PCM considering only the conduction heat transfer mode. The authors found that the whole melting time is the summation of the start of melting time and the time of total melting of PCM. Majumdar and Saha [90] have presented a numerical model for analyzing the thermal performance of heat storage tanks for the SWH system. The authors found that thermic oil has a better thermal performance for heat transfer instead of water. Kousksou et al [91] have introduced a numerical model for domestic SWH systems along with PCMs. The authors found that the prime design parameter is the melting temperature of the PCM, for successfully designing a PCM-based SWH system. Zivkovic and Fujii [92] have demonstrated a mathematical study for the isothermal phase change of encapsulated PCMs. The authors found that for the same volume and same area of heat transfer rectangular geometry is more efficient in comparison to cylindrical geometry. The rectangular geometry needs approximately half of the time for melting of PCM when compared with the cylindrical geometry. S. Kilickap et al. [93] have investigated the efficiency of the storage tank with and without the application of PCM through the experimental setup in Elazig climatic conditions. The authors found the highest efficiency of the PCM storage tank at 58 % at around 13:30 in the month of July. M. Mahfuz et al. [94] have determined experimentally the performance of paraffin wax as PCM encapsulated in shell and tube for the storage tank of the SWH system for different flow rates of water. The author's study includes the energy, exergy, and life cycle costs of PCMs for various flow rates. The authors found that with the increase in flow rates of water, the total life cycle cost of PCMs decreases. M. Mazman et al. [95] have experimentally investigated the impact of PCM graphite compounds in the upper part of the storage tank of a domestic SWH system in real environmental conditions. The authors used eutectic mixtures in 80:20 weight percentage of the paraffin and stearic acid, paraffin and palmitic acid, and stearic acid and myristic acid. The authors found that the paraffin and stearic acid mixture is the most suitable PCM compound for domestic SWH systems for enhancing thermal efficiency by about 74 %. S. Jaisankar et al. [96] have presented a review study for improving the thermal efficiency of SWH systems. The authors depicted the convective heat transfer method for the improvement of the thermal efficiency of the SWH system. R. Shukla et al. [97] have presented a review study for the latest advancements in SWH systems. The authors suggested that a new design of the heat pump-based SWH system could be proficient in the lesser solar energy areas.

### 5.1.4 Recommend design modules of PCMs for the SWH system

In this section, some favorable design modules for encapsulation purposes are described as shown in Figure 5.2. It is evident from several studies that PCM modules should be arranged in such a manner that they should be able to perform maximum thermal stratification for the storage tank. It is observed that the biggest challenge of encapsulation is that PCMs should be completely melted and solidified as per the design temperature range of the storage tank. In this regard, PCMs should be encapsulated in the shape of cylindrical cans, spherical balls, and inside hollow tubes as shown in Figure 5.2. Even some other parameters also play an important role like the mass flow rate of water, spacing among the PCM encapsulation, and container materials for encapsulation. It is recommended that the flow rate should not be very high in place it should be in a moderate range so that proper heat interaction between water and encapsulated PCMs can take place. Some experimental studies suggested that random packaging of PCMs is more useful for enhancing thermal stratification in place of a special packaging system. The material selection of containers for the encapsulation of PCM is an also essential characteristic of heat interaction in the storage tank of the SWH system. These materials should be capable of allowing the maximum amount of heat without any hindrance and these should be non-corrosive. Some common container materials are stainless steel, tin, aluminum, aluminum mixed, copper, etc.

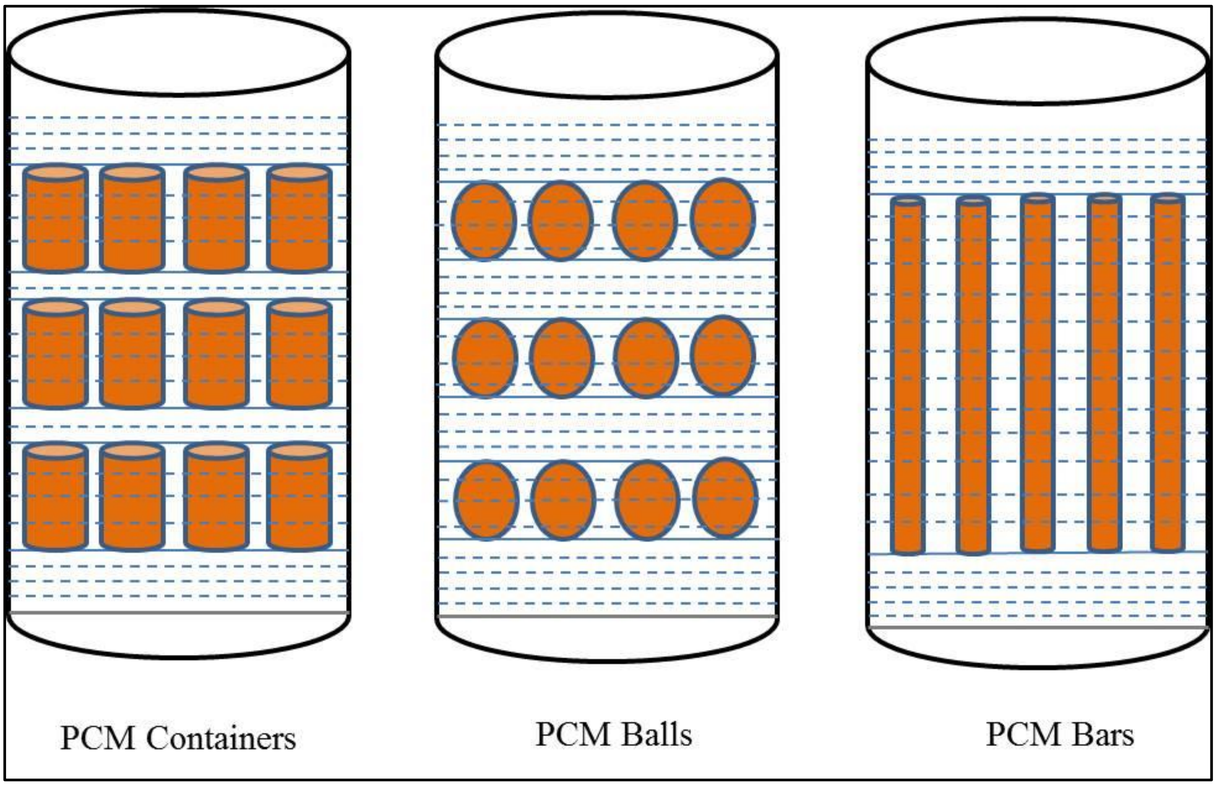


**Figure 5.2 Encapsulated PCM modules**

## 5.2. Description of the physical model

The physical model considered in this study has a similar equivalence to the experimental model of S. Canbazoglu et al. [23]. The complete physical model is presented in Figure 5.3. Here two cases for the storage tanks of SWH systems are considered, in the first case, the storage tank without PCM is considered as shown in Figure 5.4 (a), and in the second case, the storage tank with PCM is considered as shown in Figure 5.4 (b). The well-insulated cylindrical storage tank of galvanized steel of 900 mm in height and 600 mm in diameter was used with and without PCM. This model is an open-loop system of solar energy for natural circulation and it is usually applicable for providing warm water supplies for domestic purposes i.e., domestic SWH system. For this model, the prescribed insulation material is glass wool. The volume of the storage tank is 190 L and it is combined with PCM as shown in Figure 5.4 (b), the PCM is encapsulated in each polyethylene bottle of 0.44 L. Each polyethylene bottle contains 0.7347 kg of PCMs. In this model, a total of 107.8 L PCM was filled into 245 bottles and used with 82.2 L of water in the heat storage tank for making an efficient thermal stratification system. The flat aluminum solar collector with a fixed plate of 1.94 m × 0.94 m × 0.10 m having a single glass cover and painted black absorber plate was used along with a storage tank for heating water through incident solar radiation on it. The net area for absorption of solar radiation of the collector was 1.65 $m^2$ for each one and the 30° tilt angle to the horizontal was used. For supplying cold water to the SWH system an 18 L volume separate tank was also fitted. The water temperature at the midpoint of the heat storage tank, collector outlet temperature, and ambient temperature are used for simulation calculations.

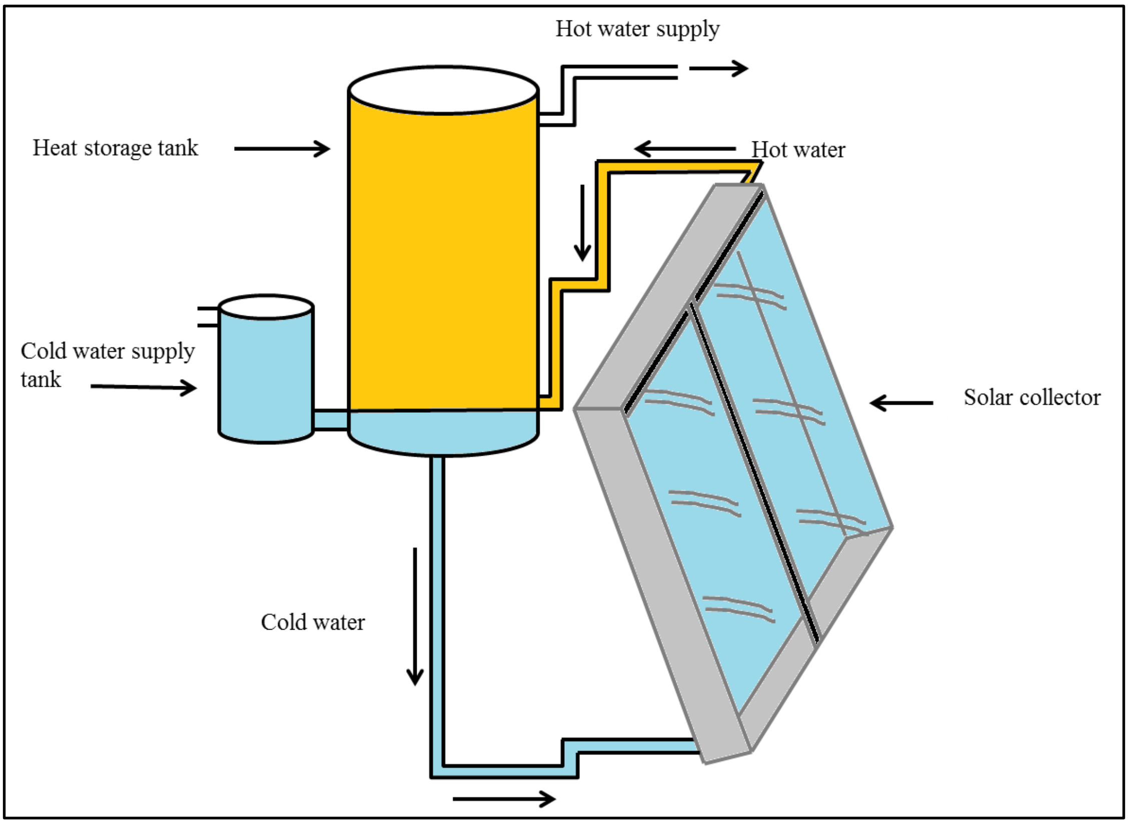


**Figure 5.3. The complete physical model**

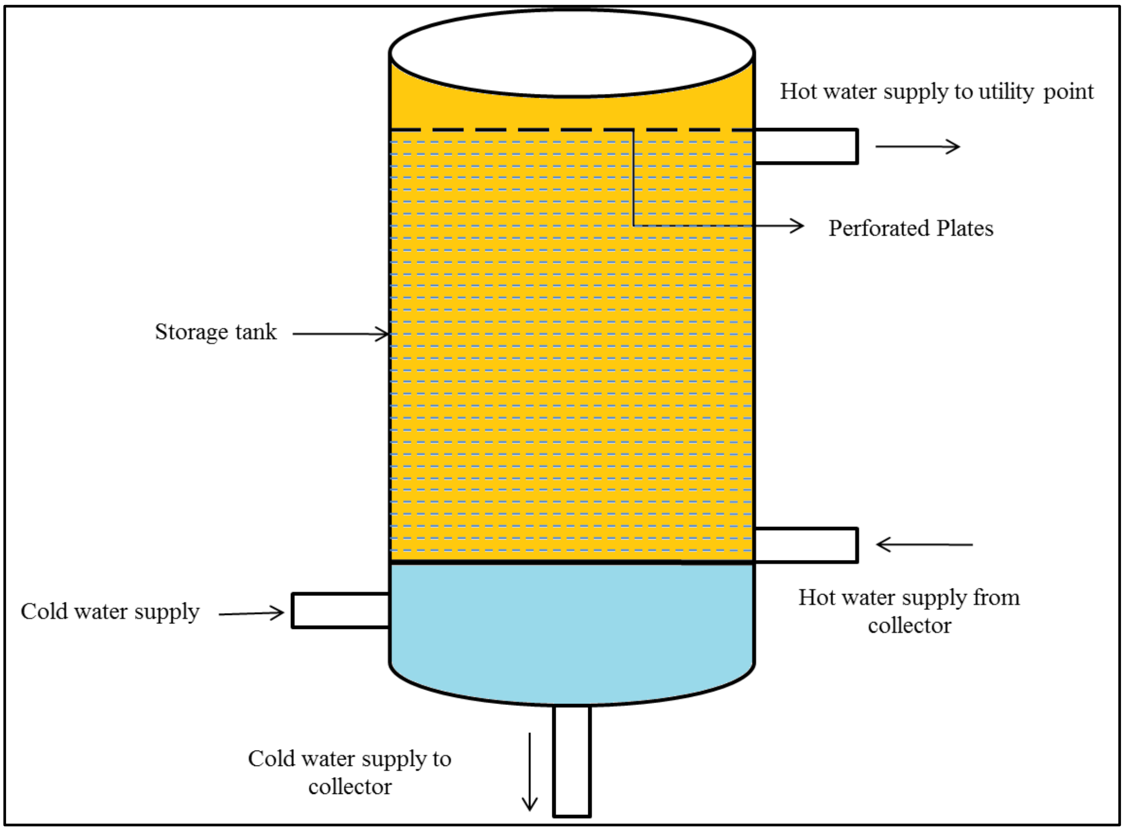


**Figure 5.4 (a). Storage tank without PCM**

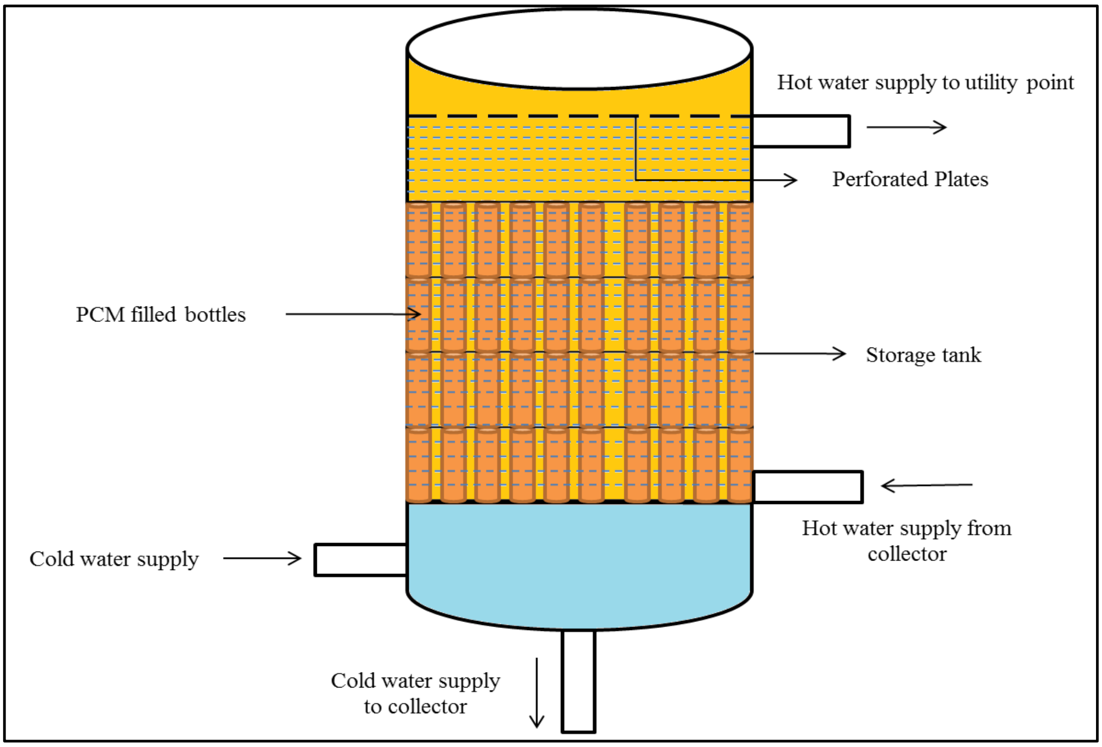


**Figure 5.4 (b). Storage tank with PCM**

### 5.3. Numerical simulation of PCMs

In this section, the numerical model for the simulation of different melting ranges of PCMs in the storage tank of the SWH system, as shown in Figure 5.4 (b), has been presented. Here eleven PCMs have been simulated to analyze their effectiveness, like Sodium hydrogen phosphate dodecahydrate (SHPD), OM 37, N-Eicosane (NE), Lauric acid (LA), Paraffin wax (PW), OM 48, Paraffin wax C20-33 (PW-C20-33), Sodium acetate trihydrate (SAT), Palmitic acid (PA), Myristic acid (MA), and Stearic acid (SA). Their thermophysical properties for simulation purposes have been presented in Table 5.6.

**Table 5.6. Thermophysical properties of PCMs**

| PCMs | Melting point, °C (a) | Melting latent heat, kJ/kg (b) | Specific heat, $C_p$, kJ/kg K | | Density, kg/m$^3$ | | Thermal conductivity, W/m K | | Reference |
|---|---|---|---|---|---|---|---|---|---|
| | | | Solid (c) | Liquid (d) | Solid (e) | Liquid (f) | Solid (g) | Liquid (h) | |
| SHPD | 36.00 | 280.00 | 1.60 | 1.90 | 1520 | 1520 | 0.613 | 0.613 | [98–100] |
| OM 37 | 36.00 | 231.00 | 2.55 | 2.63 | 973 | 860 | 0.160 | 0.130 | [90] |
| NE | 36.70 | 247.00 | 2.20 | 2.00 | 856 | 778 | 0.150 | 0.150 | [98,99] |
| LA | 44.00 | 177.40 | 1.70 | 2.30 | 1007 | 862 | 0.147 | 0.147 | [101] |
| PW | 44.00 | 174.12 | 2.44 | 2.53 | 830 | 783 | 0.210 | 0.210 | [98,99,102] |
| OM 48 | 45.00 | 173.50 | 2.02 | 2.35 | 960 | 875 | 0.200 | 0.120 | [90] |
| PW-C20-33 | 49.00 | 189.00 | 2.10 | 2.10 | 912 | 769 | 0.210 | 0.210 | [98,99,103] |
| SAT | 57.31 | 173.00 | 4.00 | 3.60 | 1340 | 1300 | 0.700 | 0.700 | [98,99,104] |
| MA | 58.00 | 186.60 | 1.70 | 2.40 | 990 | 861 | 0.150 | 0.150 | [101] |
| PA | 64.00 | 185.40 | 1.90 | 2.80 | 989 | 850 | 0.162 | 0.162 | [101] |
| SA | 69.00 | 202.50 | 1.60 | 2.20 | 965 | 848 | 0.172 | 0.172 | [101] |

The presented model of numerical simulation is based on certain assumptions like incompressible fluid flow in the steady-state, a well-insulated heat storage tank used, no heat generated inside of the heat storage tank, fluid flow in the vertical direction only taking place, loss of heat transfer from the storage tank is neglected, and variations in the thermophysical properties of PCMs are neglected. The stored heat per unit time without PCMs in the ordinary heat storage tank, as shown in figure 5.4 (a), is calculated by using equation (5.1) as,

$$\dot{Q_w} = \dot{m}_w c_{p,w} \, (T_h - T_c) \tag{5.1}$$

here, $\dot{m}_w$ is the mass flow rate of hot water required, and taken as 0.1 kg/s; $c_{p,w}$ is the specific heat of water (i.e. 4.1868 kJ/kg °C); $T_h$ is the hot water temperature required for domestic application here it is taken as 45 °C, this temperature can be varied as per the requirement and location of the SWH system; $T_c$ is the temperature of cold water feeding from the ground pipe network of the municipal corporation of the city, here it is taken as 15.5 °C, this temperature is also varied as per the geographical location of the SWH system. By the application of these values in equation (5.1) the heat stored per unit of time is calculated as,

$$\dot{Q}_w = (0.1)(4.1868)(45 - 15.5)$$

$$\dot{Q_w} = 12.351 \text{ kW}$$

The complete heat stored in the form of sensible heat in 190 kg of water mass in the heat storage tank without PCM, as shown in figure 5.4 (a), of 190 L can be calculated by using the equation (5.2) as,

$$Q_w = m_w c_{p,w} (T_{max} - T_{mean}) \tag{5.2}$$

$$Q_w = (190)(4.1868)(70 - 45)$$

$$Q_w = 19{,}887.30 \text{ kJ}$$

here, $T_{max}$ and $T_{mean}$ are taken as 70 °C and 45 °C respectively for sensible heat stored in the water without PCM. Now time $(t_w)$ for storage of warm water in the ordinary heat storage tank without PCM is calculated from equations (5.1) and (5.2) as,

$$t_w = \frac{Q_w}{\dot{Q}_w} = \frac{19887.3}{12.351} = 1610\ s = 26.83\ \text{min.}$$

The warm water mass $(m)$ developed for taken by utility point in case of the storage tank without PCM is calculated as,

$$m = \dot{m}_w \times t_w = 161\ \text{kg}$$

The sensible heat $(Q_S)$, latent heat $(Q_L)$, and total heat $(Q_{PCM})$ for the PCM storage tank, as shown in figure 5.4 (b), is explained by the equations (5.3) – (5.5) as,

$$Q_S = m_w c_{p,w} \Delta T + m_{PCM}\left(c_{P,PCM-L} \Delta T_1 + c_{P,PCM-S} \Delta T_2\right) \tag{5.3}$$

$$Q_L = m_{PCM} h_{SL} \tag{5.4}$$

$$Q_{PCM} = Q_S + Q_L \tag{5.5}$$

here, $m_w$ is the mass of water of 82.2 kg in the tank of heat storage including PCM; $c_{p,w}$ is the specific heat of water; $\Delta T$ is the required temperature difference for heating the mass of water in the heat storage tank including PCM, given by equation (2) i.e. (70 – 45 = 25 °C); $m_{PCM}$ is the mass of PCM; $C_{P,PCM-L}$ is the liquid-state specific heat of PCM; $\Delta T_1$ is the temperature difference between PCM melting and the maximum temperature of warm water in the heat storage tank ; $C_{P,PCM-S}$ is a solid-state specific heat of PCM ; $\Delta T_2$ is the temperature difference between the hot water of the tank and the PCM melting temperature; $h_{SL}$ is the specific melting latent heat of PCM during the phase change; $Q_{PCM}$ is the total stored heat in the PCM. The time of storage of hot water ($t_{PCM}$) and the mass ($m_{w,PCM}$ ) of hot water prepared to use through the PCM heat storage tank can be calculated as,

$$t_{PCM} = \frac{Q_{PCM}}{\dot{Q}_w}$$

$$m_{w,PCM} = \dot{m}_w \times t_{PCM}$$

Now each PCM listed in Table 5.6 is examined through numerical simulation by applying equations (5.1) - (5.5) for encapsulated PCMs in the storage tank of the SWH system, as shown in Figure 5.4 (b), and the results are summarized in Table 5.7.

**Table 5.7. Numerical simulation of PCMs in the storage tank of the SWH system**

| PCMs | Mass, kg [e×107.8 l volume of PCM] (i) | Latent heat of PCM, kJ [i × b] (j) | Sensible heat of PCM, kJ | | Sensible heat of water, kJ [$m_w C_{P,w} \Delta T$] (m) | Total heat, kJ [j+ k+ l+ m] (n) | Time, min. [n/$\dot{Q}_w$] (o) | Prepared hot water mass, kg [o × $\dot{m}_w$] (p) | Effectiveness factor [p/(warm water mass= $161\ kg$)] |
|---|---|---|---|---|---|---|---|---|---|
| | | | Solid [$m_{PCM}\ C_{P,PCM-S}\ \Delta T_2$] (k) | Liquid [$m_{PCM} C_{P,PCM-l} \Delta T_1$] (l) | | | | | |
| SHPD | 163.85 | 45879.68 | -- | 10584.71 | 8603.874 | 65068.26 | 87.80 | 526.82 | 3.27 |
| OM 37 | 104.88 | 24229.45 | -- | 9378.36 | 8603.874 | 42211.68 | 56.96 | 341.76 | 2.12 |
| NE | 92.27 | 22792.36 | -- | 6145.18 | 8603.874 | 37541.41 | 50.65 | 303.95 | 1.88 |
| LA | 108.55 | 19257.58 | -- | 6491.29 | 8603.874 | 34352.744 | 46.35 | 278.10 | 1.72 |

| | | | | | | | | | |
|---|---|---|---|---|---|---|---|---|---|
| PW | 89.47 | 15579.21 | -- | 5885.33 | 8603.874 | 30068.41 | 40.57 | 243.44 | 1.51 |
| OM 48 | 103.48 | 17955.16 | -- | 6079.45 | 8603.874 | 32638.48 | 44.04 | 264.25 | 1.64 |
| PW-C20-33 | 98.31 | 18581.27 | 825.80 | 4335.47 | 8603.874 | 32346.41 | 43.64 | 261.89 | 1.62 |
| SAT | 144.45 | 24990.19 | 7112.71 | 6599.05 | 8603.874 | 47305.82 | 63.83 | 383.01 | 2.37 |
| MA | 106.72 | 19914.32 | 2358.51 | 3073.53 | 8603.874 | 33950.23 | 45.81 | 274.87 | 1.70 |
| PA | 106.61 | 19766.27 | 3848.62 | 1791.04 | 8603.874 | 34009.80 | 45.89 | 275.36 | 1.71 |
| SA | 104.02 | 21065 | 3994.36 | 228.84 | 8603.874 | 33892.07 | 45.73 | 274.40 | 1.70 |

### 5.4. Melt fraction analysis of PCMs

It is also imperative to evaluate the affinity of PCMs along with some majorly used container materials (i.e. glass, stainless steel, tin, aluminum, aluminum mixed, and copper) apart from their effectiveness for the heat storage tank of the SWH system. The thermophysical properties of these container materials are listed in Table 5.8.

**Table 5.8.Thermophysical properties of different container materials [105]**

| Materials | Density (kg/m$^3$) | Thermal conductivity (W/m °C) | Specific heat (kJ/kg °C) |
|---|---|---|---|
| Glass | 2700 | 0.78 | 0.840 |
| Stainless Steel | 8010 | 7.7 | 0.500 |
| Tin | 7304 | 64 | 0.226 |
| Aluminum | 2707 | 204 | 0.896 |
| Aluminum mixed | 2659 | 137 | 0.867 |
| Copper | 8954 | 386 | 0.383 |

It is well known that the PCMs are kept inside container materials for exchanging heat from outside water to PCMs or vice versa. For this purpose, a melt fraction study of all selected PCMs is performed here with the help of the FORTRAN programming language by making a numerical code of it. This numerical code is based on some assumptions, like (i) The PCM and container material has constant thermophysical properties over the variation of temperature, (ii) The PCM has different constant thermophysical properties in solid and liquid states, (iii) It is considered an initial state of PCM is in solid-state, (iv) The homogenous and isotropic characteristics of PCM is considered, (v) All subunits of PCM are identical and independent of each other.

### 5.4.1 Mathematical model

If material is going in a change of phase from solid to liquid or liquid to solid then for constant thermophysical properties the transfer of energy can be expressed in the form of temperature and total volumetric enthalpy as,

$$\frac{\partial H}{\partial t} = \nabla[k_k(\nabla T)] \tag{5.6}$$

here, $k_k$ is the thermal conductivity of phase $k$ in PCM (W/m °C), and total volumetric enthalpy (H) is acquired by the addition of sensible and latent heat of the PCM as,

$$H(T) = h(T) + \rho f(T)\lambda \tag{5.7}$$

where, $h(T) = \int_{T_m}^{T} \rho_k\, c_k dT$ (5.8)

here, $\rho_k$ is the density of phase $k$ in PCM in kg/m$^3$, λ is the latent heat of fusion in kJ/kg, and $c_k$ is the specific heat of phase $k$ in PCM in J/kg °C. For phase change at a constant temperature, the melt fraction (f) is expressed as,

$$f = \begin{cases} 0 & if\ T < T_m \quad (solid), \\ 0-1 & if\ T = T_m\ (mushy), \\ 1 & if\ T > T_m \quad (liquid). \end{cases} \tag{5.9}$$

The enthalpy of PCM in solid, mushy, and liquid regions is obtained by using equations (5.7) and (5.8) as,

$$H = \int_{T_m}^{T} \rho_s\, c_s dT, \qquad T < T_m \ \ (solid) \tag{5.10}$$

$$H = \rho_l f \lambda, \qquad T = T_m\ (mushy) \tag{5.11}$$

$$H = \int_{T_m}^{T} \rho_l\, c_l\, dT + \rho_l \lambda, \quad T > T_m \ \ (liquid) \tag{5.12}$$

here, $\rho_s$ & $\rho_l$ are the densities of PCM in solid and liquid states in kg/m$^3$, $c_s$ & $c_l$ are the specific heat of PCM in solid and liquid states in J/kg °C. The value of PCM temperature for solid, mushy, and liquid regions are expressed by using equations (5.10), (5.11), and (5.12) as,

$$T = T_m + H/\rho_s\, c_s, \qquad H < 0 \quad (solid) \tag{5.13}$$

$$T = T_m, \qquad 0 < H < \rho_l \lambda \quad (mushy) \tag{5.14}$$

$$T = T_m + (H - \rho_l \lambda)/\rho_l\, c_l, \qquad H > \rho_l \lambda \quad (liquid) \tag{5.15}$$

The expression for heat transfer in the PCM can be expressed by equation (5.6) by using equations (5.7) and (5.8) as,

$$\frac{\partial h}{\partial t} = \frac{\partial}{\partial x}\left(\alpha \frac{\partial h}{\partial x}\right) + \frac{\partial}{\partial y}\left(\alpha \frac{\partial h}{\partial y}\right) - \rho_l \lambda \frac{\partial f_l}{\partial t} \tag{5.16}$$

And for the fin expressed as,

$$\frac{\partial h_f}{\partial t} = \frac{\partial}{\partial x}\left(\alpha_f \frac{\partial h_f}{\partial x}\right) + \frac{\partial}{\partial y}\left(\alpha_f \frac{\partial h_f}{\partial y}\right) \tag{5.17}$$

here, $\alpha$ is the thermal diffusivity in m$^2$/s, $\alpha_f$ is the thermal diffusivity of the fin in m$^2$/s, and $h_f$ is the sensible volumetric enthalpy of the fin in J/m$^3$.

### 5.4.2 Solution of a mathematical model

The solution of equations (5.16) and (5.17) is provided by employing the finite difference method in a fully implicit manner. While solving these equations it is considered that the initial state of PCM is solid and its initial temperature is well below its melting temperature, as given here along with boundary conditions,

$$h_{init} = \rho_s c_s (T_m - T_{init}) \tag{5.18}$$

for face $x = 0$ the boundary condition is given as,

$$h_{ff}(0,t) = \rho_k c_k (T_{wall} - T_m) \tag{5.19}$$

from equation (5.19) the volumetric enthalpy is known for each time step. For the face of $x = L, y = 0, and\ y = L$ being of adiabatic given as,

$$dh_f/dx\ |_{x=L} = 0 \tag{5.20}$$

$$dh_f/dy\ |_{y=0} = 0 \tag{5.21}$$

$$dh_f/dy\ |_{y=L} = 0 \tag{5.22}$$

The integration of equation (5.16) for the PCM is obtained as a finite difference equation for each control volume as given by Voller [106] and Patankar [107]. The discretized form of equation (5.16) for $\Delta x = \Delta y$ (shown in fig.3.) is given as,

$$h_p = h_P^o + \alpha R[h_E - 4h_P + h_W + h_N + h_S] + \rho_l \lambda \left[f_P^o - f_P^k\right] \tag{5.23}$$

$$a_E h_E + a_W h_W + a_P h_P + a_N h_N + a_S h_S = Q \tag{5.24}$$

where,

$$a_E = a_W = a_N = a_S = -\alpha R, \qquad a_P = 1 - a_E - a_W - a_P - a_N - a_S,$$

$$Q = h_P^o + \rho_l \lambda \left(f_P^o - f_P^k\right), \qquad and\ R = dt/(dx)^2$$

here, subscripts W, E, P, N, and S denote the west, east, center, north, and south nodes of iteration respectively, as shown in Figure 5.5. $h_P^o\ and\ f_P^o$ are shows the amount of enthalpy and fraction of liquid of PCM respectively for the foregoing time step. The alphabet a is the internal nodes coefficient. The value of $Q$ represents the heat estimation regarding PCM. The meaning of superscript $k$ is that the $k^{th}$ iteration for $f$ at node $P$ and o is the old value of iteration. The equation (5.24) is solved in the same way and by using of same boundary condition in the program as presented by Costa et al. [108]. To analyze the melt fraction of PCM for different container materials a grid matrix of (32×32) has been considered along with a (30×30) grid matrix of PCM containing a length of the grid of 2 mm and a time step of the 20 s, as shown in Figure 5.5. In the mathematical model, considering that the initial temperature of PCM is 5 ºC lower than the melting temperature of PCM (i.e. $T_m - T_{init} = 5$ ℃) and the wall temperature of heat transfer container material is kept 15 ℃ higher than the melting temperature of PCM (i.e. $T_{wall} - T_m = 15$ ℃). Here this section of study simulated all eleven PCMs (as listed in the Table 5.6) to predict the variation of melt fraction of PCMs due to different thermophysical properties of container materials and PCMs; the results of the simulation are summarized and presented in Table 5.9.

**Table 5.9. PCMs melt fraction for different container materials within 300 min. (thickness=2mm, $T_m - T_{init} = 5$ ℃, $T_{wall} - T_m = 15$ ℃)**

| **PCMs** | **Glass** | | **Stainless steel** | | **Tin** | | **Aluminum mixed** | | **Aluminum** | | **Copper** | |
|---|---|---|---|---|---|---|---|---|---|---|---|---|
| | $t^*$ | $f$ | $t^*$ | $f$ | $t^*$ | $f$ | $t^*$ | $f$ | $t^*$ | $f$ | $t^*$ | $f$ |
| SHPD | 300 | 0.42 | 300 | 0.70 | 300 | 0.90 | 281 | 1.00 | 254 | 1.00 | 178 | 1.00 |
| OM 37 | 300 | 0.34 | 300 | 0.68 | 300 | 0.79 | 300 | 0.90 | 300 | 0.92 | 300 | 1.00 |
| NE | 300 | 0.43 | 300 | 0.80 | 300 | 0.94 | 275 | 1.00 | 256 | 1.00 | 186 | 1.00 |
| LA | 300 | 0.44 | 300 | 0.83 | 300 | 0.94 | 281 | 1.00 | 264 | 1.00 | 194 | 1.00 |
| PW | 300 | 0.53 | 300 | 0.95 | 262 | 1.00 | 187 | 1.00 | 173 | 1.00 | 128 | 1.00 |
| OM 48 | 300 | 0.40 | 300 | 0.79 | 300 | 0.88 | 300 | 0.97 | 300 | 1.00 | 238 | 1.00 |
| PW-C20-33 | 300 | 0.57 | 300 | 0.98 | 235 | 1.00 | 165 | 1.00 | 153 | 1.00 | 111 | 1.00 |
| SAT | 300 | 0.47 | 300 | 0.83 | 300 | 1.00 | 218 | 1.00 | 200 | 1.00 | 144 | 1.00 |
| MA | 300 | 0.42 | 300 | 0.81 | 300 | 0.92 | 298 | 1.00 | 280 | 1.00 | 206 | 1.00 |
| PA | 300 | 0.41 | 300 | 0.80 | 300 | 0.91 | 300 | 1.00 | 292 | 1.00 | 215 | 1.00 |
| SA | 300 | 0.46 | 300 | 0.84 | 300 | 0.96 | 253 | 1.00 | 237 | 1.00 | 173 | 1.00 |

*Units:* $t^*(time\ in\ minutes, 0 - 300)$; $f(dimentionless\ melt\ fraction, 0 - 1)$

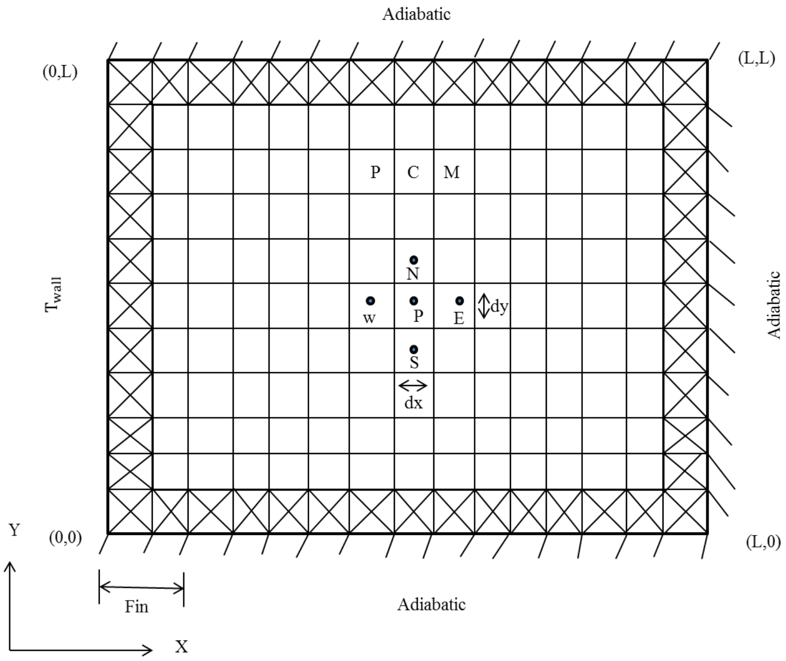


**Figure 5.5. PCM melt fraction domain**

### 5.4.3 Model and code validation

The model and code validation of this study have been done through the previously published model of Costa et al. [108]. The comparison graph of melt fraction for our study and Costa et al.'s study has been drawn and presented in Figure 5.6. From the figure, it is clear that the model of our study has close tolerances with the study of Costa et al. In this viewpoint, our model has a good validation agreement with the Costa et al. model.

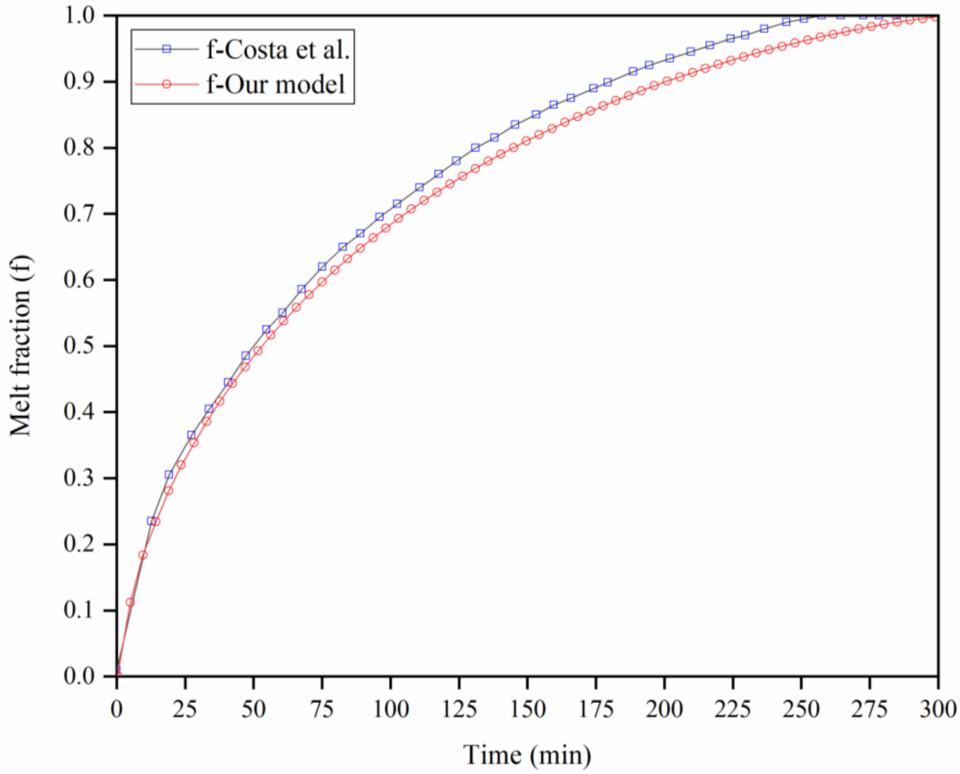


**Figure 5.6 Comparison graph of our model and Costa et al. model**

## 5.5. Result and discussion

### 5.5.1 Effectiveness of encapsulated PCMs

The effectiveness of different PCMs listed in Table 5.6 is evaluated through the numerical simulation model and presented in Figure 5.7.

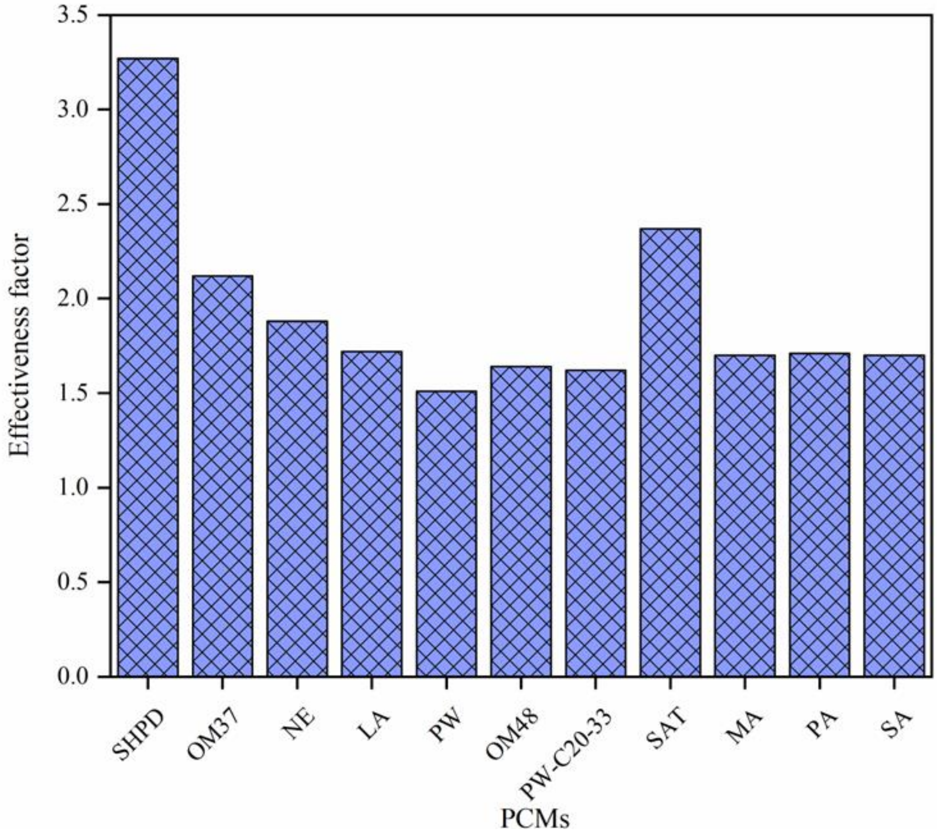


**Figure 5.7. Effectiveness of PCMs**

The performance of different encapsulated PCMs is defined by the term effectiveness factor. It is the ratio of the mass of hot water produced in the heat storage tank with PCM to the mass of hot water produced in the heat storage tank without PCM. It describes how much PCM is effective in improving the thermal stratification of the storage tank with encapsulated PCMs. If any PCM has an effectiveness factor of 2 it means that the performance of the heat storage tank has been improved two times than the conventional heat storage tank due to encapsulated particular PCM in the heat storage tank. From Figure 5.7, it can be evaluated that the lowest value of effectiveness is found for PW at 1.51 and the highest value is found for SHPD at 3.27, so PW is least recommended while SHPD is highly recommended as encapsulated PCM for the SWH system. The other PCMs which have an effectiveness factor greater than 2 have also quite eligible PCMs for improving the thermal performance of the storage tank of the SWH system.

### 5.5.2 Effect of melting temperature of different encapsulated PCMs

The variation of melting temperature is observed in the effectiveness of encapsulated PCMs and presented in Figure 5.8.

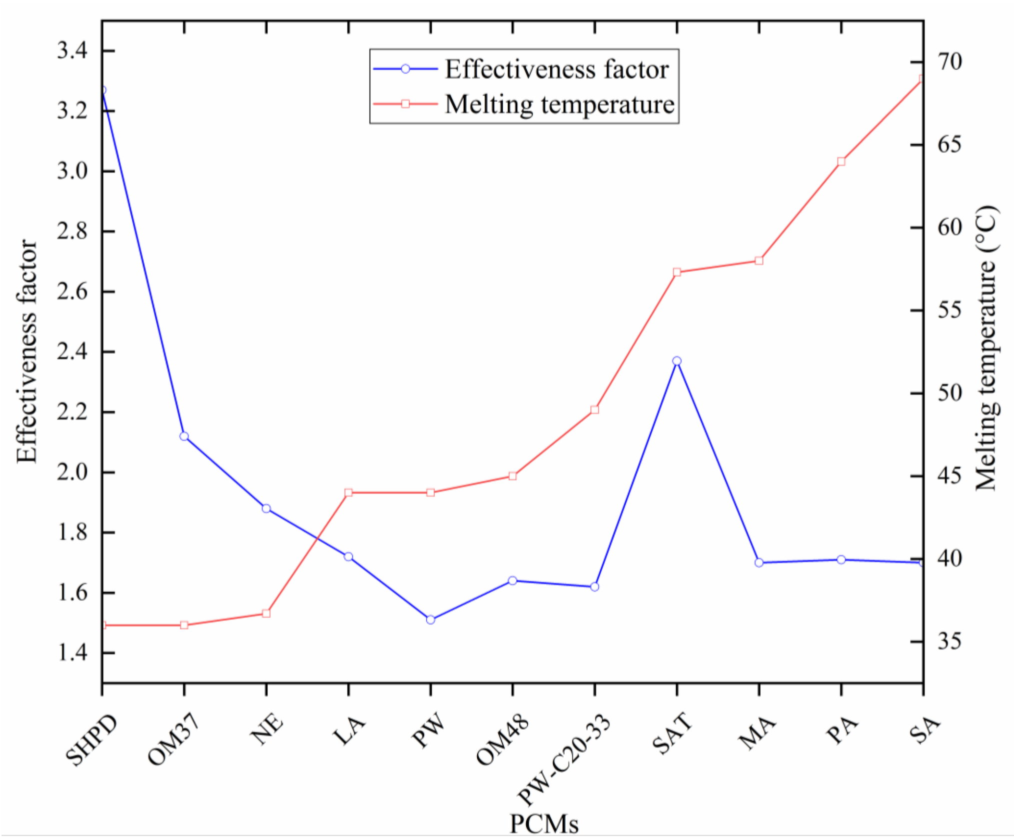


**Figure 5.8 Variation of melting temperature of PCMs**

It is observed from the figure that there is not any direct relationship exists between the effectiveness of a particular PCM to melting temperature. While for the highest value of effectiveness factor of 3.27 for SHPD, the melting temperature of it is 36 °C. In the case of the lowest value of effectiveness factor of 1.51 corresponding to the PW, it has a melting temperature of 89.47 °C. So, for designing a storage tank with encapsulated PCM, the effectiveness of PCM is a more important criterion in comparison to melting temperature for the selection of encapsulated PCMs.

### 5.5.3 Effect due to variation in mass flow rate

The effect of the variable mass flow rate is studied for a particular encapsulated PCM. It is observed from Figure 5.7 that the highly recommended PCM for encapsulation for the storage tank of the SWH system is SHPD, so the variation of mass flow rate is studied by considering this PCM only and presented in Figure 5.9. It is observed from the figure that as the mass flow rate increases from 0.10 to 0.30 kg/sec for the storage tank and the effectiveness of PCM also increases linearly, it means that the suggested PCM is performing well for the given range of mass flow rate. Based on the given range i.e. 0.10 to 0.30 kg/sec, it can be evaluated that the suggested encapsulated PCM is suitable for a lower range of mass flow rate and it will follow a linear relation as shown in Figure 5.9.

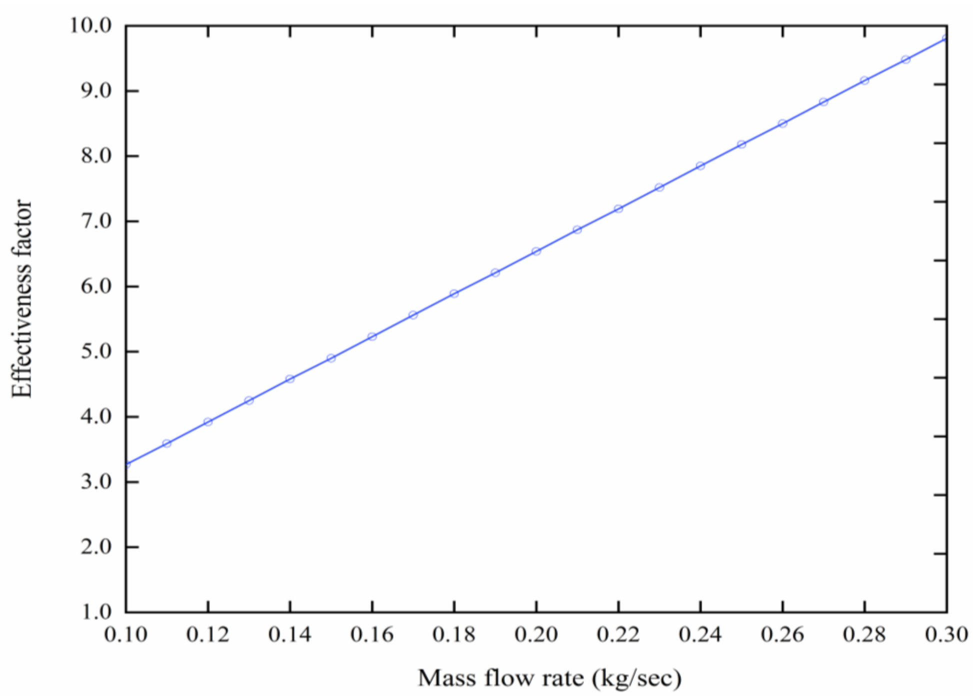


**Figure 5.9 Variation of mass flow rate**

### 5.5.4 Effect of the variable mean temperature of the heat storage tank

The effect of variable mean temperature is studied by considering the SHPD as an encapsulated PCM for the storage tank of the SWH system. Here the mean temperature is varied from 30 to 50 °C and the effect of this variation on the effectiveness factor is noted down. Previously the effectiveness factor of SHPD (i.e. 3.27) was calculated for a mean temperature of 45 °C as mentioned in Table 5.7. This variation of mean temperature is presented in figure 5.10, indicating that when the mean temperature increases from 30 to 36 °C, the effectiveness of PCM decreases, and after 36 °C the effectiveness becomes constant for further increase of mean temperature, it is due to the melting point of encapsulated PCM i.e. 36 °C. So, it can be observed from Figure 5.10 that if the selected PCM has a higher value of melting point from the mean temperature of the storage tank then there is no impact on the performance of encapsulated PCMs and if the selected PCM has the melting point lower than the mean temperature then it has considerable impact on the performance of thermal stratification of encapsulated PCMs i.e. with an increase in the mean temperature effectiveness factor of PCM decreases.

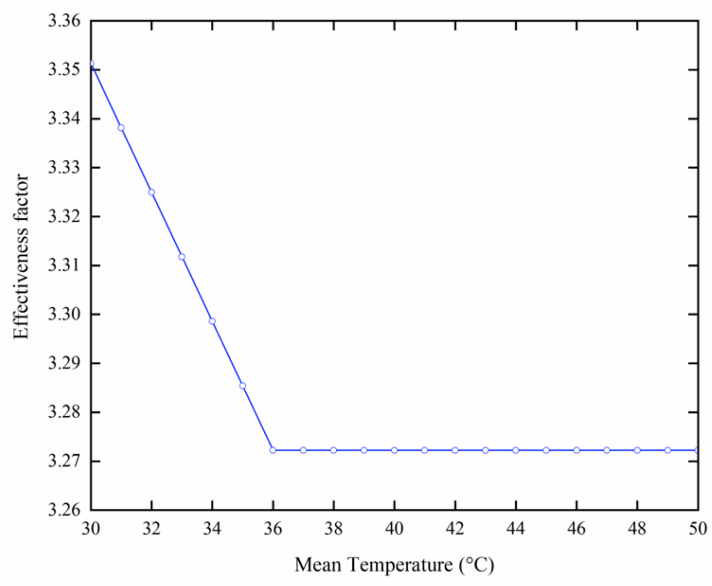


**Figure 5.10 Variation of mean temperature**

### 5.5.5 Desired range of thermophysical properties for encapsulated PCMs

The generalized desirable range of thermophysical properties has been examined by considering SHPD as a reference encapsulated PCM for the heat storage tank of the SWH system and presented in Table 5.10.

**Table 5.10. The desired range of thermophysical properties of encapsulated PCM materials**

| Thermophysical property | Unit | Range |
|---|---|---|
| Density-solid | kg/m$^3$ | 1400-1620 |
| Latent heat | kJ/kg | 150-350 |
| Specific heat $C_p$-liquid | kJ/kg K | 1.0-3.0 |

The density of PCM in a solid state varied from 1400 to 1620 kg/m$^3$ while keeping other properties constant and it is plotted with effectiveness factors of PCM as shown in Figure 5.11 (a). From the figure, it is observed that encapsulated PCM density varied almost linearly with the effectiveness factor of PCM. So, for designing a storage tank of SWH systems for encapsulated PCMs the higher value of encapsulated PCM density is most preferred. In this manner, the latent heat of encapsulated PCM is also analyzed by varying its value from 150 to 350 kJ/kg while keeping other properties constant. The variation of latent heat is plotted with the effectiveness of encapsulated PCMs and presented in Figure 5.11 (b). From the figure, it is observed that the latent heat of encapsulated PCM also makes an almost linear relation with the effectiveness factor of PCM. It is obvious that for designing the encapsulated PCM storage tank of SWH systems, a higher value of latent heat is preferred. The specific heat variation in the liquid state of encapsulated PCM is also noted here by varying its value from 1.0 to 3.0 kJ/kg K and plotted with the effectiveness factor as shown in Figure 5.11 (c). It is observed that specific heat variations are also found in an almost linear manner. So it is preferred to use encapsulated PCM of the higher value of specific heats for designing the storage tank of SWH systems.

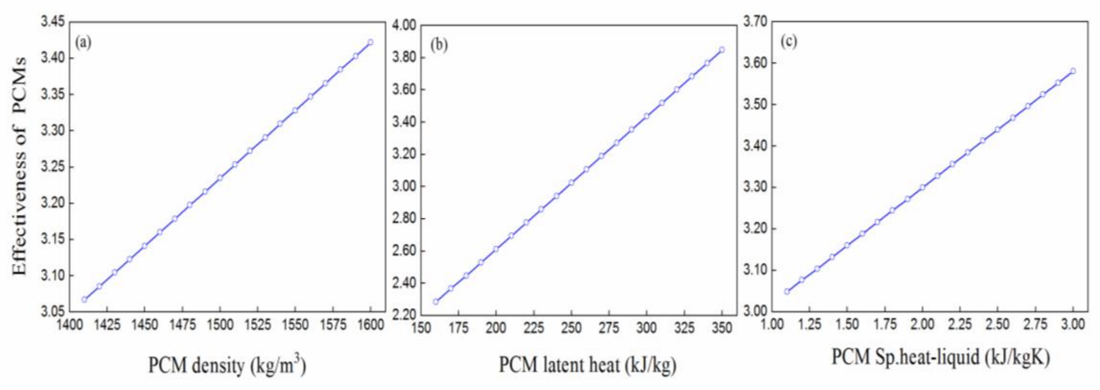


**Figure 5.11-(a). Variation of PCM density, (b).Variation of PCM latent heat, (c) Variation of PCM-specific heat**

### 5.5.6 Effect on melt fraction due to various thermophysical properties of PCM and heat transfer container material

From Table 5.9, the various values of melt fraction are presented for 2 mm thickness of container materials of glass, stainless steel, tin, aluminum mixed, aluminum, and copper. The values of melt fractions in Table 5.9 are calculated within 300 min through the simulation model of the FORTRAN programming language. It is evident from Table 5.9 that as the thermal conductivity of container material improves the melt fraction of PCMs also improves. Among all container materials, copper has the highest value of thermal conductivity so it has the highest value of melt fraction ($f$ =1) for all PCMs within different short time intervals in comparison to other container materials. The melt fraction of all PCMs corresponding to the container material of copper is plotted and presented in Figure 5.12. From the figure, it is clear that for the complete melting of all PCMs, there is a different time due to the different thermophysical properties of each PCM.

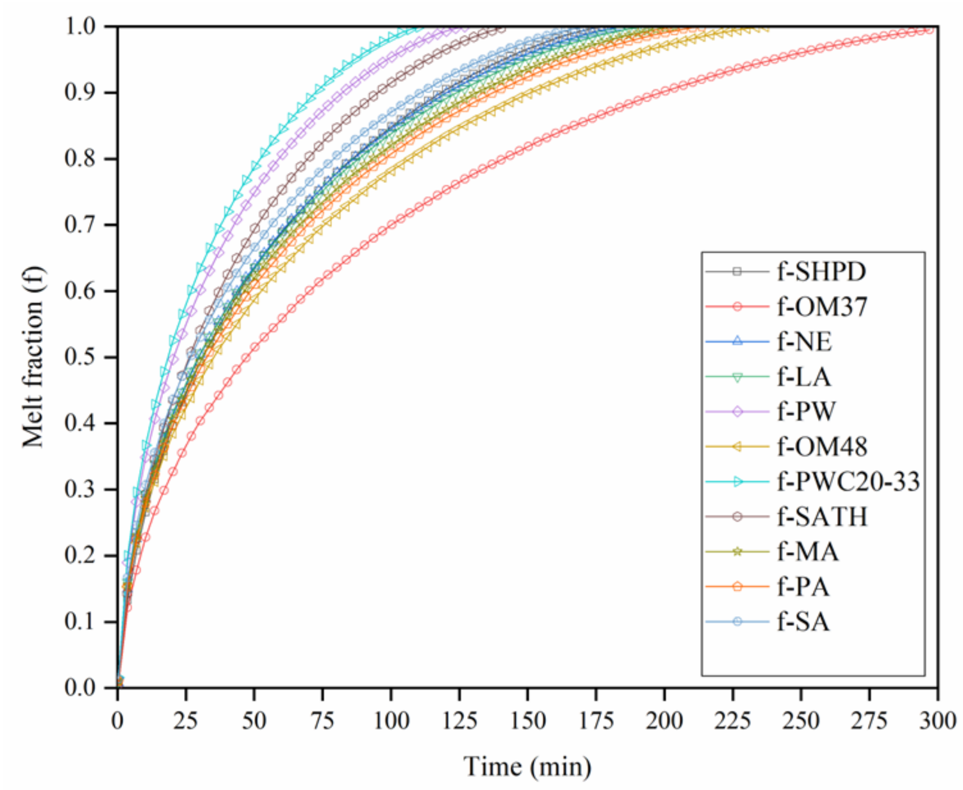


**Figure 5.12 Melt fraction of all PCMs corresponding to only copper container material (thickness=2mm,$T_m - T_{init} = 5$ ℃, $T_{wall} - T_m = 15$ ℃)**

While the second most favorable container material emerges as aluminum, it has also the highest values of melt fractions, except OM37 ($f$ = 0.92), but in a long time in comparison to copper container material. In the case of aluminum mixed container material, except for OM37 ($f$ = 0.90) and OM48 ($f$ = 0.97), all PCMs are completely melted which shows also a quite satisfactory melting phenomenon of PCMs. But in the case of tin container material, only three PCMs are completely melted namely PW, PW-C20-33, and SAT, and the rest are not melted completely. In this sequence, stainless steel and glass container materials also do not show the complete melting of any PCMs. The incomplete melting of PCMs inside of container material, as shown in Table 5.9, is not recommended for designing any TES system because it lowers the thermal efficiency of the system. So, it is advantageous to choose container material for a higher value of thermal conductivity.

In the case of the copper container material from Table 5.9, it is also observed that a minimum melting time of 111 min. is found corresponding to PW-C20-33. Even all listed PCMs are completely melted but with different times of melting, it is due to the different thermophysical properties of each PCM. The PW-C20-33 is considered here as a reference PCM, for analyzing the different container materials, because it has the least time of melting (i.e. 111 min.) corresponding to the copper container material. The SHPD is not considered a reference PCM because it has a higher value of melting time (i.e. 178 min.) in comparison to PW-C20-33.

To exhibit the effect of the thermal conductivity of various container materials on melt fraction, a comparative diagram showing the melting of PW-C20-33 corresponding to all container materials within the time of 111 min. is drawn and presented in Figure 5.13. The rate of melting of each PCM corresponding to all container materials within the time interval of 111 min. is also presented in Table 5.11, for representing the effect of the thermal conductivity of each container material on the melt fraction. It is found from the table that container material of higher thermal conductivity (> 100 W/m ˚C) has a significant effect on the melt fraction of each PCM.

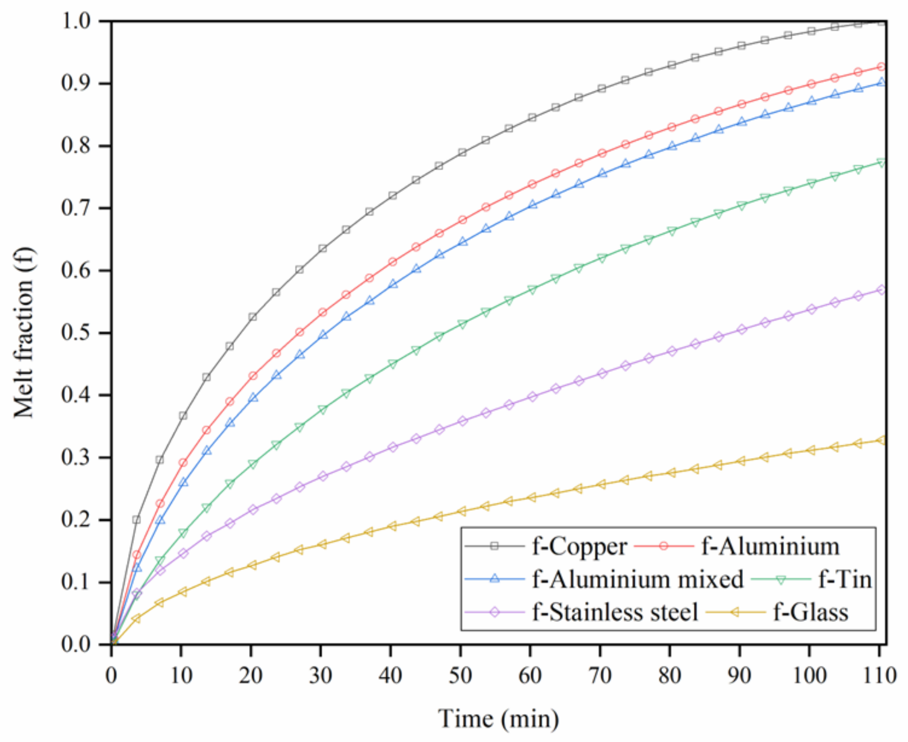


**Figure 5.13. Melt fraction variation of PW-C20-33 with all container materials within 111 min. (thickness=2 mm, $T_m - T_{init} = 5$ ℃, $T_{wall} - T_m = 15$ ℃)**

**Table 5.11. All PCMs melt fraction for different container materials within 111 min. (thickness=2mm, $T_m - T_{init} = 5$ ℃, $T_{wall} - T_m = 15$ ℃)**

| PCMs | Glass *f* | Stainless steel *f* | Tin *f* | Aluminum mixed *f* | Aluminum *f* | Copper *f* |
|---|---|---|---|---|---|---|
| SHPD | 0.24 | 0.40 | 0.55 | 0.71 | 0.76 | 0.88 |
| OM 37 | 0.19 | 0.36 | 0.50 | 0.60 | 0.63 | 0.72 |
| NE | 0.25 | 0.45 | 0.62 | 0.74 | 0.77 | 0.87 |
| LA | 0.25 | 0.46 | 0.63 | 0.74 | 0.77 | 0.86 |
| PW | 0.30 | 0.54 | 0.74 | 0.86 | 0.89 | 0.97 |
| OM 48 | 0.23 | 0.43 | 0.58 | 0.69 | 0.71 | 0.81 |
| PW-C20-33 | 0.32 | 0.57 | 0.77 | 0.90 | 0.92 | 1.0 |
| SAT | 0.26 | 0.45 | 0.65 | 0.80 | 0.83 | 0.94 |
| MA | 0.24 | 0.45 | 0.61 | 0.72 | 0.75 | 0.85 |
| PA | 0.24 | 0.44 | 0.60 | 0.71 | 0.74 | 0.83 |
| SA | 0.26 | 0.47 | 0.65 | 0.77 | 0.80 | 0.90 |

*Unit:* $f\,(dimentionless\ melt\ fraction, 0-1)$

### 5.5.7 Thickness effect of container material on melt fraction of PCMs

To comprehend the effect of container material thickness on melt fraction, the PCM of PW-C20-33 has been selected as being of minimum melting time corresponding to copper container material. The melt fraction results of this PCM for 1, 2, and 4 mm thickness for all container materials are listed and presented in Table 5.12.

**Table 5.12. Melt fraction variation of PW-C20-33 for different thicknesses of heat exchanger container materials within 300 min. ($\boldsymbol{T_m - T_{init} = 5}$℃, $\boldsymbol{T_{wall} - T_m = 15}$ ℃)**

| Thickness (mm) | Glass | | Stainless steel | | Tin | | Aluminum mixed | | Aluminum | | Copper | |
|---|---|---|---|---|---|---|---|---|---|---|---|---|
| | $t^*$ | $f$ | $t^*$ | $f$ | $t^*$ | $f$ | $t^*$ | $f$ | $t^*$ | $f$ | $t^*$ | $f$ |
| 1 | 300 | 0.51 | 300 | 0.80 | 300 | 1.0 | 213 | 1.0 | 193 | 1.0 | 139 | 1.0 |
| 2 | 300 | 0.57 | 300 | 0.98 | 235 | 1.0 | 165 | 1.0 | 153 | 1.0 | 111 | 1.0 |
| 4 | 300 | 0.72 | 170 | 1.0 | 158 | 1.0 | 114 | 1.0 | 107 | 1.0 | 79 | 1.0 |

*Units:* $t^*(time\ in\ minutes, 0-300)$; $f(dimentionless\ melt\ fraction, 0-1)$

It is noted from the table that as the thickness of container material increases the rate of melt fraction also increases. It is due to the increase in the thickness area of container material and the decrease in the amount of PCM inside the container. In the case of copper container material, the values of melt fraction corresponding to different container thicknesses are plotted and presented in Figure 5.14. It is also observed from Table 5.12 and Figure 5.14 that the difference amount of melt fraction is very much less as compared to the increase in thickness of container material. But for obvious, if the thickness of container material is increased then the amount of PCM decreases, so ultimately time taken in the complete melting of PCM also decreases accordingly. So that it can be accomplished that the thickness increment of container material does not contribute any significant influence on the melt fraction of PCMs.

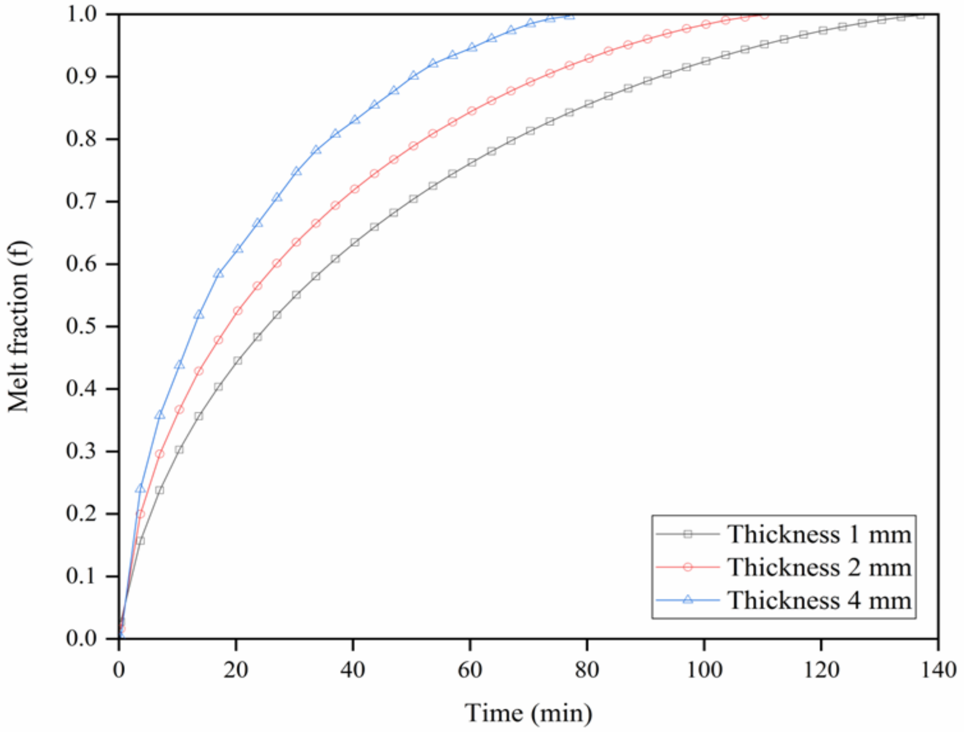


**Figure 5.14. Melt fraction variation of PW-C20-33 corresponding to only copper container material ($T_m - T_{init} = 5$℃, $T_{wall} - T_m = 15$ ℃)**

### 5.5.8 Effect of initial temperature of PCM on melt fraction

To perceive the effect of the initial temperature of PCM on the melt fraction, the values of melt fractions corresponding to 5, 10, 15, and 20 ˚C temperature difference (i.e. $T_m - T_{init}$) for PW-C20-33 have been noted down and presented in Table 5.13. It can be observed from the table that with the increase in temperature difference, the melt fraction decreases slightly. But if the conductivity of container material increases then the melt fraction of PCM will increase. From Table 5.13, this decrease in melt fraction is very much less as compared to the increase in the temperature difference. To exhibit the variation of melt fraction for different values of temperature difference in the case of copper container material, a graph has been plotted and presented in

Figure 5.15. From the figure, it can be easily observed that there is no sharp effect on melt fraction due to variation in the temperature difference. So it can be summarised that the effect of initial temperature of PCMs does not have a significant effect on the melt fraction.

**Table 5.13. Melt fraction variation of PW-C20-33 for different values of ($T_m - T_{init}$) with various heat exchanger container materials within 300 min. (thickness=2mm, $T_{wall} - T_m = 15$ ℃)**

| $T_m - T_{init}$ | Glass | | Stainless steel | | Tin | | Aluminum mixed | | Aluminum | | Copper | |
|---|---|---|---|---|---|---|---|---|---|---|---|---|
| | $t^*$ | $f$ | $t^*$ | $f$ | $t^*$ | $f$ | $t^*$ | $f$ | $t^*$ | $f$ | $t^*$ | $f$ |
| 5 | 300 | 0.57 | 300 | 0.98 | 235 | 1.0 | 165 | 1.0 | 153 | 1.0 | 111 | 1.0 |
| 10 | 300 | 0.54 | 300 | 0.96 | 239 | 1.0 | 169 | 1.0 | 156 | 1.0 | 114 | 1.0 |
| 15 | 300 | 0.52 | 300 | 0.94 | 243 | 1.0 | 171 | 1.0 | 158 | 1.0 | 116 | 1.0 |
| 20 | 300 | 0.50 | 300 | 0.93 | 247 | 1.0 | 174 | 1.0 | 161 | 1.0 | 118 | 1.0 |

*Units:* $t^*(time\ in\ minutes, 0-300)$; $f(dimentionless\ melt\ fraction, 0-1)$

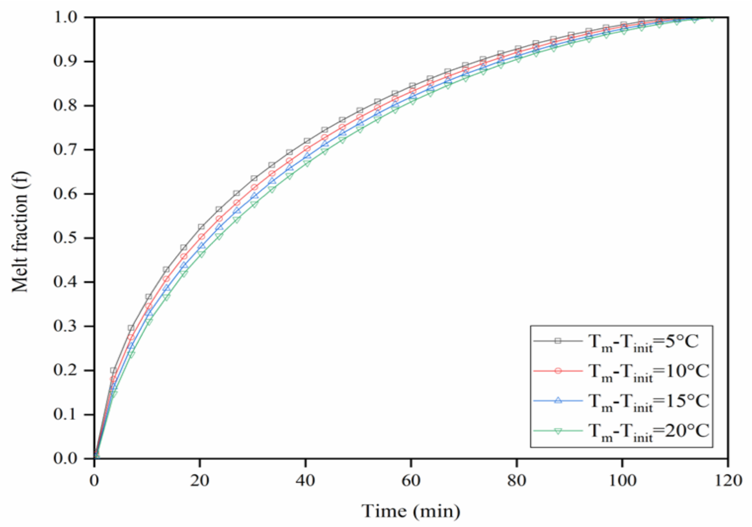


**Figure 5.15. Melt fraction variation corresponding to different temperature differences ($T_m - T_{init}$) for the initial temperature of PW-C20-33(thickness=2mm, $T_{wall} - T_m = 15$ ℃)**

### 5.5.9 Effect of wall temperature of container material on melt fraction

To analyze the effect of wall temperature on PCMs melt fraction, the melt fraction analogous to the 5, 10, 15, and 20 ˚C temperature difference (i.e. $T_{wall} - T_m$) has been calculated for PW-C20-33 and presented in Table 5.14.

**Table 5.14. Melt fraction variation of PW-C20-33 for different values of ($T_{wall} - T_m$) with various heat exchanger container materials within 300 min. (thickness=2mm, $T_m - T_{init} = 15$ ℃)**

| $T_{wall} - T_m$ | Glass | | Stainless steel | | Tin | | Aluminum mixed | | Aluminum | | Copper | |
|---|---|---|---|---|---|---|---|---|---|---|---|---|
| | $t^*$ | $f$ | $t^*$ | $f$ | $t^*$ | $f$ | $t^*$ | $f$ | $t^*$ | $f$ | $t^*$ | $f$ |
| 5 | 300 | 0.31 | 300 | 0.57 | 300 | 0.76 | 300 | 0.90 | 300 | 0.92 | 290 | 1.0 |
| 10 | 300 | 0.46 | 300 | 0.82 | 300 | 0.97 | 236 | 1.0 | 218 | 1.0 | 157 | 1.0 |
| 15 | 300 | 0.57 | 300 | 0.98 | 235 | 1.0 | 165 | 1.0 | 153 | 1.0 | 111 | 1.0 |
| 20 | 300 | 0.66 | 252 | 1.0 | 182 | 1.0 | 130 | 1.0 | 120 | 1.0 | 88 | 1.0 |

*Units:* $t^*(time\ in\ minutes, 0-300)$; $f(dimentionless\ melt\ fraction, 0-1)$

It can be observed from the table that with the increase in temperature difference, the rate of melt fraction also increases an appreciable amount. Even if the thermal conductivity of container materials increases then the melt fraction also increases. In the case of the copper container material, it can be easily noted from Table 5.14 that at the temperature difference of 5, 10, 15, and 20 ˚C the time required for complete melting are 290, 157, 111, and 88 min. respectively. This successive decrease in time for complete melting shows the high rate of melting due to an increase in the wall temperature of container material. To show this variation of melt fraction for temperature difference (i.e. 5, 10, 15, and 20 ˚C) in a more explicit manner, a graph has been plotted only for copper container material and presented in Figure 5.16.

From Figure 5.16 and Table 5.14, it can be easily observed that the wall temperature variation of container material has a significant effect on the melt fraction of PCMs.

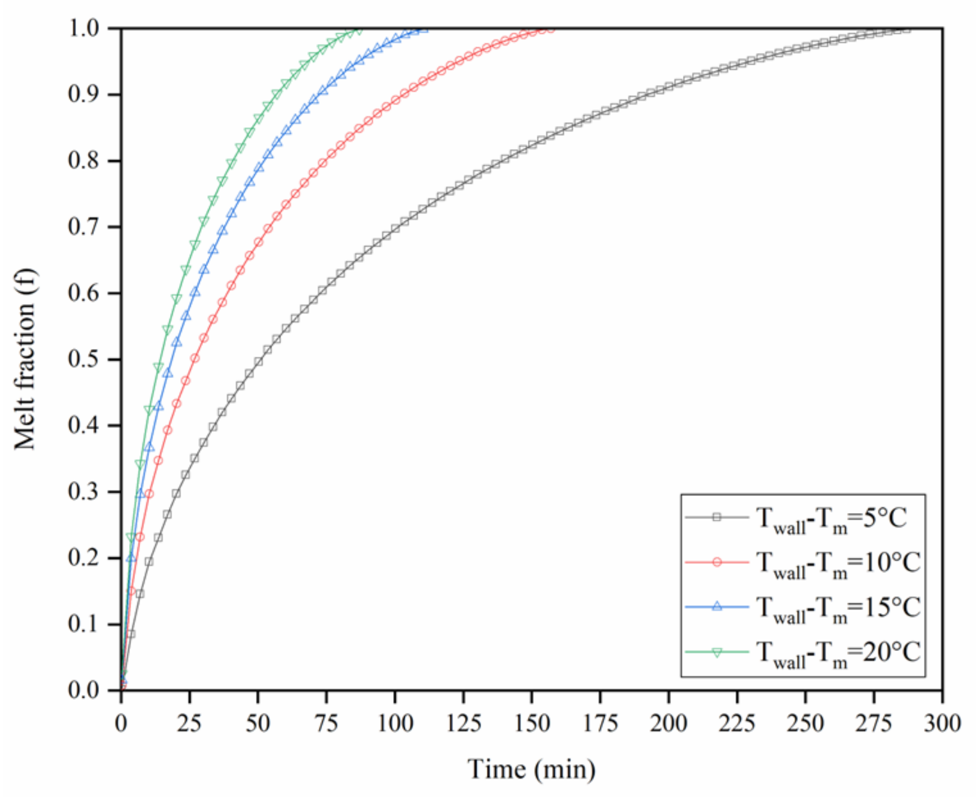


**Figure 5.16. Melt fraction comparison of PW-C20-33 for different values of $(T_{wall} - T_m)$ in case of only copper container material (thickness=2mm, $T_m - T_{init} = 15$ ℃)**

# Chapter 6: Summary, conclusion, and future prospects

In the present study technical, environmental, and economic feasibility analyses of the SWH system for domestic applications have been carried out. Further, a comparative study of the SWH system for residential, commercial, and industrial applications has been performed. This study also suggested an effective method of improving the thermal performance of the SWH system by the application of encapsulated PCMs in the storage tank of the SWH system. The probably suitable compounds that are eligible for PCM were also exhibited. The study depicts a numerical simulation model for testing different PCMs according to their effectiveness for the storage tank of the SWH system. The melting phenomena of PCMs inside container material for the storage tank of the SWH system are also presented. The detailed summary and conclusion of the presented thesis work are given in subsequent sections as,

## 6.1 Feasibility study of the SWH system for domestic applications

The technical and financial feasibility analysis of the evacuated tube-type SWH system has been done in this chapter. The seven cities of different geographical locations were selected for the study of the financial viability and performance of the SWH system in India. Among the selected cities Shimla (5.28 kWh/m$^2$/day) gets the highest daily solar radiation and Guwahati (4.69 kWh/m$^2$/day) gets the minimum value. Shimla is the most preferred location for the SWH installation. It is also observed that all cities are receiving daily solar radiation of more than 4.5 kWh/m$^2$/day which is a good precursor for SWH installation. The solar fractions of all cities are greater than 60 %, which is a good indicator of the performance of the SWH system at all geographical locations. The maximum value of 80.2 % is observed for Shimla and the minimum value of 64 % is obtained for Hyderabad. The Gross GHG emission reduction for the whole project life (25 yrs.) is 739 $tCO_2$ for all selected cities of the SWH system which may be more if the number of projects, will be more in each city and it could be an attractive parameter for getting approval of CDM project. The Energy savings through the SWH system at all locations of installation are 21 MWh which is equivalent to 68.8 barrels of crude oil not consumed. The energy savings increase if the number of installations increases in each city. The payback period analysis indicates that at least a 50 % incentive must be given by the Government to increase the interest of individuals in the household. It is more beneficial to give subsidies to SWH projects in place of giving subsidies to grid-connected electricity for heating water through electric geysers. These findings could be of great interest to CDM approval projects in India.

## 6.2 Techno-comparative study of SWH system for residential, commercial, and industrial applications

The techno-comparative feasibility of residential, commercial, and industrial models for the application of the SWH system was found feasible in this chapter. The model had been found environmentally sound and capable of reducing a large amount of GHGs. The optimum tilt angles for residential, commercial, and industrial models at the facility location for the collectors are 35°, 25°, and 30° along with maximum heat delivered of 3974.76 kWh, 313385.71 kWh, and 9020.51 kWh respectively. The range of SF obtained for all simulated models was well above the desired range which shows the satisfactory performance of SWH systems. The SF range for residential, commercial, and industrial sectors was 65 % - 90 %, 64.1 % - 64.7 %, and 13 % respectively. The average values of SF for residential, commercial, and industrial sectors are 74 %, 64.48 %, and 13 % respectively. The cumulative values of energy saved for residential, commercial, and industrial models were 111.3 MWh, 1728.6

MWh, and 313.8 MWh respectively. The cumulative values of gross annual GHGR potential for residential, commercial, and industrial models were 155.9 $tCO_2$, 2419.3 $tCO_2$, and 492.3 $tCO_2$ per year, these values could be of great interest for the purchase of carbon credits by developed countries. The range of SPP for residential, commercial, and industrial models was 2.5 - 9.4 years, 4.5 - 19.6 years, and 1.9 - 9.3 years respectively. The average values of SPP are 4.83 years, 8.99 years, and 3.90 years corresponding to residential, commercial, and industrial models respectively. The range of EPP for residential, commercial, and industrial models was 2.3 - 7.6 years, 3.1 - 15.3 years, and 1.7 - 7.5 years respectively and average values of EPP are 4.16 years, 7.78 years, and 3.39 years respectively. The average values of pre-tax IRR equity were 30.36 %, 27.89 %, and 38.77 % corresponding to residential, commercial, and industrial models. The average values of pre-tax MIRR equity for residential, commercial, and industrial models were 14.70 %, 16.16 %, and 15.34 % respectively. These presented values of simulation models were making feasible and proven advantages of SWH systems for the residential, commercial, and industrial sectors of India. All three simulation models presented in the study showed an enriched amount of GHG reduction potential by application of the proposed energy model of SWH systems. If the proposed energy model is not implemented then the same amount of $CO_2$ generation is continued at its rate and it will create a most dangerous impact on the environment. So, to make SWH projects most popular around the globe, different policies should be made for each specific sector like residential, commercial, and industrial. For increasing the application of the number of SWH projects around the world, there is a need to improve the efficiency of SWH systems in terms of the latent heat storage medium in the storage tank of hot water as well as to make this technology more cost-effective.

### 6.3 Numerical simulation for the storage tank of the SWH system

This chapter provides the theoretical simulation model to analyze the effectiveness of PCMs incorporated inside the storage tank of the SWH system. The study also includes the melt fraction analysis for the prediction of the melting behavior of PCMs inside container materials like glass, stainless steel, tin, aluminum mixed, aluminum, and copper through the program of the FORTRAN programming language. Through the simulation, eleven PCMs ranging in different melting temperatures of 36 to 69 °C had been investigated. It was found that among all eleven PCMs, SHPD had the highest value of effectiveness of 3.27, and the lowest value was found for PW at 1.51. The other PCMs also have values greater than 1.5. These values indicate that SHPD is the most effective encapsulated PCM for the storage tank of the SWH system. Even the rest of the PCMs are also having a high potential for increasing the thermal efficiency of the storage tank. It was observed that along with melting temperature the effectiveness of PCMs should also be considered for designing efficient thermal storage for the SWH system. It was noted that even if the mass flow rate of water increases for the storage tank then PCMs also capable of storing and releasing heat for improving the thermal efficiency of the storage tank. It is due to an almost linear relationship between the increase in mass flow rate and the effectiveness of PCM. It is recommended that the selected PCM should have a melting temperature higher than the designed mean temperature of the storage tank. For the making of efficient thermal stratification inside of storage tank. It is suggested that the selected PCM should have higher values of density, latent heat, and specific heat for the storage tank of the SWH system. Because these parameters almost have a linear relation with the increase of these values concerning the effectiveness of PCM. The melt fraction analysis showed that container material made of copper is the most favorable container material for the encapsulation of PCMs. It has the least time for the complete melting of PCMs due to its high value of thermal conductivity. Simulation analysis also suggested that some other container materials were also good for melting PCMs like aluminum and aluminum mixed. It had been found that if the thickness of container material increases it does not make any valuable effect on improving the melt fraction of PCMs. So, while designing the thickness of container material it is good to keep the minimum thickness of it, as possible from an economical point of view. It was noted that the melt fraction is independent of the initial temperature of PCMs. It was also found that the boundary wall temperature of container materials has a greater impact on the melt fractions of PCMs. The rate of melting of PCMs increases appreciably if the wall temperature is at a high value. It is evident through the results of the simulation model that PCMs could be the most eligible candidates to improve the thermal efficiency of the storage tank of the SWH systems along with good container material for encapsulation. The key facts of this study will help to design the suitable encapsulated PCM along with the container material for the storage tank to improve the thermal efficiency of the system.

### 6.4 Future scope of the work

The present day's need for energy in our country cannot be fulfilled alone through conventional sources of energy. We are facing severe energy crises in all sectors of the economy. It has been observed that we are majorly dependent on the Gulf countries to fulfill their energy needs. In spite, of having sufficient renewable energy potential to withstand the energy demand. The presented study explains the importance of the SWH system for application in the residential, commercial, and industrial sectors of India. This type of study is very rare focusing on the benefits of the SWH system in different sectors of the economy of India.

The presented simulation model uses the NASA database for various values of environment parameters for the simulation purpose like daily solar radiation, air temperature, wind speed, earth temperature, relative humidity, heating degree days, and cooling degree days. These parameters play an important role in the energy estimation of a project. It is recommended that the values of these environmental parameters should be measured practically through the measuring devices for more realistic results of the simulation models.

The study also suggested a method of improving the thermal efficiency of the storage tank of the SWH system through numerical simulation. In the simulation model, eleven PCMs have been analyzed. It is recommended that some more PCMs other than these eleven should be analyzed for the identification of more compatible PCMs for encapsulation in the storage tank of the SWH system. The thermal cycle testing of the suggested PCMs is also recommended for analyzing of thermal stability of the PCMs. It is well evident that encapsulated PCMs melt and solidify inside of the container material for many cycles so a corrosion test should also be performed for container materials.

The presented simulation model could be applied to the targeted sector of the economy for the fulfillment of the hot water need so the results could be of great interest to policymakers of the government of India.

# REFERENCES


[1] P.D. Lund, Clean energy systems as mainstream energy options, Int. J. Energy Res. 40 (2016) 4–12. https://doi.org/10.1002/ER.3283.

[2] R. Clift, A.J. Longley, Introduction to clean technology, Clean Technol. Environ. (1995) 174–198. https://doi.org/10.1007/978-94-011-1312-0_6.

[3] IPCC Special Report, Global Warming of 1.5 Degree Celsius, World Meteorological Organization, Geneva, Switzerland, 32 pp., 2015. www.ipcc.ch.

[4] M. Bahrami, P. Abbaszadeh, An overview of renewable energies in Iran, Renew. Sustain. Energy Rev. 24 (2013) 198–208. https://doi.org/10.1016/j.rser.2013.03.043.

[5] N. Kannan, D. Vakeesan, Solar energy for future world: - A review, Renew. Sustain. Energy Rev. 62 (2016) 1092–1105. https://doi.org/10.1016/j.rser.2016.05.022.

[6] K.H. Solangi, M.R. Islam, R. Saidur, N.A. Rahim, H. Fayaz, A review on global solar energy policy, Renew. Sustain. Energy Rev. 15 (2011) 2149–2163. https://doi.org/10.1016/j.rser.2011.01.007.

[7] A.P. Tyagi, Solar Radiant Energy Over India, New Delhi, 2009. https://www.imdpune.gov.in/library/public/Solar Radiant Energy Over India.pdf.

[8] N.L. Panwar, S.C. Kaushik, S. Kothari, Role of renewable energy sources in environmental protection: A review, Renew. Sustain. Energy Rev. 15 (2011) 1513–1524. https://doi.org/10.1016/j.rser.2010.11.037.

[9] N. Kannan, D. Vakeesan, Solar energy for future world: - A review, Renew. Sustain. Energy Rev. 62 (2016) 1092–1105. https://doi.org/10.1016/j.rser.2016.05.022.

[10] Global Solar Atlas, (n.d.). https://globalsolaratlas.info/download/world (accessed July 13, 2022).

[11] W. Spork-Dur, Solar Heat World Wide, Austria, 2022. https://www.iea-shc.org/Data/Sites/1/publications/Solar-Heat-Worldwide-2021.pdf.

[12] MNRE Report, Development of Conceptual Framework For Renewable Energy Certificate Mechanism for India, Ministry of New and Renewable Energy (Government of India), ABPS Infrastructure Advisory Private Limited, New Delhi, 2009. https://mnre.gov.in/knowledge-center/reports.

[13] S.K. Kar, A. Sharma, B. Roy, Solar energy market developments in India, Renew. Sustain. Energy Rev. 62 (2016) 121–133. https://doi.org/10.1016/j.rser.2016.04.043.

[14] MNRE Report, Annual Report of Year 2020-21, Ministry of New and Renewable Energy, Government of India., New Delhi, 2021. https://mnre.gov.in/.

[15] Z. Wang, W. Yang, F. Qiu, X. Zhang, X. Zhao, Solar water heating: From theory, application, marketing and research, Renew. Sustain. Energy Rev. 41 (2015) 68–84. https://doi.org/10.1016/j.rser.2014.08.026.

[16] C.M. Kemp, US Patent no. 451384, April 28th, 1891, (n.d.). https://patents.google.com/patent/US451384A/en (accessed September 20, 2022).

[17] F.A. Brooks, Solar energy and its use for heating water in California,Agricultural Bulletin 602. California Agricultural Experiment Station. Berkeley, California, USA, Univ. Calif. (1936). https://www.osti.gov/biblio/5096831 (accessed September 20, 2022).

[18] M. Smyth, P.C. Eames, B. Norton, Integrated collector storage solar water heaters, Renew. Sustain. Energy Rev. 10 (2006) 503–538. https://doi.org/10.1016/j.rser.2004.11.001.

[19] I. Tanishita, Present situation of commercial solar water heaters in Japan., Trans. Use Sol. Energy, Sci. Basis, Tucson, Arizona. (1955) 67–78.

[20] I. Tanishita, Present situation of commercial solar water heaters in Japan, in: Proc. ISES Conf. Melbourne, Aust., 1970: p. Paper no. 2/73. https://www.osti.gov/biblio/5092813 (accessed September 20, 2022).

[21] Natural Resources Canada, Clean Energy Project Analysis, 2005.

[22] MNRE Report, Solar Water Heaters, New Delhi, 2012. https://www.undp.org/india/publications/user's-handbook-solar-water-heaters.

[23] S. Canbazoğlu, A. Şahinaslan, A. Ekmekyapar, Ý.G. Aksoy, F. Akarsu, Enhancement of solar thermal energy storage performance using sodium thiosulfate pentahydrate of a conventional solar water-heating system, Energy Build. 37 (2005) 235–242. https://doi.org/10.1016/j.enbuild.2004.06.016.

[24] A. Felix Regin, S.C. Solanki, J.S. Saini, An analysis of a packed bed latent heat thermal energy storage system using PCM capsules: Numerical investigation, Renew. Energy. 34 (2009) 1765–1773. https://doi.org/10.1016/j.renene.2008.12.012.

[25] R.M. Reddy, N. Nallusamy, K.H. Reddy, Experimental Studies on Phase Change Material-Based Thermal Energy Storage System for Solar Water Heating Applications, J. Fundam. Renew. Energy Appl. 2 (2012) 1–6. https://doi.org/10.4303/jfrea/R120314.

[26] M.A. Fazilati, A.A. Alemrajabi, Phase change material for enhancing solar water heater, an experimental approach, Energy Convers. Manag. 71 (2013) 138–145. https://doi.org/10.1016/j.enconman.2013.03.034.

[27] H. Huang, Z. Wang, H. Zhang, B. Dou, X. Huang, H. Liang, M.A. Goula, An experimental investigation on thermal stratification characteristics with PCMs in solar water tank, Sol. Energy. 177 (2019) 8–21. https://doi.org/10.1016/j.solener.2018.11.004.

[28] S. Bazri, I.A. Badruddin, M.S. Naghavi, O.K. Seng, S. Wongwises, An analytical and comparative study of the charging and discharging processes in a latent heat thermal storage tank for solar water heater system, Sol. Energy. 185 (2019) 424–438. https://doi.org/10.1016/j.solener.2019.04.046.

[29] M. Dadollahi, M. Mehrpooya, Modeling and investigation of high temperature phase change materials (PCM) in different storage tank configurations, J. Clean. Prod. 161 (2017) 831–839. https://doi.org/10.1016/j.jclepro.2017.05.171.

[30] T. Bouhal, T. El Rhafiki, T. Kousksou, A. Jamil, Y. Zeraouli, PCM addition inside solar water heaters: Numerical comparative approach, J. Energy Storage. 19 (2018) 232–246. https://doi.org/10.1016/j.est.2018.08.005.

[31] Z. Wang, F. Qiu, W. Yang, X. Zhao, Applications of solar water heating system with phase change material, Renew. Sustain. Energy Rev. 52 (2015) 645–652. https://doi.org/10.1016/j.rser.2015.07.184.

[32] S. Sadhishkumar, T. Balusamy, Comparison of Solar Water Heater with and without Phase Change Material as Latent heat storage, Adv. Nat. Appl. Sci. 11 (2017) 605–611. http://www.aensiweb.com/http://creativecommons.org/licenses/by/4.0/.

[33] H.M. Teamah, M.F. Lightstone, J.S. Cotton, An alternative approach for assessing the benefit of phase change materials in solar domestic hot water systems, Sol. Energy. 158 (2017) 875–888. https://doi.org/10.1016/j.solener.2017.10.033.

[34] J. Zhao, Y. Ji, Y. Yuan, Z. Zhang, J. Lu, Energy-saving analysis of solar heating system with PCM storage tank, Energies. 11 (2018). https://doi.org/10.3390/en11010237.

[35] L. Xie, L. Tian, L. Yang, Y. Lv, Q. Li, Review on application of phase change material in water tanks, Adv. Mech. Eng. 9 (2017) 1–13. https://doi.org/10.1177/1687814017703596.

[36] M. Mofijur, T.M.I. Mahlia, A.S. Silitonga, H.C. Ong, M. Silakhori, M.H. Hasan, N. Putra, S.M. Ashrafur Rahman, Phase change materials (PCM) for solar energy usages and storage: An overview, Energies. 12 (2019) 1–20. https://doi.org/10.3390/en12163167.

[37] A.K. Pandey, M.S. Hossain, V. V. Tyagi, N. Abd Rahim, J.A.L. Selvaraj, A. Sari, Novel approaches and recent developments on potential applications of phase change materials in solar energy, Renew. Sustain. Energy Rev. 82 (2018) 281–323. https://doi.org/10.1016/j.rser.2017.09.043.

[38] G. Murali, K. Mayilsamy, T. V. Arjunan, An experimental study of PCM-incorporated thermosyphon solar water heating system, Int. J. Green Energy. 12 (2015) 978–986. https://doi.org/10.1080/15435075.2014.888663.

[39] E. Douvi, C. Pagkalos, G. Dogkas, M.K. Koukou, V.N. Stathopoulos, Y. Caouris, M.G. Vrachopoulos, Phase change materials in solar domestic hot water systems: A review, Int. J. Thermofluids. 10 (2021) 100075. https://doi.org/10.1016/j.ijft.2021.100075.

[40] Z. Wang, F. Qiu, W. Yang, X. Zhao, Applications of solar water heating system with phase change material, Renew. Sustain. Energy Rev. 52 (2015) 645–652. https://doi.org/10.1016/j.rser.2015.07.184.

[41] S. Faisal Ahmed, M. Khalid, M. Vaka, R. Walvekar, A. Numan, A. Khaliq Rasheed, N. Mujawar Mubarak, Recent progress in solar water heaters and solar collectors: A comprehensive review, Therm. Sci. Eng. Prog. 25 (2021) 100981. https://doi.org/10.1016/j.tsep.2021.100981.

[42] J.A. Duffie, W.A. Beckman, Solar Engineering of Thermal Processes, John Wiley & Sons, Inc., Hoboken, NJ, USA, 2013. https://doi.org/10.1002/9781118671603.

[43] A. Anand, A. Shukla, A. Sharma, Recapitulation on latent heat hybrid buildings, Int. J. Energy Res. 44 (2020) 1370–1407. https://doi.org/10.1002/er.4920.

[44] IPCC, Global warming of 1.5°C, Cambridge, 2018. https://doi.org/10.1017/CBO9781107415324.004.

[45] MNRE Report, Final Report On Market Assessment Of Solar Water Heating, Submitted to Ministry Of New And Renewable Energy (Government of India) Prepared by:ABPS Infrastructure Advisory Private Ltd, 2011.

[46] ABPS, Final Report On Scheme and Framework for Promotion of Solar Water Heating Systems by Utilities and Regulators Submitted to Ministry of New and Renewable Energy, 2010.

[47] Greentech, Solar Water Heaters in India: Market Assessment Studies And Surveys For Different Sectors and Demands Segments, 2010.

[48] A. Houri, Solar water heating in Lebanon : Current status and future prospects, 31 (2006) 663–675. https://doi.org/10.1016/j.renene.2005.08.003.

[49] P. Purohit, A. Michaelowa, CDM potential of solar water heating systems in India, Sol. Energy. 82 (2008) 799–811. https://doi.org/10.1016/j.solener.2008.02.016.

[50] A. Gastli, Y. Charabi, Solar water heating initiative in Oman energy saving and carbon credits, Renew. Sustain. Energy Rev. 15 (2011) 1851–1856. https://doi.org/10.1016/j.rser.2010.12.015.

[51] S. Stevanović, M. Pucar, Financial measures Serbia should offer for solar water heating systems, Energy Build. 54 (2012) 519–526. https://doi.org/10.1016/j.enbuild.2012.02.054.

[52] M. Abd-ur-rehman, F.A. Al-sulaiman, Optimum selection of solar water heating ( SWH ) systems based on their comparative techno-economic feasibility study for the domestic sector of Saudi Arabia, 62 (2016) 336–349. https://doi.org/10.1016/j.rser.2016.04.047.

[53] Y. Asyar, Technical and Financial Assessment of Glazed and Evacuated Tubes Solar Collectors for Domestic Water Heating ..., An-Najah Univ. j. Res.(N.Sc.). 31(1) (2017).

[54] M.A. Ben Taher, Z. Benseddik, A. Afass, S. Smouh, M. Ahachad, M. Mahdaoui, Energy life cycle cost analysis of various solar water heating systems under Middle East and North Africa region, Case Stud. Therm. Eng. 27 (2021) 101262. https://doi.org/10.1016/j.csite.2021.101262.

[55] M. Hazami, N. Naili, I. Attar, A. Farhat, Solar water heating systems feasibility for domestic requests in Tunisia: Thermal potential and economic analysis, Energy Convers. Manag. 76 (2013) 599–608. https://doi.org/10.1016/j.enconman.2013.07.079.

[56] M. Sadiq, Solar water heating system for residential consumers of Islamabad, Pakistan: A cost benefit analysis, J. Clean. Prod. 172 (2018) 2443–2453. https://doi.org/10.1016/j.jclepro.2017.11.166.

[57] J.K. Kaldellis, K. El-Samani, P. Koronakis, Feasibility analysis of domestic solar water heating systems in Greece, Renew. Energy. 30 (2005) 659–682. https://doi.org/10.1016/j.renene.2004.07.004.

[58] T. Cruz, R. Schaeffer, A.F.P. Lucena, S. Melo, R. Dutra, Solar water heating technical-economic potential in the household sector in Brazil, Renew. Energy. 146 (2020) 1618–1639. https://doi.org/10.1016/j.renene.2019.06.085.

[59] P. Veeraboina, G.Y. Ratnam, Analysis of the opportunities and challenges of solar water heating system (SWHS) in India: Estimates from the energy audit surveys & review, Renew. Sustain. Energy Rev. 16 (2012) 668–676. https://doi.org/10.1016/j.rser.2011.08.032.

[60] M. Raisul Islam, K. Sumathy, S. Ullah Khan, Solar water heating systems and their market trends, Renew. Sustain. Energy Rev. 17 (2013) 1–25. https://doi.org/10.1016/j.rser.2012.09.011.

[61] Government of India Ministry of Power, CO 2 Baseline Database for the Indian Power Sector User Guide, Rep. by Minist. Power Govt India. (2011) 1–34.

[62] R.E.N. Members, Renewables 2019 global status report 2019, 2019.

[63] G.K.S.P. Ltd., Solar Water Heaters in India : Market Assessment Studies and Surveys

for Different Sectors, Knowl. Creat. Diffus. Util. 110078 (2010).

[64] P.M. Unit, H. Project, Development Of An Area Based Energy Service Company (ESCO) Model For Solar Water Heating In India. Final Report Prepared for: Project Management Unit, UNDP/GEF Assisted Global Solar Water Heating Project, Ministry of New and Renewable Energy, GOI, 2010.

[65] B. Chandrasekar, T.C.Ã. Kandpal, Techno-economic evaluation of domestic solar water heating systems in India, 29 (2004) 319–332. https://doi.org/10.1016/S0960-1481(03)00198-8.

[66] P. Viability, A. For, I. Swh, S. In, G. Of, P. Of, EJ EAFChe, (n.d.).

[67] D.A. Hagos, A. Gebremedhin, B. Zethraeus, Solar Water Heating as a Potential Source for Inland Norway Energy Mix, 2014 (2014).

[68] A. Yasin, Technical and Financial Assessment of Glazed and Evacuated Tubes Solar Collectors for Domestic Water Heating Application in Palestine, (2017).

[69] S. Mekhilef, R. Saidur, A. Safari, A review on solar energy use in industries, Renew. Sustain. Energy Rev. 15 (2011) 1777–1790. https://doi.org/10.1016/j.rser.2010.12.018.

[70] A. Gautam, S. Chamoli, A. Kumar, S. Singh, A review on technical improvements, economic feasibility and world scenario of solar water heating system, Renew. Sustain. Energy Rev. 68 (2017) 541–562. https://doi.org/10.1016/j.rser.2016.09.104.

[71] R. Zhang, G.Q.P. Shen, M. Ni, J.K.W. Wong, Techno-economic feasibility of solar water heating system: Overview and meta-analysis, Sustain. Energy Technol. Assessments. 30 (2018) 164–173. https://doi.org/10.1016/j.seta.2018.10.004.

[72] L.F. Cabeza, H. Mehling, Review on thermal energy storage with phase change : materials , heat transfer analysis and applications, 2003.

[73] A. Abhat, Low temperature latent heat thermal energy storage: Heat storage materials, Sol. Energy. 30 (1983) 313–332. https://doi.org/10.1016/0038-092X(83)90186-X.

[74] R. Naumann, H.H. Emons, Results of thermal analysis for investigation of salt hydrates as latent heat-storage materials, J. Therm. Anal. 35 (1989) 1009–1031. https://doi.org/10.1007/BF02057256.

[75] D.W. Hawes, D. Feldman, D. Banu, Latent heat storage in building materials, Energy Build. 20 (1993) 77–86. https://doi.org/10.1016/0378-7788(93)90040-2.

[76] D. Ibrahim, Thermal energy storage : systems and applications / Ibrahim Dinçer and Marc Rosen., 2011.

[77] P. Taylor, G.A. Lane, G.A. Lane, Low temperature heat storage with phase change materials Low temperature heat storage with phase change materials, (2011) 37–41. https://doi.org/10.1080/01430750.1980.9675731.

[78] K. Sasaguchi, R. Viskanta, Phase Change Heat Transfer During Melting and Resolidification of Melt Around Cylindrical Heat Source ( s )/ Sink ( s ), 111 (2016).

[79] D.Feldman, M.M.Shapiro, D.Banu, Organic phase change materials for thermal energy storage, Sol. Energy Mater. Sol. Cells. 13 (1986) 1–10.

[80] A. Sari, K. Kaygusuz, Thermal performance of palmitic acid as a phase change energy storage material, 43 (2002) 863–876.

[81] A. Sari, K. Kaygusuz, Thermal energy storage system using stearic acid as a phase change material, Sol. Energy. 71 (2001) 365–376. https://doi.org/10.1016/S0038-

092X(01)00075-5.

[82] M. Dzikevics, A. Zandeckis, Mathematical Model of Packed Bed Solar Thermal Energy Storage Simulation, Energy Procedia. 72 (2015) 95–102. https://doi.org/10.1016/j.egypro.2015.06.014.

[83] S. Ebadi, S.H. Tasnim, A. a. Aliabadi, S. Mahmud, Melting of nano-PCM inside a cylindrical thermal energy storage system: Numerical study with experimental verification, Energy Convers. Manag. 166 (2018) 241–259. https://doi.org/10.1016/j.enconman.2018.04.016.

[84] E. Hahne, Y. Chen, Numerical study of flow and heat transfer characteristics in hot water stores, Sol. Energy. 64 (1998) 9–18. https://doi.org/10.1016/S0038-092X(98)00051-6.

[85] K.A.R. Ismail, J.R. Henríquez, Numerical and experimental study of spherical capsules packed bed latent heat storage system, Appl. Therm. Eng. 22 (2002) 1705–1716. https://doi.org/10.1016/S1359-4311(02)00080-7.

[86] L. Xia, P. Zhang, R.Z. Wang, Numerical heat transfer analysis of the packed bed latent heat storage system based on an effective packed bed model, Energy. 35 (2010) 2022–2032. https://doi.org/10.1016/j.energy.2010.01.018.

[87] A. Raul, M. Jain, S. Gaikwad, S.K. Saha, Modelling and experimental study of latent heat thermal energy storage with encapsulated PCMs for solar thermal applications, Appl. Therm. Eng. 143 (2018) 415–428. https://doi.org/10.1016/j.applthermaleng.2018.07.123.

[88] S. Bellan, T.E. Alam, J. González-Aguilar, M. Romero, M.M. Rahman, D.Y. Goswami, E.K. Stefanakos, Numerical and experimental studies on heat transfer characteristics of thermal energy storage system packed with molten salt PCM capsules, Appl. Therm. Eng. 90 (2015) 970–979. https://doi.org/10.1016/j.applthermaleng.2015.07.056.

[89] Z. Liu, C. Ma, Numerical analysis of melting with constant heat flux heating in a thermal energy storage system, Energy Convers. Manag. 43 (2002) 2521–2538. https://doi.org/10.1016/S0196-8904(01)00190-X.

[90] R. Majumdar, S.K. Saha, Effect of varying extent of PCM capsule filling on thermal stratification performance of a storage tank, Energy. 178 (2019) 1–20. https://doi.org/10.1016/j.energy.2019.04.101.

[91] T. Kousksou, P. Bruel, G. Cherreau, V. Leoussoff, T. El Rhafiki, PCM storage for solar DHW: From an unfulfilled promise to a real benefit, Sol. Energy. 85 (2011) 2033–2040. https://doi.org/10.1016/j.solener.2011.05.012.

[92] B. Zivkovic, I. Fujii, An Analysis of Isothermal Phase Change of Phase Change, Sol. Energy. 70 (2001) 51–61.

[93] S. Kılıçkap, E. El, C. Yıldız, Investigation of the effect on the efficiency of phase change material placed in solar collector tank, Therm. Sci. Eng. Prog. 5 (2018) 25–31. https://doi.org/10.1016/j.tsep.2017.10.016.

[94] M.H. Mahfuz, M.R. Anisur, M.A. Kibria, R. Saidur, I.H.S.C. Metselaar, Performance investigation of thermal energy storage system with Phase Change Material (PCM) for solar water heating application, Int. Commun. Heat Mass Transf. 57 (2014) 132–139. https://doi.org/10.1016/j.icheatmasstransfer.2014.07.022.

[95] M. Mazman, L.F. Cabeza, H. Mehling, M. Nogues, H. Evliya, H.Ö. Paksoy, Utilization of phase change materials in solar domestic hot water systems, Renew.

Energy. 34 (2009) 1639–1643. https://doi.org/10.1016/j.renene.2008.10.016.

[96] S. Jaisankar, J. Ananth, S. Thulasi, S.T. Jayasuthakar, K.N. Sheeba, A comprehensive review on solar water heaters, Renew. Sustain. Energy Rev. 15 (2011) 3045–3050. https://doi.org/10.1016/j.rser.2011.03.009.

[97] R. Shukla, K. Sumathy, P. Erickson, J. Gong, Recent advances in the solar water heating systems: A review, Renew. Sustain. Energy Rev. 19 (2013) 173–190. https://doi.org/10.1016/j.rser.2012.10.048.

[98] Lane GA., Solar Heat Storage: Latent Heat Materials, 1983.

[99] G.A. Lane, Solar Heat Storage : Latent Heat Materials Volume II :, CRC Press, 2018.

[100] Q. Xu, N. Akkurt, Z. Zou, Y. Liu, J. Feng, C. Yu, C. Ding, Y. Xiong, J. Zhou, Y. Zang, Y. Ding, Synthesis and Characterization of Disodium Hydrogen Phosphate Dodecahydrate-Lauric-Palmitic Acid Used for Indoor Energy Storage Floor Units, J. Therm. Sci. 29 (2020) 477–485. https://doi.org/10.1007/s11630-020-1273-7.

[101] A. Sharma, A. Shukla, C.R. Chen, S. Dwivedi, Development of phase change materials for building applications, Energy Build. 64 (2013) 403–407. https://doi.org/10.1016/j.enbuild.2013.05.029.

[102] E.-B.S. Mettawee, G.M.R. Assassa, Thermal conductivity enhancement in a latent heat storage system, Sol. Energy. 81 (2007) 839–845. https://doi.org/10.1016/j.solener.2006.11.009.

[103] N. Ukrainczyk, S. Kurajica, J. Šipušić, Thermophysical comparison of five commercial paraffin waxes as latent heat storage materials, Chem. Biochem. Eng. Q. 24 (2010) 129–137. https://doi.org/10.15255/CABEQ.2014.240.

[104] M. Dannemand, J.B. Johansen, S. Furbo, Solidification behavior and thermal conductivity of bulk sodium acetate trihydrate composites with thickening agents and graphite, Sol. Energy Mater. Sol. Cells. 145 (2016) 287–295. https://doi.org/10.1016/j.solmat.2015.10.038.

[105] A. Anand, A. Shukla, A. Sharma, Numerical heat transfer study of energy storage materials used in the latent heat storage system, Mater. Sci. Energy Technol. 3 (2020) 633–639. https://doi.org/10.1016/j.mset.2020.06.007.

[106] V.R. Voller, Numerical Heat Transfer , Part B : Fundamentals : An International Journal of Computation and Methodology, Fast imlicit finite-difference method for the analysis of phase change problems, Numer. Heat Transf. 17 (1990) 155–169.

[107] Patankar SV, Numerical heat transfer and fluid flow. Hemisphere Publishing Corporation, Washington - New York - London. McGraw Hill Book Company, New York 1980., 53 (1980) 225–225.

[108] M. Costa, A. Oliva, Numerical Simulation of a Latent Heat Thermal Energy Storage System With, Energy Convers. Manag. 39 (1998) 319–330.

# LIST OF PUBLICATIONS

## PUBLICATION IN PEER-REVIEWED JOURNALS

1. **Shailendra Singh**, Abhishek Anand, Amritanshu Shukla, Atul Sharma, Technical, financial, and environmental feasibility of solar water heater for residential, commercial, and industrial application: A theoretical approach, Materials Science for Energy Technologies. 3 (2020) 648-671.
2. **Shailendra Singh**, Abhishek Anand, Amritanshu Shukla, Atul Sharma, Environmental, technical and financial feasibility study of domestic solar water heating system in India, Sustainable Energy Technologies and Assessments. 43 (2021) 100965.
3. **Shailendra Singh**, Abhishek Anand, Amritanshu Shukla, Atul Sharma, Numerical analysis of phase change and container materials for thermal energy storage in the storage tank of solar water heating system, Journal of Thermal Science. Online first (2023) 1-17.
4. **Shailendra Singh**, Majed Alharthi, Abhishek Anand, Amritanshu Shukla, Atul Sharma, Hitesh Panchal, Performance evaluation and financial viability analysis of grid associated 10 $MW_P$ solar photovoltaic power plant at UP India, Scientific Reports. 12 (2022) 22380.
5. Abhishek Anand, Vartika Srivastava, **Shailendra Singh**, Amritanshu Shukla, Abhay Kumar Choubey, Atul Sharma, Development of nano-enhanced phase change materials using manganese dioxide nanoparticles obtained through green synthesis, Energy Storage (2022).

# BOOK CHAPTERS

1. **Shailendra Singh**, Abhishek Anand, Amritanshu Shukla, Atul Sharma, Role of phase change materials in solar water heating applications. Apple Academic Press (USA), (2020).
2. Atul Sharma, Abhishek Anand, **Shailendra Singh**, Amritanshu Shukla, Solar cooking applications through phase change materials (PCMs). Apple Academic Press (USA), (2020).
3. **Shailendra Singh**, Abhishek Anand, Amritanshu Shukla, D. Buddhi, F. Bruno, and Atul Sharma, Application of latent heat storage materials in the storage tank of the SWH system. Springer Nature Singapore, (2022).

# CONFERENCES

1. **Shailendra Singh**, Abhishek Anand, Amritanshu Shukla, Atul Sharma, Development of phase change materials for thermal application, "International Conference on Energy Storage Technologies and Systems (ICOEST)", Center of Excellence in Renewable and Sustainable Energy Studies, Suresh Gyan Vihar University, Jaipur, (2018).
2. **Shailendra Singh**, Abhishek Anand, Amritanshu Shukla, Atul Sharma, Application of thermal energy storage for solar water heating systems, "International Symposium on Advances in Functional and Biological Materials (ISAFBM)", Humboldt Academy, Department of Physics, University of Lucknow. (2019).